Universidad de Huelva

Departamento de Ingeniería Electrónica, de Sistemas Informáticos y Automática

Nuevas estrategias de planificación de la producción en plantas termosolares con almacenamiento térmico

Memoria para optar al grado de doctor
presentada por:

Emilian Gelu Cojocaru

Fecha de lectura: 10 de febrero de 2020

Bajo la dirección de los doctores:

José Manuel Bravo Caro

Manuel Jesús Vasallo Vázquez

Huelva, 2020

Universidad de Huelva

Departamento de Ingeniería Electrónica, de Sistemas Informáticos y Automática

Nuevas estrategias de planificación de la producción en plantas termosolares con almacenamiento térmico

Memoria para optar al grado de doctor presentada por:

Emilian Gelu Cojocaru

Bajo la dirección de los doctores:

José Manuel Bravo Caro

Manuel Jesús Vasallo Vázquez

Huelva, 2019

Universidad de Huelva

Departamento de Ingeniería Electrónica,
de Sistemas Informáticos y Automática

Programa de Doctorado

Economía, Empresas, Finanzas y Computación

Tesis Doctoral

Nuevas estrategias de planificación de la producción en plantas termosolares con almacenamiento térmico

Autor:

Emilian Gelu Cojocaru

Directores:

José Manuel Bravo Caro
Manuel Jesús Vasallo Vázquez

Huelva, 2019

A mi abuela Lucia

Agradecimientos

En primer lugar, a los directores de esta Tesis, José Manuel Bravo Caro y Manuel Jesús Vasallo Vázquez por su paciencia, por el tiempo que me han dedicado y por todo lo que he aprendido de ellos durante estos años. No podría haber realizado este trabajo sin su apoyo.

A los doctores Diego Marín Santos y Manuel Emilio Gegúndez Arias por su colaboración en los distintos trabajos publicados.

A Juan Antonio Gómez Galán por hacerme saber de la oportunidad de realizar esta Tesis, y por escucharme y darme ánimos en muchas ocasiones.

A mi familia por todo lo que compartimos.

A Haru por su amistad y sus enseñanzas.

Finalmente, a Lavinia, por todo su cariño, por estar a mi lado.

Índice general

Siglas

CSP *Concentrating solar power* (energía solar por concentración).

DNI *Direct normal irradiance* (irradiancia solar directa).

HTF *Heat transfer fluid* (fluido caloportador).

LCOE *Levelized cost of electricity* (coste medio de generación eléctrica).

LFR *Lineal Fresnel reflector* (concentrador solar de tipo Fresnel lineal).

MILP *Mixed-integer lineal programming* (programación lineal entera mixta).

MPC *Model-based predictive control* (control predictivo basado en modelo).

PCM *Production cost model* (modelo de coste de producción).

PT *Price taker* (enfoque de tomador de precios).

PTC *Parabolic trough collector* (concentrador solar de tipo cilindro parabólico).

PV *PhotoVoltaic* (tecnología fotovoltaica).

SPD *Solar power dish* (concentrador solar de tipo disco parabólico).

SPT *Solar power tower* (tecnología solar de tipo torre).

TES *Thermal energy storage* (almacenamiento de energía térmica).

Capítulo 1

Planteamiento general de la Tesis

1.1. Introducción

Esta Tesis está vinculada al Proyecto de Investigación PI2016-76493-C3-2-R, de título *Data-driven inference and applications*, perteneciente al Programa Estatal de Investigación, Desarrollo e Innovación Orientada a los Retos de la Sociedad. Se presenta como un compendio de tres artículos publicados en revistas del *Journal Citation Reports*.

Los objetivos principales de la Tesis son el diseño de nuevas estrategias de planificación óptima de la producción para una planta termosolar con almacenamiento térmico, y el estudio mediante simulación del rendimiento económico de cada estrategia cuando se considera la participación de la planta en el mercado diario de la electricidad. En este sentido, en cada articulo se desarrolla y estudia cada una de las estrategias propuestas.

En respuesta a problemas como el cambio climático, la dependencia energética exterior de los países y el agotamiento de los combustibles fósiles, la generación eléctrica basada en fuentes de energía renovable intermitente, como la energía solar y eólica, ha crecido significativamente durante los últimos años gracias a la disminución de costes. Este tipo de generación presenta un carácter intermitente, variable y de difícil predicción, lo que dificulta su integración en la red eléctrica. Sin embargo, la energía solar por concentración (también llamada energía termosolar, solar termoeléctrica o solar térmica) presenta ciertas características que pueden compensar en parte las desventajas anteriores. Esta tecnología captura la radiación solar en forma de energía térmica por medio del calentamiento de un fluido y la convierte en energía eléctrica mediante un ciclo termodinámico, una turbina y un generador. Por el hecho de emplear energía térmica como forma de energía intermedia, se complementa muy bien con sistemas de almacenamiento térmico. Gracias a este almacenamiento energético, este tipo de plantas presenta cierto grado de gestionabilidad, existiendo la posibilidad de adaptar la producción al perfil de demanda eléctrica. Esta propiedad favorece su participación en el mercado eléctrico.

El objetivo de un productor de electricidad cuando participa en el mercado eléctrico es maximizar los beneficios económicos derivados de la venta de electricidad. Este objetivo puede lograrse cuando se planifica la generación de potencia en función del perfil de precios de venta de la electricidad. Puede plantearse, por tanto, un problema de optimización dinámica conocido en la literatura como problema de planificación óptima de la generación (*optimal generation scheduling problem*). Considerando sólo el mercado diario de la electricidad, la resolución del problema de planificación óptima permite obtener el plan diario de generación, que debe enviarse al mercado normalmente el día anterior. Se deduce de lo anterior que en el caso de plantas renovables, además de la necesidad de disponer de una predicción de los precios de la electricidad, se requiere una predicción del recurso natural para poder abordar el problema.

La herramienta matemática más usada para resolver este tipo de problemas es la programación lineal entera mixta (*mixed integer lineal programming*, MILP). Un problema lineal entero mixto es un problema de optimización en el que se combinan variables de decisión reales con variables de decisión binarias (enteras en su formato más general). Este método permite formular de manera sencilla la toma de decisiones sobre qué generador y qué modo de operación se aplican en la producción. También se facilita el modelado de restricciones operativas asociadas a arranques, paradas, gradientes de la producción

eléctrica y otros factores. Una ventaja final es la existencia de *resolvedores* (*solvers* en inglés) con capacidad para encontrar la solución óptima global del problema en tiempos de cómputo relativamente cortos. En este sentido, las estrategias de planificación propuestas en esta Tesis se han basado en la programación lineal entera mixta. La función objetivo se ha adaptado al criterio establecido en cada estrategia. Las restricciones incluidas en el problema de optimización modelan las conversiones energéticas y las restricciones operativas de la planta.

Un aspecto que dificulta el problema de planificación óptima es la existencia de incertidumbre en las predicciones de precios de la electricidad y del recurso solar. Una predicción imprecisa de los precios trae consigo una planificación subóptima, que no lograría alcanzar el máximo de los beneficios. Lo mismo ocurre con una predicción inexacta del recurso natural. Además, cuando el recurso natural se ha sobrestimado, se pueden producir desvíos de la generación respeto al plan comprometido con el mercado, lo que puede suponer costes de penalización.

En este contexto, esta Tesis abarca los siguientes trabajos:

- Desarrollo de una estrategia de planificación inspirada en el *control predictivo basado en modelo* (**estrategia de replanificación horaria**). Este tipo de control es una estrategia de *horizonte deslizante*, que se caracteriza por la resolución periódica del problema de optimización en el horizonte considerado, que va desplazándose hacia el futuro, y por la actualización del estado de la planta mediante mediciones en cada desplazamiento. Estas propiedades generan un esquema de control en bucle cerrado. La estrategia de replanificación horaria empleada tiene como particularidad la división del horizonte en dos intervalos. El primero, intervalo de seguimiento, comprende todas las horas desde la hora actual hasta la finalización del día actual y, por tanto, presenta un compromiso de cumplimiento del plan de generación de dicho día. El segundo intervalo abarca el día siguiente. Cada hora, la solución del problema establece qué nivel de generación se debe aplicar en la hora actual y, según la información conocida hasta ese momento, cómo seguir el plan comprometido y qué plan se debe ejecutar el día siguiente. La función objetivo es de tipo económico, contabilizando los ingresos por ventas de electricidad y estimando los costes de penalización por desvío de la generación respecto al plan comprometido. El criterio para la optimización es la maximización de los beneficios económicos. El mercado define una hora límite para el envío del plan de generación. A esa hora se envía la solución del problema para el segundo intervalo. La ventaja de la replanificación es que permite introducir en el problema de manera periódica, horaria en este caso, el estado actual de la planta, las mejoras en la predicción del recurso solar y el conocimiento exacto de los precios de la electricidad para el día actual. Es por tanto un mecanismo para abordar la incertidumbre presente en las predicciones y en el propio modelado del problema. Esta estrategia es presentada en el artículo *Calculating the profits of an economic MPC applied to CSP plants with thermal storage system.*
- Diseño de una estrategia de planificación orientada a la disminución de las variaciones en la producción (**estrategia anti-*cycling***). El termino inglés *cycling* se usa para referirse a dichas variaciones. Esta reducción de la variabilidad en la generación tiene como ventajas una extensión en la vida útil de los elementos del bloque de potencia

de la planta, una reducción de sus costes de mantenimiento y una simplificación de la operación de la planta. Si bien la posibilidad de variar la producción en este tipo de plantas es el factor que añade valor, es interesante limitar esta variación de manera que no comprometa los beneficios económicos y produzca las ventajas antes mencionadas. Esta estrategia es presentada en el artículo *Optimal scheduling in concentrating solar power plants oriented to low generation cycling*.

- Desarrollo de una estrategia de planificación que combine la replanificación horaria y la reducción de la variabilidad de la producción (**estrategia de replanificación horaria con anti-*cycling***). Esta estrategia sumará las ventajas de las dos estrategias anteriores. Esta estrategia es presentada en el artículo *A binary-regularization-based model predictive control applied to generation scheduling in concentrating solar power plants.*

Se ha desarrollada una plataforma de pruebas para la simulación a escala horaria de las tres estrategias propuestas sobre una planta termosolar de 50 MW de tipo cilindro parabólico localizada en la provincia de Granada (España). Concretamente, la planta empleada como referencia es *Andasol* 2, propiedad del Grupo ACS. El objetivo de las simulaciones es estudiar el impacto económico de las estrategias propuestas. Se considera el mercado diario de electricidad español y la hipótesis de que la producción de la planta no altera los precios. Las simulaciones tienen una resolución horaria y abarcan un periodo de 6 ó 12 meses, según el caso, lo que permite testear diversas condiciones meteorológicas y de mercado. La plataforma incluye el planificador de la producción que implementa las tres estrategias, un simulador del campo solar de la planta, e información realista sobre el recurso solar, los precios de la electricidad, los costes de penalización y las predicciones de todos estos datos. Esta información está asociada al año 2013.

1.2. Rendimiento científico de la Tesis

Los trabajos llevados a cabo en esta Tesis están vinculados al Proyecto de Investigación PI2016-76493-C3-2-R, de título *Data-driven inference and applications*, perteneciente al Programa Estatal de Investigación, Desarrollo e Innovación Orientada a los Retos de la Sociedad. Los datos de este proyecto son los siguientes:

- Título: *Data-driven inference and applications*.
- Entidad financiadora: Ministerio de Economía, Industria y Competitividad.
- Cantidad financiada: 116160 euros.
- Referencia: DPI2016-76493-C3-2-R.
- Entidad participante: Universidad de Huelva.
- Duración: desde 30/12/2016 hasta 31/12/2019.
- Investigador principal: José Manuel Bravo Caro.
- Número de investigadores participantes: 5.

A continuación se enumeran los trabajos publicados por el doctorando en el periodo de realización de la Tesis. La relación se muestra en orden cronológico inverso, estando los artículos además ordenados según el tipo de publicación. Los tres trabajos publicados en revistas internacionales son los que componen esta Tesis, presentada como compendio de artículos. Las revistas en los que fueron publicados pertenecen al primer cuartil (*Solar Energy* y *Renewable Energy*) y segundo cuartil (*Optimal Control Applications and Methods*) de sus respectivas categorías del *Journal Citation Reports*.

Los trabajos (1), (2) y (3) de la lista de publicaciones en congresos internacionales y los trabajos (4) y (5) de la relación de publicaciones en congresos nacionales son trabajos previos a los artículos publicados en revistas.

Los trabajos (4) de la lista de publicaciones en congresos internacionales y (3) de la relación de publicaciones en congresos nacionales son trabajos relacionados con el desarrollo de un simulador de planta termosolar orientado a la docencia, que finalmente no se incluyó en la Tesis.

Los trabajos (1) y (2) de la relación de publicaciones en congresos nacionales son trabajos relacionados con una de las lineas futuras de investigación indicadas en la Sección 2.4 del Capítulo 2.

Finalmente, en la categoría *Otras publicaciones* se indica un trabajo que está fuera del contexto de la Tesis.

Publicaciones en revistas internacionales:

1. Emilian Gelu Cojocaru, José Manuel Bravo, Manuel Jesús Vasallo and Diego Marín. A binary-regularization-based model predictive control applied to generation scheduling in concentrating solar power plants. *Optimal Control Applications and Methods*,1-24, 2019 (in press). Índice de Impacto (JCR, 2018) = 1.452, Cuartil: Q2 (81/254) en la categoría *Mathematics, Applied*.

2. Emilian Gelu Cojocaru, José Manuel Bravo, Manuel Jesús Vasallo and Diego Marín. Optimal scheduling in concentrating solar power plants oriented to low generation cycling. *Renewable energy*, 135:789-799, 2019. Índice de Impacto (JCR, 2018) = 5.439. Cuartil: Q1 (17/103) en la categoría *Energy & Fuels*.

3. Manuel Jesús Vasallo, José Manuel Bravo, Emilian Gelu Cojocaru and Manuel Emilio Gegúndez. Calculating the profits of an economic MPC applied to CSP plants with thermal storage system. *Solar Energy*, 155 (Supplement C): 1165 - 1177, 2017. Índice de Impacto (JCR, 2017) = 4.374 , Cuartil: Q1 (23/97) en la categoría *Energy & Fuels*.

Publicaciones en congresos internacionales:

1. E. G. Cojocaru, J. M. Bravo, M. J. Vasallo and D. Marín. Scheduling in concentrating solar power plants based on mixed-integer optimization and binary-regularization. In *2018 IEEE Conference on Decision and Control (CDC)*, pages 1632-1637, Dec 2018.

2. E. G. Cojocaru, M. J. Vasallo, J. M. Bravo and D. Marin. Scheduling in concentrating solar power plants based on model predictive control and binary-regularization methods. In *2018 IEEE Conference on Control Technology and Applications (CCTA)*, pages 1008-1013, Aug 2018.

3. E. G. Cojocaru, M. J. Vasallo, J. M. Bravo and D. Marín. A lifetime-extending model-based predictive control for scheduling in concentrating solar power plants. In *2018 IEEE International Conference on Industrial Technology (ICIT)*, pages 1732-1737, Feb 2018.

4. E. G. Cojocaru, M. J. Vasallo, J. M. Bravo and D. Marín. Concentrated solar power plant simulator for education purpose. In *2018 IEEE International Conference on Industrial Technology (ICIT)*, pages 1829-1834, Feb 2018.

Publicaciones en congresos nacionales:

1. Emilian Cojocaru, José Manuel Bravo Caro, Manuel Vasallo, and Manuel Emilio Gegúndez-Arias. Modelos empíricos del campo solar en plantas termosolares de concentración. Aplicación a la planificación. In *XL Jornadas de Automática*, pages 1829-1834, Feb 2018.

2. Emilian Gelu Cojocaru, José Manuel Bravo, Manuel Jesús Vasallo and Manuel Emilio Gegúndez-Arias. Planificación de la producción en plantas termosolares. Modelado del campo solar orientado a datos. In *XXXIX Jornadas de Automática*, pages 664-671, Sep 2018.

3. Emilian Gelu Cojocaru, Manuel Jesús Vasallo, José Manuel Bravo and Diego Marín. Simulador de planta termosolar con fines educativos. In *IV Simposio CEA de Modelado, Simulación y Optimización*, pages 53-58. Valladolid, España, Jan 2018.

4. Emilian Gelu Cojocaru, Manuel Jesús Vasallo, José Manuel Bravo and Diego Marín. Planificación de la producción en plantas térmicas de concentración solar, una perspectiva para el mercado eléctrico. In *IV Simposio CEA de Modelado, Simulación y Optimización*, pages 72-77. Valladolid, España, Jan 2018.

5. M. J. Vasallo, J. M. Bravo, E. Cojocaru and M. E. Gegúndez. Planificación de la producción basada en control predictivo para plantas termosolares. In *XXXVIII Jornadas de Automática* pages 641-648, Sep 2017.

Otras publicaciones:

- José Manuel Bravo, Emilian Cojocaru, Manuel Vasallo, and Teodoro Alamo. Interval predictor based on supporting hyperplanes. In *2018 European Control Conference (ECC)*, pages 2830-2835. IEEE, 2018.

1.3. Estructura de la Tesis

La memoria de esta Tesis está organizada en cuatro capítulos según la distribución que se describe a continuación.

En el **Capitulo 1**, *Planteamiento general de la Tesis*, se realiza una introducción a la temática de la misma, se señalan las principales aportaciones y se indica la producción científica generada mediante los trabajos realizados en el ámbito de esta Tesis. Finalmente, se describe la estructura del documento de Tesis.

En el **Capitulo 2**, *Resumen*, se exponen los objetivos propuestos, la metodología seguida para alcanzarlos, los resultados obtenidos y las conclusiones derivadas a partir de dichos resultados. Finalmente, se exponen las conclusiones generales de la Tesis y algunos posibles trabajos futuros.

En el **Capitulo 3**, *Antecedentes*, se realiza una introducción a los sistemas y tecnologías que tienen relación con los desarrollos realizados en esta Tesis, junto con una descripción del problema abordado. Los elementos tratados son los sistemas y mercados eléctricos, las tecnologías de energía renovable, las tecnologías termosolares, la programación lineal entera mixta, el control predictivo basado en modelo y el problema de planificación de la producción en sistemas eléctricos en general, y en plantas termosolares en particular.

El **Capitulo 4**, *Copia de trabajos publicados*, contiene los artículos publicados en su orden de aparición.

Finalmente, se indica la bibliografía referenciada en el documento de Tesis.

Capítulo 2

Resumen

En este capítulo se realiza un resumen de la Tesis. Se exponen los objetivos propuestos, la metodología seguida para alcanzarlos, los resultados obtenidos y sus conclusiones, las conclusiones generales y algunos posibles trabajos futuros.

2.1. Objetivos y metodología

Los objetivos de esta Tesis son el desarrollo de tres nuevas estrategias para la planificación de la producción en plantas termosolares, descritas brevemente en la Sección 1.1 del capítulo 1, y el estudio del impacto económico de cada estrategia en un contexto de simulación. Se indican a continuación los recursos iniciales que el doctorando tuvo a su disposición al inicio de los trabajos de esta Tesis, que fueron desarrollados por los directores de la Tesis para las publicaciones [1] y [2]:

1. Un modelo MILP (*mixed-integer linear programming*) que resuelve el problema de planificación para el día siguiente, cuya función objetivo incluye sólo los ingresos económicos derivados de la venta de electricidad. Este modelo de optimización fue implementado en MATLAB con ayuda de una herramienta de acceso libre para el modelado y resolución de problemas de optimización llamada YALMIP [3].

2. Un modelo MILP que resuelve el problema de planificación para una posición de la ventana deslizante de la estrategia de control predictivo basado en modelo (*model-based predictive control*, MPC). A diferencia de la estrategia de replanificación horaria propuesta en esta Tesis, en este modelo la función objetivo contabiliza en el primer intervalo del horizonte los desvíos respecto al plan comprometido y calcula en el segundo intervalo los ingresos derivados de la venta de electricidad. Las herramientas MATLAB y YALMIP también se emplearon para implementar este modelo de optimización.

3. Un modelo detallado del campo solar de la planta objeto de estudio, implementado en MATLAB, que permite calcular la potencia térmica disponible a partir de la irradiancia solar directa (*direct normal irradiance*, DNI), que es el tipo de radiación solar aprovechable en la tecnología termosolar.

Empleando estos elementos como recursos iniciales, los trabajos que se han llevado a cabo son los siguientes:

1. Desarrollo de la estrategia de replanificación horaria. La nueva función objetivo contabiliza los ingresos derivados de la venta de electricidad en todo el horizonte y estima las penalizaciones provocadas por los desvíos en el intervalo de seguimiento. Se trata, por tanto, de una función objetivo con un enfoque totalmente económico. El nivel de penalización del desvío se emplea como parámetro de ajuste de la estrategia. Se supone la existencia de un predictor a corto plazo de la radiación solar con una precisión regulable.

2. Diseño de la estrategia anti-*cycling*. La nueva función objetivo incluye un mecanismo que penaliza los cambios en la producción. Además, este mecanismo penaliza de manera diferente, mediante el uso de variables binarias, las variaciones según el estado del bloque de potencia: operación normal, arranque y parada. De esta manera se consigue aumentar el número de grados de libertad del problema en busca de mejores soluciones. Los grados de penalización de las variaciones en operación normal, arranque y parada son los parámetros de ajuste de esta estrategia.

3. Desarrollo de la estrategia de replanificación horaria con anti-*cycling*. Se combinan las dos estrategias anteriores.

4. Desarrollo e implementación en MATLAB de una plataforma de pruebas para realizar las simulaciones a escala horaria que permitan evaluar el impacto económico de las estrategias. Las simulaciones abarcan un periodo de seis meses para las estrategias de replanificación horaria con y sin mecanismo anti-*cycling*, y de 12 meses para la estrategia anti-*cycling*. Se eligieron estos tamaños de los periodos de simulación con base en el tiempo de computación requerido por cada estrategia. La plataforma consta de los siguientes bloques:

    - Planificador de la producción. En este bloque están implementadas las tres estrategias de planificación. Cada estrategia lleva asociada una función de MATLAB que contiene el problema de optimización correspondiente, donde se definen la función objetivo y las restricciones operativas y de balance energético de la planta. De nuevo se emplea la herramienta YALMIP para el modelado del problema y su resolución.
    - Simulador de la planta para el análisis económico. La planta se representa mediante un problema de optimización basado en MILP que se ejecuta cada paso de simulación (una hora). Este problema recibe como datos de entrada la potencia térmica disponible en el campo solar y la consigna de producción establecida por el planificador. Presenta las mismas restricciones que los modelos MILP de las tres estrategias. El objetivo de mayor prioridad del problema es la reducción del error de generación, seguido de la maximización de la energía que se puede guardar en el almacenamiento térmico (*thermal energy storage*, TES). La herramienta YALMIP también se emplea para el modelado y resolución de este problema. El modelo detallado del campo solar se empleó para convertir valores reales de DNI en potencia térmica disponible, que es un dato de entrada para el modelo MILP de la planta, como se comentó anteriormente.
    - Predictor de la potencia térmica disponible en el campo solar. Este bloque tiene por objeto crear un escenario de predicciones realistas de la potencia térmica disponible en el campo solar. Se apoya en un conjunto de predicciones sintéticas de DNI, que se han generado buscando un valor anual del error cuadrático medio normalizado del 32 % para la predicción a un día, que es una valor encontrado en la literatura para una localización como el sur de España [4]. Finalmente, se empleó el modelo detallado del campo solar para convertir las predicciones de DNI en predicciones de potencia térmica disponible en el campo solar. Existe también la posibilidad de generar un escenario de predicción perfecta de la potencia térmica disponible.

- Predictor de precios de la electricidad. Este bloque genera un escenario realista de predicciones para el precio de la electricidad. También se basa en conjunto de predicciones sintéticas, que se han generado para obtener un valor medio anual del error cuadrático medio de 2.7 €/MW h para la predicción a un día, valor orientativo encontrado en la literatura [5]. También es posible generar un escenario de predicción perfecta de pecios.
- Proveedor de valores reales de DNI, precios de la electricidad y costes de penalización por desvío de la producción. Los valores reales de DNI se han obtenido a partir de un conjunto de medidas de radiación solar procedentes de una planta fotovoltaica cercana a la localización en cuestión. Los datos económicos fueron tomados de las paginas web del Operador del Mercado Eléctrico [6] y del Operador del Sistema Eléctrico en España [7] para el año 2013.

5. Análisis del impacto económico de las tres estrategias. Se realizaron varias simulaciones por cada estrategia, haciendo un barrido de los valores de los parámetros de ajuste de cada una de ellas. Como referencia para la comparación se empleó una estrategia básica de planificación, esto es, sin replanificación ni mecanismo anti-*cycling*.

2.2. Resultados y discusión

A continuación se indican los principales resultados obtenidos tras la realización de las simulaciones. Una estrategia básica de planificación, esto es, sin replanificación ni mecanismo anti-*cycling*, se empleó como referencia para realizar las comparaciones.

La estrategia de replanificación horaria se aplicó en el periodo 01/01/2013 a 30/06/2013. Para este análisis se supuso una predicción perfecta de precios. De los resultados se pueden extraer las siguientes conclusiones:

1. La estrategia de replanificación horaria mejora los resultados económicos de la estrategia de referencia, incluso cuando no se utiliza ninguna predicción a corto plazo de la radiación solar.

2. La precisión y el alcance de la predicción a corto plazo de la radiación solar mejoran los resultados económicos de la estrategia de replanificación horaria.

3. La mejora económica es más significativa en periodos de baja precisión en la predicción de radiación solar. Concretamente, la mejora de los beneficios económicos respecto a la estrategia de referencia se sitúa en torno a un 7 % el mes de Marzo.

4. En relación a la máxima mejora posible, obtenida si se considerasen predicciones perfectas del recurso solar y los precios, se observan mejoras económicas que oscilan entre un 13.9 % y un 33.3 %, según la precisión de la predicción a corto plazo.

5. El nivel de penalización aplicado a los desvíos en la estrategia (parámetro de ajuste) puede basarse en los valores de los costes de penalización del año anterior. Se comprobó que esta estimación ofrece buenos resultados.

La estrategia anti-*cycling* se aplicó en el periodo 01/01/2013 a 31/12/2013, considerando predicciones imperfectas de precios de la electricidad y radiación solar. Analizando los resultados se pueden extraer las siguientes conclusiones:

1. La solución óptima presenta poca sensibilidad a variaciones de alta frecuencia en el perfil de generación, lo que favorece la aplicación de esta estrategia.
2. Se observan importantes reducciones de las variaciones de la generación (hasta cerca de un 70 % en la media del incremento horario en valor absoluto de la generación eléctrica en operación normal), sin afectar los beneficios económicos.
3. El comportamiento de la estrategia es similar cuando se emplean predicciones perfectas del recurso solar, indicando cierta independencia frente a la precisión de las predicciones.
4. Se propone un método basado en datos históricos para estimar el nivel de penalización que permita minimizar las variaciones de la generación sin influir en los beneficios económicos
5. Otro beneficio observado es la reducción de los desvíos respecto al plan comprometido, un aspecto positivo que simplificaría la tarea del Operador del Sistema Eléctrico

La estrategia de replanificación horaria con anti-*cycling* se aplicó en el periodo 1/01/2013 a 30/06/2013, considerando predicciones imperfectas de precios de la electricidad y radiación solar. Esta estrategia aplica el mecanismo de penalización de las variaciones tanto en la síntesis del plan de generación para el día siguiente como en el seguimiento del plan actual.

De los resultados se pueden extraer las siguientes conclusiones:

1. La inclusión de un término de penalización de las variaciones en la estrategia de replanicación horaria proporciona buenos resultados al reducir el porcentaje de variaciones (hasta cerca de un 60 % en la media del incremento horario en valor absoluto de la generación eléctrica en operación normal) sin empeorar los resultados económicos obtenidos, empleando esta vez la estrategia de replanificación horaria sin anti-*cycling* como referencia.
2. El rendimiento económico de la estrategia de replanificación horaria con anti-*cycling* es superior al de la estrategia simple con anti-*cycling*, como era de esperar.
3. Al igual que lo deducido tras los resultados de la estrategia anti-*cycling*, el comportamiento con predicción perfecta del recurso solar es similar al observado con predicción imprecisa, y el nivel de penalización que minimiza las variaciones y mantiene los beneficios económicos puede estimarse con datos históricos.

2.3. Conclusiones generales

En esta Tesis se han propuesto varias estrategias de planificación óptima de la producción para plantas termosolares con almacenamiento térmico. Además se han realizado varios estudios del rendimiento económico resultante tras aplicar dichas estrategias. Los estudios se han basado en simulaciones realistas de distintos escenarios climáticos y de mercado.

Se ha diseñado una plataforma de simulación que permite estudiar el impacto económico de los sistemas de planificación propuestos. La plataforma incluye el planificador de la producción, un simulador de la planta termosolar e información realista sobre el recurso solar, los precios de la electricidad, las penalizaciones económicas por desvío y las predicciones de todos estos datos. La plataforma permite la simulación de las estrategias de planificación a lo largo de todo un año de producción con el fin de estudiar el impacto de condiciones climáticas y de mercado diferentes.

Se ha empleado una formulación del problema de planificación óptima basada en la programación lineal entera mixta. La formulación de dicho problema utiliza predictores de recursos solares y precios de venta de electricidad para obtener los datos necesarios en la optimización. La función de coste refleja el objetivo buscado por la estrategia de planificación correspondiente. Un conjunto de restricciones de igualdad y desigualdad se utilizan para modelar las conversiones energéticas y la operativa realizada en el proceso de producción de la planta.

Con el fin de atenuar la incertidumbre presente en el modelo de optimización y en las predicciones de radiación solar y precios de venta de la electricidad, se ha formulado una estrategia de replanificación horaria basada en ventana deslizante (inspirada en la estrategia usada por el control pedictivo basado en modelo). La replanificación horaria tiene como objetivo repartir los desvíos respecto a la producción comprometida de la forma más beneficiosa económicamente, considerando la nueva información disponible cada hora.

Se han diseñado dos estrategias de planificación de la producción orientadas a aumentar la vida útil de los elementos del bloque de potencia, a reducir los costes de mantenimiento y a facilitar la operabilidad de la planta, pero sin disminuir los beneficios por venta de electricidad. Estas estrategias incluyen un método de penalización de las variaciones no necesarias en la producción. La diferencia entre estas dos estrategias propuestas es la inclusión o no de la replanificación horaria.

Se han realizado varios estudios del impacto económico de las diferentes estrategia de planificación propuestas usando la plataforma de pruebas diseñada. Se ha usado como referencia para la comparación una estrategia básica de planificación (sin replanificación y sin penalización de variaciones). Los estudios confirman las mejoras esperadas en cada una de las estrategias de planificación desarrolladas.

2.4. Trabajos futuros

A continuación se enumeran algunas líneas de investigación que podrían dar continuidad a la investigación iniciada con esta Tesis. Algunas de estas líneas ya se han iniciado, como se puede apreciar en la lista de publicaciones en congresos nacionales (Sección 1.2 del Capítulo 1).

- Proponer nuevas estrategias de planificación orientadas a disminuir la energía desenfocada. La planificación orientada a precios de venta genera un incremento de la energía desenfocada y, por tanto, no convertida en electricidad. El objetivo de esta línea sería plantear una nueva estrategia de planificación que sin empeorar los resultados económicos minimice la energía no aprovechada.
- Obtener modelos empíricos del campo solar e integrarlos en la estrategia de planificación. La obtención de modelos empíricos simplifica enormemente la tarea de modelado del comportamiento de la planta termosolar.
- Estudiar técnicas de programación estocástica y optimización robusta en la estrategia de replanificación. El objetivo es modelar la incertidumbre presente en los modelos para obtener mejores resultados económicos y garantizar un mínimo de beneficios.

Capítulo 3

Antecedentes

En este capítulo se lleva a cabo una introducción a los sistemas y tecnologías que tienen relación con los trabajos de la Tesis, junto con una descripción del problema abordado.

En primer lugar, en la Sección 3.1, se realiza una introducción al sistema eléctrico, donde se indican las distintas entidades que lo constituyen y las funciones que desempeñan. El mercado eléctrico y sus tipos son descritos brevemente en la Sección 3.1.1. La Sección 3.1.2 se dedica a las tecnologías de energías renovables, como partes integrantes del sistema eléctrico. Se abordan aspectos como su desarrollo, despliegue y evolución de costes, con el fin de dar una idea global sobre su estado actual y futuro.

En la Sección 3.2 se realiza una introducción a las plantas termosolares. Se expone una breve descripción del funcionamiento de esta tecnología y las características más importantes. También se describen sus tipos y los componentes fundamentales de esta clase de plantas.

El método empleado en esta Tesis para resolver el problema de planificación de la producción en plantas termosolares se basa en la programación lineal entera mixta, por lo que en la Sección 3.3 se ofrece una introducción a este tipo de problema de optimización, donde se exponen las características que se reflejan en su formulación y los enfoques de resolución existentes.

Algunas de las estrategias de planificación propuestas en esta Tesis están inspiradas en el control predictivo basado en modelo. En la Sección 3.4 se describe con brevedad este tipo de control, se realiza un breve recorrido sobre su desarrollo y se indican sus principales ventajas e inconvenientes.

En la Sección 3.5 se aborda el problema de la planificación de la producción en sistemas eléctricos, con especial énfasis en plantas termosolares, describiéndose los dos enfoques aplicables a este tipo de problemas. Finalmente, en la Sección 3.5.1 se exponen las características del tipo de problema de planificación abordado en esta Tesis: la planificación de la producción de una planta de energía solar por concentración (*concentrating solar power*, CSP) en el mercado diario de la electricidad desde un punto de vista de tomador de precios. Al final de esta sección se indica la estrategia de planificación empleada en esta Tesis como referencia para realizar la comparación con las estrategias propuestas.

3.1. El sistema eléctrico

El sistema eléctrico español está compuesto por la infraestructura que permite la generación, el transporte, la distribución y el consumo de la electricidad, y por un mercado eléctrico que define su funcionamiento, determinando quién produce, cuánto, cuándo y a qué precio.

La potencia de los sistemas de generación eléctrica puede variar desde unos pocos kW (por ejemplo, pequeñas instalaciones fotovoltaicas) hasta varios GW (por ejemplo, plantas nucleares o de carbón). Además, los sistemas de generación eléctrica se pueden clasificar según su flexibilidad de operación (producción fija o ajustable) y según la fuente de energía empleada (no renovable o renovable). También se pueden clasificar en generadores de

capacidad firme, es decir, aquellos cuya generación no se ve alterada por factores externos, y en generadores de capacidad variable, cuya generación depende de factores no controlables, como el viento o el sol [8].

El sistema eléctrico es gestionado por el Operador del Sistema (*Transmission System Operator*, TSO), que es una entidad encargada de la planificación, operación y mantenimiento del sistema eléctrico. En España, el TSO es Red Eléctrica de España (REE) [7]. Por otro lado, el Operador del Mercado (*Market Operator*, MO) es el encargado de gestionar el mercado eléctrico bajo criterios económicos. Su principal función es la casación entre oferta y demanda, para obtener precios y cantidades de energía intercambiada. En la Península Ibérica, el operador del mercado mayorista es OMIE (Operador del Mercado Ibérico de Energía) [6].

Un aspecto importante a tener en cuenta en los sistemas eléctricos es el equilibrio entre la oferta y la demanda. Debido a las dificultades de almacenamiento de la electricidad, la casación entre ambas se obtiene principalmente variando la producción de las unidades generadoras. Las unidades fijas proporcionan la denominada potencia base, mientras que los generadores ajustables satisfacen los picos de demanda [8].

3.1.1. Mercados eléctricos

La desregularización de los sistemas eléctricos dio comienzo a finales de los años ochenta a nivel mundial, y a mediados de los años noventa en la Unión Europea [6]. Uno de sus objetivos fue la reducción de complejidades e ineficiencias asociadas con la toma centralizada de decisiones [9]. En estos sistemas, la electricidad se comercializa de manera competitiva, con la gestión generalmente realizada por entidades privadas [10; 11; 12]. Los agentes del mercado eléctrico son los distintos productores, vendedores y grandes consumidores.

Tipos de mercados

Una primera clasificación del mercado eléctrico puede hacerse en minorista y mayorista. El mercado minorista se centra en la relación entre proveedores y consumidores. Los proveedores compran electricidad a los productores y la venden a los consumidores. En el mercado mayorista, los participantes son los productores, los proveedores y los grandes consumidores. Estos mercados operan a nivel transnacional. Para la Península Ibérica, OMIE es el operador del mercado mayorista.

Debido a que la electricidad se tiene que producir cuando se necesita, las compra-ventas de electricidad se refieren siempre a una entrega que ocurrirá en el futuro. En función de las características temporales de las transacciones, existen varios tipos de mercado mayorista [11; 6]:

- mercados de futuro: transacciones para horizontes de medio a largo plazo, con rangos típicos de semanas hasta años.
- mercado diario: transacciones para las 24 horas del día siguiente.

- mercado intradiario: complementa al mercado diario; la energía se tiene que entregar dentro de un periodo de tiempo especificado, típicamente varias horas desde el fin de la sesión.
- mercado de balance o de servicios de ajuste: en este mercado la entrega se tiene que hacer en tiempo real (el horizonte temporal de los servicios de ajuste es desde 20 segundos hasta 15 minutos [7]) .

El mercado diario

Los mercados diarios son mercados al por mayor (también llamados "al contado", o mercados "spot"). En estos mercados, los productores indican los precios a los que están dispuestos a vender la electricidad que pueden generar, típicamente el día anterior. Sus ofertas indican, para cada hora del día, cantidades de energía que pueden entregar al mercado, y los precios asociados a cada cantidad. De igual forma, los compradores entregan sus ofertas de compra, basadas en la misma estructura. El Operador del Mercado acepta ofertas de compra hasta alcanzar las demandas esperadas para cada hora, en orden creciente de precios. Los precios del mercado y volúmenes de energía para cada hora se obtienen empleando un algoritmo de uso común en todos los mercados europeos llamado *Euphemia*, obteniendo planes de producción para los distintos generadores.

De forma simplificada, el precio de compra/venta del mercado es el máximo de todas las ofertas aceptadas, o el mínimos de las demandas aceptadas [13]. En el mercado diario europeo, que incluye al español, los precios son fijados diariamente a las 12:00 horas, para las 24 horas del día siguiente [6].

En un último proceso se consideran restricciones de transmisión y limitaciones de las unidades generadoras (por ejemplo, condiciones complejas de las ofertas como gradientes de carga o ingresos mínimos) [6], que pueden resultar en pequeños ajustes de los planes obtenidos del mercado, tanto en potencias generadas como en precios finales de la electricidad.

El mercado intradiario

En el mercado intradiario, los agentes del mercado pueden ajustar el programa resultante del mercado diario mediante nuevas ofertas de compra/venta de energía. Este mercado se estructura en varias sesiones de subastas donde se presentan ofertas adaptadas a las necesidades del mercado observadas en tiempo real. En el mercado Ibérico, existen seis sesiones diarias para este mercado, cada una con distintos horizontes temporales (de 12 hasta 28 horas [6]).

Al igual en el mercado diario, en el mercado intradiario las ofertas presentadas pueden incluir condiciones complejas, como límites a los gradientes de carga y a la energía disponible. La casación de las ofertas de compra y venta de energía se realiza mediante un proceso iterativo, que asegura el cumplimiento de todas las condiciones de las ofertas aceptadas, además de las restricciones del sistema eléctrico [6].

Mercado de servicios de ajuste

El mercado de servicios de ajuste asegura el balance entre la oferta y la demanda mediante las distintas reservas disponibles. Estos servicios se ofrecen principalmente por los productores (también pueden ser ofrecidos por consumidores mediante reducción de su consumo) a través de una serie de mercados organizados por el Operador del Sistema [7]. Las actuaciones realizadas se centran en resolver congestiones en la red, control de frecuencia y tensión, reservas de potencia y gestión de desvíos [14].

3.1.2. Energías renovables

Las tecnologías renovables están en un continuo proceso de desarrollo y despliegue. Actualmente, a nivel mundial, las aportaciones de las fuentes renovables en el consumo de energía siguen siendo bastante reducidas. Sin embargo, debido al rápido agotamiento de los combustibles fósiles [15; 16], a la necesidad de reducir la dependencia energética mejorando la producción nacional [17], y a la aceleración del calentamiento global, existe un gran impulso a nivel mundial para el desarrollo de estas fuentes [18; 19].

Las energías renovables tienen varias ventajas. Son prácticamente inagotables, no contaminan y están disponibles en todo el planeta. Sin embargo, suelen presentar intermitencias importantes en la producción y elevados costes de inversión [19].

El problema de la intermitencia en la producción se puede afrontar mediante el uso de plantas híbridas o la inclusión de sistemas de almacenamiento energético [20]. Las plantas de generación híbrida combinan varias fuentes de generación. Pueden aprovechar los recursos renovables cuando estén disponibles y producir energía usando otras fuentes renovables (como biocombustibles) o no renovables, en ausencia de la fuente renovable intermitente. Por otro lado, las distintas tecnologías de almacenamiento energético son de gran interés en el ámbito de las energías renovables ya que permiten almacenar la energía sobrante y desplazar la producción, mejorando la gestionabilidad del sistema de generación [21].

En cuanto al despliegue de las tecnologías renovables, en 2017, la potencia eléctrica total instalada a nivel global alcanza 2179 GW [22]. El porcentaje del consumo global de energía primaria que proviene de fuentes renovables alcanzó el 3.6 % en 2017 (sin contar la energía hidráulica), un valor bastante bajo, aunque en un proceso de crecimiento importante [16]. Muchos países están planificando una producción energética con una gran parte basada en energías renovables. Existen estudios que apuestan por una generación 100 % renovable [23; 24; 25].

Energía fotovoltaica

Las tecnologías fotovoltaicas (*PhotoVoltaic*, PV) se han desarrollado ampliamente en los últimos años. La reducción de costes de producción debido a la economía de escala, mejoras de los procesos de producción, la existencia de cadenas de suministro competitivas a nivel global, o la existencia de proyectos internacionales experimentales han tenido como resultado importantes reducciones de costes, haciendo que la tecnología PV sea cada vez

más rentable. Conforme con el informe de IRENA [26], en los proyectos a escala comercial basados en tecnología PV los costes han bajado un 73 % desde 2010. Considerando los costes medios de generación eléctrica (*levelized cost of electricity*, LCOE), la tecnología PV llega a 0.10 $/kWh[1] para proyectos encargados en 2017. Los costes de los módulos PV han bajado un 81 % en el mismo periodo, haciendo que esta tecnología sea cada vez más rentable. La media global de los costes totales de instalación de sistemas fotovoltaicos ha bajado un 68 % entre 2010 y 2017.

Energía eólica

Las tecnologías eólicas han experimentado un crecimiento importante en los últimos años. Se trata de una tecnología madura y de costes de inversión relativamente bajos, lo que la hace atractiva para muchos lugares en el mundo. Los proyectos eólicos en tierra han tenido una disminución de costes del 23 % en el periodo 2010-2017. Esta disminución se debe sobre todo a la reducción de los precios de las turbinas, que han bajado entre un 39 % y un 58 % (dependiendo del mercado). En los proyectos encargados para 2017, el coste de la energía eléctrica eólica marítima llega a valores LCOE de 0.14 $/kWh, mientras que el LCOE para proyectos eólicos en tierra ronda los 0.06 $/kWh, con precios de subastas para proyectos eólicos en tierra llegando a valores de 0.03 $/kWh [26].

Energía hidroeléctrica

La hidroelectricidad, aunque continúa generando electricidad a precios muy bajos, ha sufrido una subida de costes medios, con LCOE aumentando desde 0.036 $/kWh en 2010 a 0.046 $/kWh para proyectos a gran escala encargados en 2017. Este aumento se debe a que la cantidad de emplazamientos idóneos para proyectos hidroeléctricos disponibles está bajando, por lo que los nuevos proyectos se vuelven más desafiantes, con más costes de ingeniería y de desarrollo del proyecto [26].

Energía solar por concentración

La energía solar por concentración (*concentrating solar power*, CSP) permite transformar la energía solar en electricidad empleando distintas tecnologías que permiten obtener altas temperaturas mediante elevados niveles de concentración de la radiación solar sobre un elemento receptor. Una ventaja de esta tecnología es el almacenamiento térmico (*thermal energy storage*, TES), que permite almacenar la energía procedente del campo solar de forma eficiente y económicamente viable, haciendo que este tipo de plantas presenten cierto grado de gestionabilidad, es decir, tienen la posibilidad de ajustar su producción de electricidad bajo demanda [27]. Esto permite optimizar la producción de la planta, de tal forma que la generación eléctrica se concentre en horas de precios altos. De esta forma, aunque el TES aumenta el coste de la planta, el desacople entre la disponibilidad de energía solar y la producción permite aumentar el rendimiento económico de la planta [28].

[1] $ se refiere a dólar estadounidense

El almacenamiento térmico es una solución de bajo coste comparada con las otras alternativas de almacenamiento (25-75 €/kWh-el, eficiencia >95 %), con costes menores incluso que el almacenamiento hidroeléctrico por bombeo (70 €/kWh-el, eficiencia <80 %), y bastante menores que el almacenamiento por baterías (>147 €/kWh-el) [29; 30].

El precio de la energía eléctrica para nuevos proyectos con tecnología CSP ha bajado un 33 % desde 2010, desde 0.27 $/kWh en 2016 a un LCOE estimado de 0.22 $/kWh en 2017. Además, se esperan nuevas bajadas de precios para esta tecnología [19; 31].

3.2. Plantas termosolares

Las tecnologías CSP emplean espejos o lentes para conseguir una alta concentración de radiación solar sobre una pequeña superficie receptora, produciendo el calentamiento de una sustancia, generalmente un fluido (fluido caloportador, *heat transfer fluid*, HTF). Esta energía térmica se transforma en energía mecánica mediante un ciclo termodinámico. Normalmente, una turbina de vapor se acopla a un generador eléctrico para realizar la conversión a energía eléctrica.

La principal ventaja de la tecnología CSP es la posibilidad de almacenar temporalmente la energía térmica, para ser usada posteriormente en la generación de electricidad. De esta forma se consigue desacoplar la producción de la planta de las intermitencias de la fuente solar, permitiendo la producción durante periodos nublados o por la noche [20]. La integración del almacenamiento térmico hace que las tecnologías CSP sean semi-gestionables (no completamente gestionables porque la capacidad de almacenamiento es finita). El bloque de potencia es totalmente compatible con el uso de otras fuentes de energía térmica, como biocombustibles o combustibles fósiles. De esta forma se pueden obtener plantas híbridas totalmente gestionables, que aprovechan la energía solar. Por ejemplo, las plantas termosolares de España obtienen entre un 12 y un 15 % de su generación de potencia a base de gas natural [32]. Por otra parte, sólo 50 plantas - circa 40 % - incorporan almacenamiento térmico [33]. En estos casos, se suelen usar combustibles convencionales como fuente de energía adicional para producir electricidad cuando la radiación solar es insuficiente o no está disponible [18; 34; 35].

La conversión de la energía térmica en energía eléctrica se realiza mediante ciclos termodinámicos de alta eficiencia, que son bien conocidos en la industria de la generación eléctrica al no ser específicos para la tecnología CSP [36; 37]. Algunos estudios estiman que las plantas CSP podrían producir un 7 % de la energía eléctrica mundial para el año 2030, y un 25 % para 2050 [38]. Con altos niveles de eficiencia energética y desarrollo industrial avanzado, las tecnologías CSP podrían cubrir un 6 % de la demanda energética global para 2030, y un 12 % para 2050 [20]. Además de la producción de electricidad, las tecnologías CSP tienen un gran potencial en la generación de empleo y reducción de CO_2 a escala global [39].

Uno de los factores que condicionan la rentabilidad de las plantas CSP es la cantidad de irradiación solar directa (*direct normal irradiance*, DNI) recibida en una ubicación determinada a lo largo del año. Normalmente se considera que los niveles de DNI para las plantas CSP comerciales deben estar en el rango 2000-2800 kWh/m^2/año para que las plantas sean rentables [40].

3.2.1. Tipos de plantas

Los concentradores solares se dividen, en función de la geometría de enfoque y tecnología receptora, en cuatro tipos, que pueden verse en la Figura 3.1: las de cilindro parabólico, de torre central, de reflectores basados en lentes de Fresnel y de disco parabólico. Cada una de las tecnologías CSP difiere en aspectos fundamentales como sus dimensiones, la potencia que pueden generar, sus rendimientos óptico y térmico, y su coste [41].

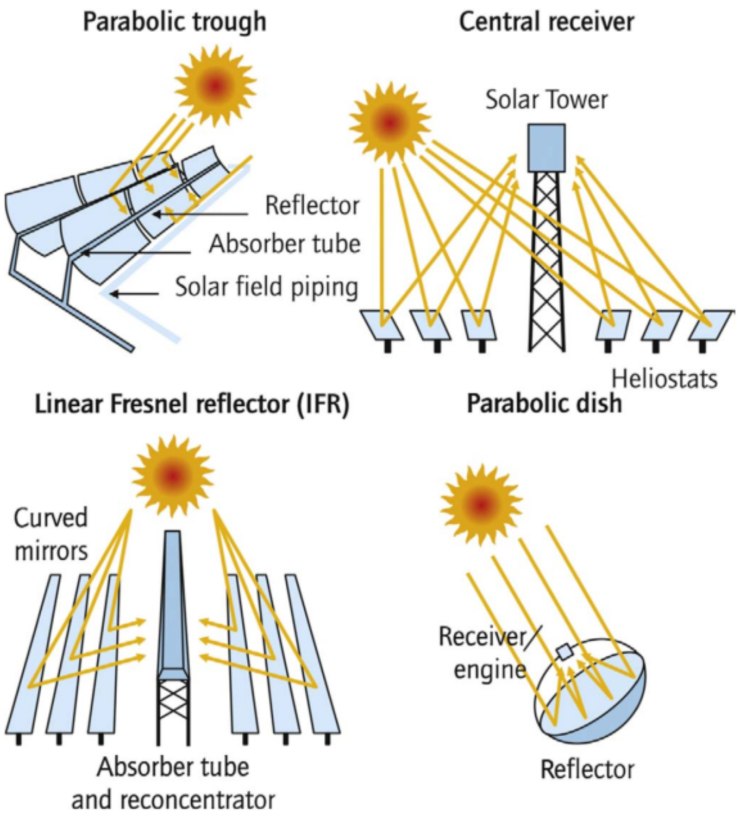

Figura 3.1: *Tipos de tecnologías CSP - de [42].*

Concentrador de tipo cilindro parabólico

Los concentradores de tipo cilindro parabólico (*parabolic trough collector*, PTC) se presentan como una alternativa a los de tipo torre, al ser también una tecnología que permite la generación de electricidad a escala comercial, además de ser una tecnología que puede ser usada en otras aplicaciones como enfriamiento solar, calentamiento industrial o desalinización [43]. Es una tecnología madura, con gran experiencia de operación y facilidad de acoplamiento con combustibles fósiles y otras fuentes de energía renovable, como la biomasa [42; 44; 45]. Este tipo de concentrador presenta una estructura modular, simple de instalar, lo que ofrece flexibilidad y escalabilidad. Mediante la interconexión de varios módulos se pueden obtener grandes potencias instaladas, aunque hay limitaciones en cuanto al tamaño del campo solar debido a las pérdidas de presión y a las pérdidas térmicas en el transporte del fluido caloportador en el campo solar.

Los receptores tipo PTC convencionales consisten de una sección parabólica de cilindro, un receptor cilíndrico lineal y una estructura de soporte metálica. El seguimiento del sol se realiza con un mecanismo de un solo eje. Normalmente, el campos solar está formado por varios lazos de colectores conectadas en paralelo. Los lazos están constituidos por varios módulos conectados en serie. Las longitudes típicas de los módulos son de unos 10 m, con un ancho de apertura de hasta 10 m [46; 47], y 10-15 módulos conectados en serie para formar un bucle. El receptor se compone de un tubo (generalmente de metal) dentro de un encapsulado de vidrio evacuado con un recubrimiento selectivo, haciendo que tenga una elevada absorbancia y una baja emisividad [48; 43]. Con niveles de concentración de 70-100 soles (1 sol = 1 kW/m^2), las temperaturas de trabajo suelen estar en el rango 350-550ºC, alcanzando una eficiencia anual solar-a-electricidad del 15 % [41; 32; 49].

El fluido caloportador puede ser un aceite sintético, sal fundida, o agua, que fluye por el tubo receptor térmico para absorber la energía térmica de la radiación solar concentrada para transferirla al generador de vapor o al sistema de almacenamiento térmico, si lo hubiera [50]. La mayor parte de los sistemas cilindro-parabólico existentes usan aceites sintéticos como HTF [51; 52], que son estables hasta 400ºC, limitando la eficiencia alcanzable del motor térmico a 38 %. Sales fundidas a 540 ºC se han empleado para la transferencia de calor en el campo solar en nuevas plantas de demostración y como medio de almacenamiento térmico en plantas comerciales [34; 53].

Concentrador de tipo torre

La tecnología de tipo torre (*solar power tower*, SPT) emplea espejos planos cuya orientación es controlada en dos ejes, permitiendo seguir el movimiento del sol para enfocar la radiación solar en el receptor ubicado en lo alto de una torre central [54]. La tecnología de torre permite obtener niveles muy altos de concentración solar (entre 300 y 1500 soles) y temperaturas de trabajo elevadas (hasta 1500ºC). La eficiencia anual solar-a-electricidad es del 20 %, con posibilidades de alcanzar el 35 % [41; 32; 49]. Como fluidos de trabajo, en los sistemas CSP de tipo torre se suelen emplear agua/vapor, sales fundidas, sodio líquido

o aire [41; 55]. Como todas las tecnologías CSP, permite la operación híbrida empleando fuentes de calor renovables o no renovables [56].

El rango de potencias de las plantas CSP-SPT es de 10-150 MW [41; 57; 35]. Actualmente a nivel mundial hay alrededor de 580 MW de tecnología SPT activos, con más de 700 MW en construcción, y 1550 MW en proyectos en desarrollo [58]. Si bien algunas de las plantas activas o en construcción no incluyen TES, para las plantas en desarrollo el almacenamiento térmico está incluido en todas ellas [58].

Concentrador de tipo Fresnel

Los concentradores lineales de tipo Fresnel (*linear Fresnel reflector*, LFR) utilizan un sistema que se aproxima a los colectores de tipo cilindro parabólico mediante el uso de espejos planos o ligeramente curvados para reflejar los rayos solares hacia un receptor lineal. Los espejos son orientados de forma individual para realizar el seguimiento del sol y reflejar la radiación solar sobre el elemento receptor. El receptor suele ser un tubo evacuado, con un concentrador secundario situado en la parte superior [59].

La principal ventaja de este sistema es su diseño simple, y el hecho de que los elementos receptores son fijos. [59]. El receptor fijo facilita la generación directa de vapor, eliminando la necesidad de fluidos de transferencia de calor y de intercambiadores de calor. Sin embargo, esta tecnología tiene niveles de concentración bajos, de 10-70 soles, y temperaturas de trabajo de 250-400ºC [59; 60], obteniendo eficiencias anuales solar-a-electricidad estimadas del 8-10 % [41; 49]. Además, la incorporación de TES en este tipo de planta es más difícil [61]. Las capacidades típicas para las plantas CSP-LFR son de 10-200 MW [41; 49].

Concentrador de tipo disco parabólico

El concentrador de tipo disco parabólico (*solar power dish*, SPD) consigue obtener los más altos niveles de concentración de la radiación solar. Este tipo de concentrador se orienta directamente hacía el sol, por lo que la orientación del reflector se tiene que hacer en dos ejes. Los diámetros típicos de los concentradores son de 5-10 m, con superficies reflectantes de 40-120 m^2. La capacidad de generación típica de los generadores CSP de este tipo está en el rango 5-50 kW [62; 63].

Típicamente, el rango de concentración de estos dispositivos es de 600-2000 soles, permitiendo alcanzar temperaturas superiores a los 1500 ºC [57]. Las temperaturas del fluido de trabajo son de unos 700-750 ºC, y presiones de 200 bar [18; 64; 65]. Las eficiencias de conversión de energía solar a eléctrica de las tecnologías SPD son de entre 25 % y 30 % [63; 66], siendo el récord de eficiencia de 31.25 % [67].

La conversión de energía térmica a electricidad se suele realizar mediante ciclos Stirling, con el motor normalmente ubicado en el punto focal del concentrador. Las ventajas de esta tecnología son el enfriamiento seco, su tamaño reducido (alta modularidad) y la posibilidad de funcionar con otra fuente de calor distinta a la solar. Sin embargo, su LCOE es el más alto

de las tecnologías CSP, y tiene dificultad en incorporar TES [34]. Las altas temperaturas de trabajo permiten alcanzar altas eficiencias de conversión a energía eléctrica, pero el elemento receptor térmico sufre importantes choques térmicos. La existencia de partes móviles en el motor térmico genera desgaste y necesidad de mantenimiento del mismo. El sistema de movimiento en dos ejes del espejo concentrador es complejo y limita las dimensiones máximas de este tipo de reflector. La fabricación del espejo parabólico es tecnológicamente compleja debido a sus dimensiones, y la precisión y durabilidad requeridas.

Varios sistemas de tipo parabólico se han construido hasta la fecha, sobre todo con fines demostrativos de la tecnología [63], pero actualmente pocas plantas están en operación [67].

3.2.2. Principales componentes de la tecnología termosolar

El campo solar

El campo solar es el elemento de la planta que recibe y concentra la radiación solar. En las tecnologías cilindro-parabólico y tipo Fresnel, el campo solar está formado por los espejos reflectores, los receptores solares y el fluido caloportador, mientras que para la tecnología de tipo torre central, se considera el campo solar solamente a los helióstatos y al sistema de bombeo, siendo la torre central y el receptor elementos distintos [68].

En las tecnologías CSP más desarrolladas, PTC y SPT, el campo solar es el bloque con mayor coste de inversión, con porcentajes del 46 % y 42 % respecto al coste total de inversión, respectivamente [29; 68]. El coste de los bloques de potencia es el 21 % para PTC y 20 % para SPT. Los costes del almacenamiento térmico son del 12 % para PTC, frente al 6 % para SPT. Otro coste importante para la tecnología SPT es la torre central, cuyos costes ascienden al 16 % de la inversión.

Los espejos deben tener una reflectividad muy alta para evitar perdidas. La calidad de construcción de las mismas es fundamental para asegurar una concentración adecuada de la radiación solar. Además, tienen que mantener sus características durante el tiempo de vida de la planta.

El receptor de la energía concentrada es uno de los principales elementos de estas tecnologías, ya que permite pasar la energía solar al fluido caloportador en forma de calor, para su posterior uso. Las características de estos elementos tienen un impacto importante en la eficiencia de la planta, ya que determina qué cantidad de la energía concentrada es absorbida. El tipo de fluido caloportador (de tipo líquido, gas o de dos fases) y la temperatura de funcionamiento considerada determinan las características generales de la planta, y también el tamaño de los principales componentes, como el receptor o el almacenamiento térmico. En el receptor solar, la transferencia de calor hacia el fluido caloportador se hace de forma indirecta; la radiación solar calienta el receptor, mientras que el HTF lo enfría, absorbiendo la energía térmica. El flujo del fluido se controla de tal forma que este alcance la temperatura deseada, y también para que la superficie del receptor térmico no aumente demasiado, ya que eso haría incrementar innecesariamente las pérdidas térmicas en el mismo. Para obtener el mejor funcionamiento, se tiene que obtener un buen coeficiente de transferencia de calor entre el fluido y la superficie del

receptor, y también una alta conductividad térmica del material del receptor. Para las tecnologías PTC y LFR, un tipo de receptor simple y frecuentemente empleado es un receptor de tipo tubo, cuyo diseño está inspirado en las calderas convencionales [46; 59]. En las plantas de tipo SPT, el receptor está situado en lo alto de una torre central. Suele estar hecho de materiales cerámicos, para resistir las altas temperaturas de funcionamiento que puede alcanzar [54].

El fluido caloportador fluye a través del receptor térmico para absorber la energía térmica de la radiación solar concentrada, y luego transferirla al generador de vapor o al sistema de almacenamiento térmico. La elección de este fluido es un factor determinante del tipo de tecnología CSP a emplear, ya que sus características indican la tecnología de concentrador a usar y el tipo de almacenamiento térmico adecuado. Los aceites sintéticos son un tipo de interés, al tener un buen coeficiente de transferencia de calor, siendo capaces de soportar temperaturas de hasta 400ºC, y teniendo temperaturas congelación de unos 15ºC. Este tipo de HTF es el más empleado en las plantas de tipo cilindro parabólico [51; 52]. Para temperaturas superiores a 400ºC se pueden emplear sales fundidas, pero tienen la desventaja de tener puntos de congelación elevados (típicamente entre 120 y 220ºC) [69; 70; 71]. Otras alternativas son el vapor de agua y el aire [41; 55].

Sistemas de almacenamiento térmico

La integración de TES en plantas de tipo CSP permite obtener un funcionamiento semi-gestionable de la planta. Las características deseadas son una alta capacidad de almacenamiento, un coeficiente de transferencia de temperatura elevado para facilitar una rápida carga y descarga de energía, y una buena estabilidad para evitar la degradación del material debido al estrés químico y mecánico [72].

La energía térmica puede ser almacenada mediante tres mecanismos: almacenamiento por calor sensible (mediante aumento/disminución de la temperatura), almacenamiento por calor latente (cambio de fase) y almacenamiento químico [72]. La cantidad de calor almacenada mediante calor sensible es una función del producto entre la masa, la capacidad calorífica y la variación de temperatura del material de almacenamiento [70]. Este tipo suele emplear sólidos y líquidos como material de almacenamiento, siendo el estado líquido el más utilizado [73; 70; 74]. Las sales fundidas son la solución más empleada en plantas comerciales [70; 71]. Si bien el almacenamiento mediante calor latente o el almacenamiento químico permiten densidades energéticas mucho mayores que el almacenamiento mediante calor latente, entre otras ventajas, también presentan inconvenientes importantes, por lo que su uso se centra actualmente en la investigación [70; 72].

Los sistema TES pueden ser activos o pasivos [75] (ver Fig. 3.2). En los sistemas activos el medio de almacenamiento fluye para realizar la carga o descarga de energía térmica, mientras que en los sistemas pasivos el medio de almacenamiento es inmóvil y el calor le es transferido haciendo circular otro fluido que hace la función de fluido caloportador (Fig. 3.2, (d)). El calor se transfiere mediante convección forzada.

Los sistemas activos a su vez pueden ser directos - cuando el medio de almacenamiento también sirve de fluido caloportador en el campo solar (Fig. 3.2, (a)), o indirectos - cuando

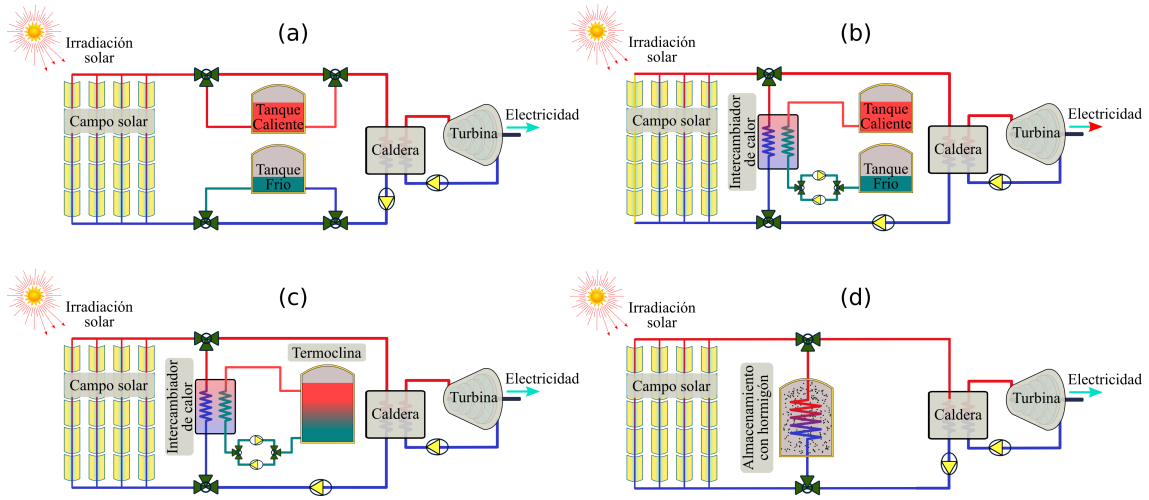

Figura 3.2: *Tipos de sistemas TES. (a) - Sistema activo directo; (b) - Sistema activo indirecto; (c) Sistema activo indirecto de un solo tanque; (d) Sistema pasivo.*

el fluido caloportador y el medio de almacenamiento son distintos (Fig. 3.2, (b) y (c)). En los sistemas directos, el fluido caloportador es almacenado directamente en un tanque caliente al salir del campo solar (carga del TES). Cuando el calor almacenado se emplea en la generación de la planta, se extrae el fluido caloportador del tanque caliente, se dirige hacia el ciclo de potencia y finalmente se almacena en el tanque frío [76]. La ventaja de este tipo de sistema es que no requiere de intercambiador de calor, pero el fluido caloportador tiene que ser adecuado para el almacenamiento. Los costes de este tipo de TES son bastante altos [70].

En los sistemas activos indirectos, el fluido caloportador es distinto del medio de almacenamiento, por lo que se necesita de un intercambiador de calor para la transferencia térmica entre fluidos. En un sistema de doble tanque (Fig. 3.2, (b)), para la carga del TES el material de almacenamiento es bombeado del tanque frío hacía el caliente, y en sentido inverso en la descarga. Una alternativa al sistema de doble tanque es el uso de un tanque único (Fig. 3.2, (c)), donde el material caliente y el frío se mantienen separados debido a la estratificación causada por la diferencia de temperatura (termoclina) [75]. La ventaja principal de este sistema es el coste, siendo hasta un 35 % más económico que el sistema de dos tanques [70].

3.3. Programación lineal entera-mixta

Una gran cantidad de problemas reales pueden ser modelados como problemas de optimización, cuyo objetivo es maximizar o minimizar una función. El propósito de la teoría de optimización es ofrecer un método sistemático para buscar una solución óptima en un espacio de alternativas. Es decir, la optimización se puede utilizar como herramienta para la toma de decisiones. Para la resolución de un problema mediante optimización, se formula un problema de programación matemática, que refleja de forma conceptual el problema real [77].

Entre las distintas formas que puede presentar el modelo de un problema de optimización, se encuentra la programación lineal entera mixta (*mixed integer linear programming*, MILP). Este tipo de problemas contienen variables reales y enteras, tanto en la función objetivo como en las restricciones. Además, las relaciones entre las variables son de tipo lineal [78]. Varios tipos de problema en el ámbito de los sistemas de potencia pueden formularse usando la MILP, por ejemplo problemas de planificación de la producción eléctrica y problemas de dimensionado de fuentes de potencia [79; 80; 1; 81].

Un problema de programación lineal entera mixta puede escribirse de la siguiente forma:

$$\begin{aligned} min \;\; & c^T x + d^T y \\ s.t. \;\; & Ax + By \leq b \\ & x \geq 0, x \in X \subseteq R^n \\ & y \in \{0,1\}^q \end{aligned} \tag{3.1}$$

En la formulación anterior, el vector x contiene las n variables reales del problema, mientras que el vector y contiene q variables binarias; c y d son vectores de parámetros, con dimensiones $n \times 1$ y $q \times 1$, respectivamente; A y B son matrices de dimensiones $m \times n$ y $m \times q$, respectivamente; b es un vector de p elementos que representan los limites para las restricciones del problema. Los vectores anteriores son vectores columna. La función objetivo es de tipo lineal, al igual que las restricciones. Las variables del problema son tanto de tipo real - las variables x, como de tipo binario - las variables y. Si los vectores d y B son 0, el problema se convierte en un problema de programación lineal (*linear problem*, LP), mientras que si los vectores c y A son 0, se trata de un problema de programación entera (*integer problem*, IP). Cualquier problema entero mixto con variables enteras en lugar de binarias puede formularse con variables binarias remplazando a las enteras, con lo cual la estructura (3.1) es general.

La existencia de las variables binarias y otorga una naturaleza combinatoria a los problemas de tipo MILP, ya que cada combinación de valores 0 ó 1 del vector y dan lugar a un problema LP a resolver, lo que dificulta su resolución. Existen varios métodos para resolver problemas de tipo MILP. Los más importantes son los métodos *branch and bound*, *cutting plane*, de descomposición y basados en lógica [78; 82].

Un concepto clave en la resolución de problemas MILP es la relajación del problema. Considerando un problema de optimización como el de las expresiones (3.1) llamado P, y su conjunto de soluciones factibles $SF(P)$, una relajación RP es un problema cuyas soluciones factibles incluyen al conjunto $SF(P)$, es decir, $SF(P) \subseteq SF(RP)$. Esta definición tiene algunas implicaciones importantes, que facilitan la resolución de los problemas MILP:

- El problema original P solamente tiene solución si el problema relajado RP la tiene.
- La solución del problema relajado es siempre mejor o igual que la solución del problema original (si existen), por lo que la solución del problema relajado ofrece un valor límite inferior a la función objetivo a minimizar.
- Como consecuencia del ítem anterior, si la solución óptima del problema relajado es una solución factible del problema original, entonces es la solución óptima del problema original.

Entre los métodos más comunes para obtener una relajación de un problema MILP se puede señalar los siguientes: 1) omitir alguna restricción; 2) fijar el valor de alguna variable binaria; y 3) convertir las variables binarias a continuas, resultando en un problema de programación lineal.

Otro concepto clave para la resolución de problemas MILP es la división del problema original en varios subproblemas de complejidad menor. Las soluciones de estos subproblemas son soluciones factibles del problema original P, de manera que la solución de uno de los subproblemas es la solución del problema original. Un método frecuente de división de un problema (P) en varios subproblemas (P_n) es considerar distintas combinaciones de valores de las variables binarias. Los algoritmos basados en la estrategia de la división del problema original disponen de mecanismos para averiguar si un determinado subproblema puede contener a la solución óptima del problema original, reduciendo de esta manera el espacio de búsqueda.

3.4. Control predictivo basado en modelo

Algunas de las estrategias de planificación de la producción propuestas en esta Tesis (las que utilizan replanificación horaria) están inspiradas en el denominado control predictivo basado en modelo (*model-based predictive control*, MPC). Esta sección muestra una pequeña introducción al mismo. El MPC es una estrategia de control avanzado, con aplicación en muchas áreas [83; 84; 85; 86; 87]. En la industria de procesos, el MPC tiene una gran aceptación [88], por estar formulado en el dominio del tiempo y ser capaz de incorporar fácilmente criterios de funcionamiento específicos.

La principal característica del MPC es la utilización de un modelo dinámico explícito del proceso a controlar para predecir la evolución del mismo al aplicarle una secuencia de señales de control. Esto permite la utilización de la optimización para determinar una secuencia óptima de entradas que permitan seguir una determinada trayectoria o comportamiento, minimizando la diferencia entre el comportamiento predicho por el modelo disponible y el comportamiento deseado. Este problema de optimización dinámica se resuelve en línea para cada paso de control. La formulación del MPC permite incorporar las restricciones del sistema en el modelo empleado de forma explícita. Además, también permite asociar incertidumbre al modelo, de tal forma que se incluya en el controlador.

Uno de los antecesores al MPC más interesantes fue el controlador linear cuadrático gaussiano (*linear quadratic Gaussian*, LQG), desarrollado a comienzos de los años sesenta del siglo pasado [89; 90]. Aunque el controlador LQG se haya vuelto un estándar para la resolución de problemas de control en un amplio rango de aplicaciones, su impacto en la industria de procesos fue bastante reducido, debido a la dificultad de incluir restricciones, no-linealidades o incertidumbres en el controlador [91].

El MPC aparece en la industria a finales de los años setenta del siglo pasado [92; 93]. La mayoría de las aplicaciones en las que el MPC emerge como enfoque de control son sistemas multivariable que incluyen restricciones. Paralelamente al desarrollo del control predictivo, se crean nuevas tecnologías de identificación de procesos basadas en datos, que permiten obtener estimaciones de los modelos dinámicos de los procesos de forma más rápida y menos costosa.

En el mundo académico, el control predictivo aparece en torno a las ideas del control adaptativo [94]. El enfoque se centra en el control de procesos monovariables con modelos de entrada/salida. El controlador de mínima varianza [95] y el control predictivo generalizado [96] se desarrollaron en este contexto.

El control predictivo basado en modelo engloba múltiples estrategias de control que comparten ciertas características. Aunque las formulaciones empleadas difieran entre sí, las siguientes ideas suelen aparecer en todas ellas [97]:

- Predicción del comportamiento futuro de la planta o proceso mediante el uso de un modelo explícito del mismo. La predicción se realiza para un periodo finito, llamado horizonte de predicción.

- Obtención de secuencias de señales de control mediante optimización de una función objetivo. El problema de optimización se resuelve mediante un algoritmo implementado en un ordenador.
- Uso de la llamada "estrategia de horizonte deslizante": en cada paso de control el horizonte considerado para la evolución del sistema es desplazado hacia el futuro. Esto implica que, aunque en cada paso se calcula una secuencia de señales de control a aplicar, solamente la primera señal se aplica al sistema. Por otra parte, la medición en cada paso de las variables de salida permite actualizar el estado del sistema. Por tanto, esta estructura genera una estrategia de control en bucle cerrado que permite compensar errores en el modelo y presencia de perturbaciones, añadiendo robustez al mecanismo de control.

Entre las ventajas más destacadas del MPC frente a otros métodos de control están las siguientes:

- Presenta una formulación en el dominio del tiempo, empleando conceptos intuitivos y una sintonización relativamente simple, por lo que es atractivo para el personal sin un conocimiento profundo de control.
- Se puede aplicar en el control de sistemas de distintos niveles de complejidad, incluyendo sistemas lineales o no lineales, multivariables, con grandes retardos, de fase no mínima o inestables.
- La ley de control responde a un criterio óptimo.
- Las restricciones del sistema se pueden incluir de manera sencilla al diseñar el controlador.

Por otra parte, el MPC no carece de inconvenientes, siendo los más importantes los siguientes:

- La necesidad de obtener un modelo preciso del sistema o proceso a controlar, al ser este un elemento clave del controlador predictivo. El desempeño del sistema de control depende, en consecuencia, de las diferencia entre el proceso real y el modelo empleado.
- La carga computacional necesaria para calcular la secuencia de señales de control puede ser bastante elevada, aunque es posible obtener soluciones explícitas [98; 99].

3.5. Planificación de la producción eléctrica

En un sistema eléctrico, un problema importante es obtener un equilibrio entre la demanda de potencia energética procedente de los usuario y la potencia ofrecida por las entidades generadoras. El reparto óptimo de la producción entre las distintas unidades generadoras es un aspecto de gran interés para el Operador del Sistema. Históricamente, el reparto de la producción se realizaba considerando los costes asociados a los incrementos de potencia solicitados por la demanda eléctrica [100; 101]. De esta manera, se asignaba un incremento de potencia a la unidad de menor coste incremental [102]. Este enfoque de asignación económica sólo ofrecía costes mínimos para las unidades en operación, por lo que el mínimo coste podría ser otro para un conjunto de unidades distintas [100]. Posteriormente se añadieron otras consideraciones a los estudios, como los efectos de las perdidas por transmisión, o los costes de los arranques y las paradas [100; 101].

Con la aparición de la programación entera [101] y más adelante de la programación entera mixta [103], el problema de la planificación de la producción de un sistema eléctrico se consiguió abordar de forma más completa, teniendo en cuenta aspectos como discontinuidades de la producción debido a la existencia de puntos mínimos de funcionamiento, costes de puesta en marcha y de parada, o costes de aumento de la producción incremental [102].

Las plantas termosolares con almacenamiento son capaces de operar en los mercados eléctricos debido a su naturaleza semi-gestionable. Para evaluar el empleo de plantas termosolares en el sistema eléctrico y las distintas estrategias de planificación de la producción en este tipo de plantas, pueden encontrase en la literatura científica dos enfoques [104]. En el primero se considera que la planta es una entidad dentro de un conjunto de generadores interconectados a una red eléctrica. En este enfoque, la optimización de la generación se hace considerando la interacción entre todos los generadores del sistema. A este enfoque se le conoce como modelo de coste de producción (*production cost model*, PCM) [105]. En el segundo enfoque se optimiza sólo la operación de la planta que es propiedad de un productor eléctrico (o conjunto de plantas para un sistema multiplanta), considerando un conjunto de precios de venta de la electricidad, y se le conoce como enfoque de tomador de precios (*price taker*, PT) [106]. Este segundo enfoque es el que se aborda en esta Tesis.

En el enfoque PCM tienen como objetivo minimizar los costes totales para satisfacer la demanda energética, considerando las restricciones inherentes del sistema, como capacidad de transmisión o limitaciones de los distintos generadores [105; 107; 108]. En este enfoque, la generación de la planta CSP es óptima en cuanto al valor ofrecido al sistema eléctrico, pero puede no serlo en cuanto a los beneficios obtenidos por el propietario de la planta.

En el enfoque PT, el criterio de optimalidad se centra en la maximización de los beneficios obtenidos por el propietario de la planta. Se busca el perfil de producción que, considerando el perfil de precios predichos de venta de la electricidad, consiga los máximos beneficios. Se suelen emplear formulaciones MILP para representar las plantas CSP y sus componentes. Los valores predichos de radiación solar directa y de precios de venta suelen considerarse o bien deterministas [109; 1; 110], o pueden incluir algún modelo de incertidumbre [111; 112; 113]. Otra alternativa al problema de la incertidumbre se encuentra en [2], donde se desarrolló un mecanismo de replanificación de la generación basado en un

enfoque MPC, que es el que inspira a dos de las estrategias de planificación propuestas en esta Tesis. Los resultados de estos estudios demuestran mejoras en los beneficios obtenidos por los propietarios de la planta. Sin embargo, este enfoque no tienen en cuenta como la operación de la planta CSP afecta al sistema eléctrico, o la influencia de un determinado plan de generación sobre los precios de la electricidad.

3.5.1. Planificación de la producción de una planta termosolar en el mercado diario de la electricidad desde un punto de vista de tomador de precios

Esta sección resume el problema de planificación de la producción abordado en esta Tesis. La principal aportación de la Tesis es proponer varias estrategias para resolver dicho problema y estudiar la viabilidad económica de dichas estrategias en un escenario realista. El problema se centra en la participación de una planta CSP en el mercado diario de la electricidad en España. El problema de generación se basa en los siguientes puntos:

- El problema se centra en el alto nivel, con una escala temporal horaria. Se asume resuelto el problema de bajo nivel gracias a la presencia de sistemas de control automático.
- Se considera un modelo PT, asumiendo que las decisiones sobre la producción de la planta CSP no afectan de forma significativa al resto del mercado.
- Cada día D, a cierta hora predefinida por el mercado eléctrico (t_{subm}), los propietarios de la planta CSP deben proporcionar al mercado un perfil horario de producción para el siguiente día (D+1). Este perfil, que representa los valores horarios de la energía suministrada a la red, es un compromiso para el día siguiente y se puede considerar como la referencia de generación que debe alcanzar la planta CSP.
- Cada hora del día D, la energía suministrada a la red por la planta CSP debería coincidir con la energía comprometida con el mercado el día anterior ($D-1$). Cuando existe una diferencia entre los valores comprometidos y alcanzados, el mercado aplica penalizaciones económicas asociadas a esta diferencia.

Es importante tener en cuenta las siguientes consideraciones:

- El recurso solar disponible para el próximo día no es conocido de antemano. Sin embargo, sí es posible disponer de una predicción de la disponibilidad de dicho recurso con la que tomar decisiones.
- El precio de venta horario de la energía generada no está tampoco disponible. De nuevo es posible utilizar predicciones de precios para tomar decisiones.
- El TES es el mecanismo que permite a la planta trasladar producciones desde horas con precios bajos a horas con precios altos, haciéndola semi-gestionable. Las decisiones que se deben tomar son cuándo y cuánto almacenar, y cuándo y cuánta energía extraer del TES.

- La generación de energía eléctrica requiere de varias fases de conversión energética que hay que modelar. La energía incidente de la radiación solar se convierte en energía térmica almacenada en el fluido caloportador y en las sales fundidas. Mediante intercambiadores de calor, esta energía térmica se traspasa a energía térmica en forma de vapor de agua. Finalmente, mediante una turbina, esta energía térmica se transforma en energía eléctrica. El modelado adecuado de todas estas fases es necesario para tomar las decisiones correctas. Además, las restricciones operativas de la planta también deben considerarse.

Se puede dar una solución al problema descrito anteriormente con diversas estrategias. A continuación se describe la estrategia básica de planificación a un día que se utiliza como referencia, que debe ser superada económicamente por las estrategias propuestas en esta Tesis. La estrategia se basa en los siguientes pasos:

- Cada día D y cada hora se proporciona a la planta el objetivo de generación que se comprometió el día anterior ($D-1$). Los controladores de bajo nivel de la planta son los responsables de alcanzar dicho objetivo si los recursos energéticos (radiación solar y energía almacenada en TES) son suficientes.
- Cada día D, a la hora prefijada por el mercado t_{subm}, la estrategia debe resolver un problema de optimización cuya solución es la planificación óptima de la generación para el día siguiente D+1. El problema de optimización tiene como información disponible las predicciones, realizadas a la hora t_{subm} del día D, de la irradiancia solar directa y los precios de la electricidad, y el estado de la planta en ese instante de tiempo. Se utiliza un modelo detallado del campo solar para la conversión de irradiancia directa solar a potencia térmica disponible en el campo solar, que es la entrada de energía que se considera en el problema de optimización. La función objetivo del problema es la suma de los ingresos por venta de energía. El modelo MILP que resuelve este problema puede consultarse en [1].

Capítulo 4

Copia de los trabajos publicados

Artículos publicados, en su orden de aparición.

Solar Energy 155 (2017) 1165–1177

Contents lists available at ScienceDirect

Solar Energy

journal homepage: www.elsevier.com/locate/solener

Calculating the profits of an economic MPC applied to CSP plants with thermal storage system

Manuel Jesús Vasallo [a,*], José Manuel Bravo [a], Emilian Gelu Cojocaru [a], Manuel Emilio Gegúndez [b]

[a] Department of Electronic Engineering, Computer Systems, and Automatics, University of Huelva, Carretera Palos de La Frontera s/n, 21819 Palos de La Frontera, Huelva, Spain
[b] Department of Mathematics, University of Huelva, Carretera Palos de La Frontera s/n, 21819 Palos de La Frontera, Huelva, Spain

ARTICLE INFO

Article history:
Received 27 January 2017
Received in revised form 11 May 2017
Accepted 8 July 2017
Available online 29 July 2017

Keywords:
Concentrating solar power plant
Thermal energy storage
Electricity market
Optimized operation strategy
Economic model-based predictive control
Mixed-integer programming

ABSTRACT

Electricity producers participating in a day-ahead energy market aim to maximize profits derived from electricity sales. The daily generation schedule has to be offered in advance, usually the previous day before a certain moment in time. The development of an economically-optimal generation schedule is the core of the generation scheduling problem. To solve this problem, renewable energy plant owners need, besides energy prices forecast, weather prediction. Among renewable energy sources, concentrated solar power (CSP) plants with thermal energy storage (TES) may find it easier to participate in electricity markets due to their semi-dispatchable generation. In any case, the limited accuracy of forecasting solar resource brings about the risk of penalties that may be imposed to CSP plants for deviation from the submitted schedule. This paper proposes a model-based predictive control (MPC) approach with an economic objective function to tackle the scheduling problem in CSP plants with TES. By this approach, the most recent forecast and the current status of plant can be used by the proposed economic MPC approach to reschedule the generation conveniently at regular time intervals. On the other hand, a more feasible generation schedule for the next day is performed at the appropriate time thanks to the use of short-term forecast. The proposed approach is applied, in a simulation context, to a 50 MW parabolic trough collector-based CSP plant with TES under the assumptions of perfect price forecasts and participation in the Spanish day-ahead energy market. A case study based on a half-year period to test several meteorological conditions is performed. In this study, an economic analysis is carried out using actual values of energy price, penalty cost, solar resource data and its day-ahead forecast. Results show an economic improvement in comparison with a traditional day-ahead scheduling strategy, especially in periods with a bad weather forecast. To overcome the lack of short-term weather forecast data for this study, a synthetic short-term predictor, whose accuracy level can be tuned by means of a parameter, is used. Sweeping this accuracy level between the situation with no forecast improvement and perfect short-term forecast, the MPC strategy reaches an improvement in total profits during the six months period between 13.9% and 33.3% of the maximum room for improvement. This maximum ideal improvement is defined as the difference in profits between the MPC strategy with perfect forecasts and the day-ahead scheduling strategy.

1. Introduction

Concentrating solar power (CSP) is a promising technology that has drawn much attention in countries such as Spain and the USA, where subsidy policies have promoted its development. The most commercially-attractive (Purohit et al., 2013) and widely installed CSP technology (Zhang et al., 2013) is found in plants based on parabolic trough collector (PTC), which use synthetic or organic oil as the heat transfer fluid (HTF). CSP has arisen interest, primarily because of the semi-dispatchable nature of CSP plants with thermal energy storage (TES) and/or backup systems based on fossil-fuels. The benefits yielded by these systems are as follows: (1) a cutback in real-time net power variability in the event of poor solar energy, (2) an extension of the whole production period, and (3) a possible rearrangement of production towards high-price periods. More specifically, the advantages of CSP with TES have been proven on an experimental basis in Dinter and Gonzalez (2014), achieving an operability similar to that of mainstream fossil-fired power plants. Additionally, an evaluation of the

* Corresponding author.
E-mail addresses: manuel.vasallo@diesia.uhu.es (M.J. Vasallo), caro@diesia.uhu.es (J.M. Bravo), emiliangelu.cojocaru@alu.uhu.es (E.G. Cojocaru), gegundez@uhu.es (M.E. Gegúndez).

http://dx.doi.org/10.1016/j.solener.2017.07.033
0038-092X/

Nomenclature

Power variables refer to average values in the step Time indices, time steps and numbers of steps

i, j, k	time indices for the current time, the MPC model and the synthetic short-term predictor
$\Delta t_w, \Delta t_o$	time steps for control update and the MPC model
N, N_{TI}, N_{STF}	numbers of steps in the MPC sliding window, the TI interval and the ST forecast

Parameters

Δw	length of the MPC sliding window
$t_{schedule\_del}$	deadline hour in day D for the delivery of the generation schedule for the day D + 1
$t_{schedule\_end}$	end time of the committed generation schedule
ω	accuracy parameter of the synthetic short-term predictor
ϕ	constant estimation for the penalty costs per MW h of deviation
$\bar{\phi}$	mean value for the penalty costs per MW h during the studied time period
γ	relative importance of the penalty term in the economic MPC
K	constant in the terminal value term of the MPC objective function
η	efficiency factor for the conversion of stored energy to net electric energy
p_{vlow}	value much lower than the minimum electricity price in the studied period

Variables

$t(i)$	current time
$x_c(t(i))$	current continuous state of the CSP plant
$x_d(t(i))$	current discrete state of the CSP plant
$p(j/i)$	electricity price forecast made at time $t(i)$
$P_{SFmax}(j/i)$	predictions for the maximum thermal power available from the SF
$P_{SFmax\_DA}(k/i)$	day-ahead forecasted maximum thermal power available from the SF
$P_{SFmax\_STF}(k/i)$	short-term forecasted maximum thermal power available from the SF
$P_{SFmax\_actual}(k/i)$	actual maximum thermal power available from the SF
$P_{eref}(j/i)$	committed generation schedule still to be met (gross value)
$P_{erefnet}(j/i)$	committed generation schedule still to be met (net value)
$P_e(j/i)$	turbine-generated gross electric power
$P_{enet}(j/i)$	turbine-generated net electric power
$P_{e\_SP}(1/i)$	setpoint for electricity generation calculated by the MPC (gross value)
$E(j/i)$	TES energy level at the beginning of the step j
$u(j/i)$	general decision variables in the MPC approach
$\phi(j/i)$	estimation of the penalty cost per kWh of deviation
$f_{cost}(.)$	undefined function for generation costs
$s(.)$	undefined function for the terminal value term of the MPC objective function

Acronyms

CSP	concentrated solar power
DAS	day-ahead scheduling
DNI	direct normal irradiance
HTF	heat transfer fluid
MILP	mixed-integer linear programming
MIP	mixed-integer programming
MPC	model-based predictive control
NSI	next schedule interval
PTC	parabolic trough collector
SF	solar field
TES	thermal energy storage
TI	tracking interval

economic performance of CSP plants using TES can be found in Madaeni et al. (2012) demonstrating that it could be a reliable option. Nowadays, the most commercially mature technology for TES is an indirect two-tank molten salt storage system (Kuravi et al., 2013).

As mentioned above, CSP systems become semi-dispatchable power sources thanks to TES (it cannot be total dispatchable due to the limited amount of stored energy). This aspect encourages CSP plants to participate in electricity markets due to, among other things, being able to rearrange production from lower to higher price periods. Therefore, it is interesting to approach the optimal generation scheduling problem (also called *self-scheduling*). In deregulated markets, the purpose of electricity producers is to maximize profits from the sale of energy. Furthermore, power plant owners also have to offer a daily schedule in electricity markets ahead of time. As a consequence, forecast for the price of the electricity and the weather must be considered in the optimization problem.

The paper (Sioshansi and Denholm, 2010) was one of the first works on the optimal operation of a CSP plant, and it analyses the profits obtained by a CSP plant using TES in electricity markets in several different areas of the USA. The optimization problem was overcome with two models: the widely-used SAM tool (SAM, 2017), which provides the thermal power produced in solar fields (SF), and a model for optimization based on mixed-integer linear programming (MILP). More examples of the use of the MILP approach can be found in Usaola (2012), Kost et al. (2013), Vasallo and Bravo (2016b). Pousinho et al. (2014, 2016) study scheduling for energy and spinning reserve of wind/CSP plants again from an MILP approach. Different approaches to MILP can be found in Lizarraga-Garcia et al. (2013), Powell et al. (2014) where Nonlinear Programming is used, and in Wittmann et al. (2011) and Channon and Eames (2014), where Dynamic Programming is used.

One of the disadvantages of CSP plants is the predictability of its electricity production since it is limited by the accuracy of forecasting direct normal irradiance (DNI). As a result, operations carried out in electricity markets run the risk of being penalized for deviating from the generation schedule. Such penalties depend to a large extent on the actual deviation, so the accuracy of DNI forecasts is no doubt a relevant aspect (Law et al., 2014). There are papers that analyze the financial value of CSP plants based on DNI forecasts, namely (Kraas et al., 2013; Law et al., 2016a). Robust and stochastic approaches are also used to solve optimal scheduling problems due to the uncertainty of CSP production forecasts and the difficulty of forecasting market prices accurately (Domínguez et al., 2012; Pousinho et al., 2015; He et al., 2016). These papers analyze optimal operation in an MILP framework and suggest offering strategies to electricity markets.

According to the literature review, we find that the most widely-used method for modeling optimal scheduling problems in CSP plants is MILP. MILP is generally a powerful mechanism

used for optimal scheduling problems in power systems (Simoglou et al., 2012). MILP is useful for these problems given that it is capable of formulating unit, startup, shutdown and ramp-rate constraints, as well as piecewise linear functions. In addition, some efficient MILP solvers nowadays find global optimal solutions in short computation times.

As mentioned above, CSP plants operating in electricity markets run the risk of being penalized for deviating from the scheduled generation as a result of inaccurate DNI forecasts. To reduce this risk, the authors of this paper suggested using a model-based predictive control (MPC) approach for generation scheduling in CSP plants based on a mixed-integer programming (MIP) model (Vasallo and Bravo, 2016a). MPC is a control strategy amply used in the industry and in academia alike. The power systems community has recently become interested in MPC due to its ability to deal with forecasts and complex constraints. Applications to scheduling and control problems arising in power systems can be seen in the literature (Petrollese et al., 2016; Sokoler et al., 2016). MPC exercises control based on a sliding-window strategy where a cost function is optimized over a moving time-horizon. It, therefore, allows for real-time optimization. Thus, information on the status of the plant and the most recent forecast becomes useful to regularly improve its operation. Categorically speaking, the purpose of the MPC approach contained in Vasallo and Bravo (2016a) is twofold: (1) the appropriate, regular tracking of the generation schedule that the plant has committed until that moment, (2) the development, at the appropriate time, of the optimal generation schedule for the following day. The information on how to track the generation schedule committed by CSP plants allows for a better estimation of their status at the beginning of the following day, permitting the development of a more achievable generation schedule. It is worth noting that the proposed MPC approach is applied only to the generation scheduling and not to the control problem, as the later issue is supposed to be efficiently resolved. This approximation is common in works about CSP scheduling found in literature (see previous references).

This paper has been inspired by the following question: what is the impact on profits of using a MPC approach for generation scheduling in CSP plants? In this regard, an economic version of the general MPC approach presented in Vasallo and Bravo (2016a) is proposed and tested. It is based on the fact that the cost function used to track the committed generation schedule is defined such that pricing and penalty information is added, unlike the application example in Vasallo and Bravo (2016a) where the even distribution of the generation error was the objective for the tracking. This way, penalties could be partially balanced by increasing revenues thanks to the use of economic information. Since all terms of the cost function now have an economic nature, this MPC approach belongs to the class of MPC strategies called *economic MPC* in literature (Dieulot et al., 2015; Touretzky and Baldea, 2014).

The proposed approach is applied, in a simulation context, to a 50 MW PTC-based CSP plant with molten-salt-based TES under the assumptions of perfect price forecast and participation in the Spanish day-ahead energy market. Unlike the work in Vasallo and Bravo (2016a), an economic analysis is performed, taking into account a half-year period to test several weather scenarios. Actual values for energy price, penalty cost, solar resource data and its day-ahead forecast are used. Moreover, several configurations of the MPC approach are studied. An economic improvement over the traditional day-ahead scheduling is shown in results. A related approach has been presented in Law et al. (2016b) but it is applied to the Australian electricity market, i.e., with different electricity market regulations.

A general description of the economic MPC approach is given in Section 2. The case study is described in Section 3, where Sections 3.1 and 3.2 depict the models used and Section 3.3 describes the characteristics of certain input data. Section 4 draws the results and discussion. Finally, conclusions are put forward in Section 5.

2. Description of the economic MPC approach

The economic MPC approach proposed in this paper is a specific version of the general approach presented in Vasallo and Bravo (2016a). The new cost function includes the pricing and penalty information. Therefore, all the terms of the cost function are economic, and the proposed MPC approach can be classified as an economic MPC. This section includes a complete description of the economic MPC approach to provide a better understanding of the rest of the paper (the variables and parameters defined are cited in the following sections). Readers are referred to (Vasallo and Bravo, 2016a) for more details.

The proposed approach assumes the participation in a day-ahead energy market and the producer's price-taking property (i.e. its production schedules do not influence market prices). As mentioned in Section 1, the dual purpose of the proposed MPC approach is: (1) the appropriate, regular tracking of the generation schedule that has been committed and (2) the development of the optimal generation schedule for the next trading day at the appropriate time. It is worth noting that the two purposes of the MPC approach are based on the following statements: (1) information on the status of the plant and the most recent forecast (e.g. short-term DNI forecast or perfect knowledge of electricity prices) would be useful to regularly improve the operation of the plant; and (2) the status of the plant at the beginning of the following day is better estimated thanks to the latter statement, and, consequently, a more feasible generation schedule can be developed.

The two objectives of the MPC approach require its sliding window to be divided into two intervals (see Fig. 1): the tracking interval (TI) and the next schedule interval (NSI). The generation schedule must then be updated to track the schedule that has been committed to within the TI interval, while the NSI interval is used to maximize future profits and generate the schedule for the following day at the appropriate time. Several variables and parameters related to the sliding window are defined next:

- $t(i) = i\Delta t_w$, where $i = 0, 1, \ldots$ are the time instants when MPC control output is generated. The beginning time of the sliding window when in position i is set to instant $t(i)$. Case $i = 0$ refers to instant 0.0 h of the current day D. Δt_w is the time step for control update.
- $t_{schedule\_del}$ is defined as the deadline hour in day D for the delivery of the generation schedule for the following day D + 1. This deadline hour depends on each country's market.
- $t_{schedule\_end}$ is the end time of the committed generation schedule. If the current time has not reached the time $t_{schedule\_del}$, $t_{schedule\_end}$ shall usually be 24.0 h of day D. On the contrary, $t_{schedule\_end}$ shall be 24.0 h of day D + 1 because the generation schedule for this day has already been delivered.
- Δw is the length of the constant sliding window.

According to the above definitions, the endpoints of the TI and NSI intervals are shown in Fig. 1. It is also worth noting that the sliding window length is constant, but the lengths of both intervals are time-variant.

When $t(i) = t_{schedule\_del}$, the generation schedule solved by the MPC control for the NSI interval until 24.0 h of day D + 1 can be regarded as the generation schedule for this day. As the typical optimal scheduling problem has an optimization horizon based on the following one or two trading days (Wittmann et al., 2011) and an assumed constant sliding window length, the value of this

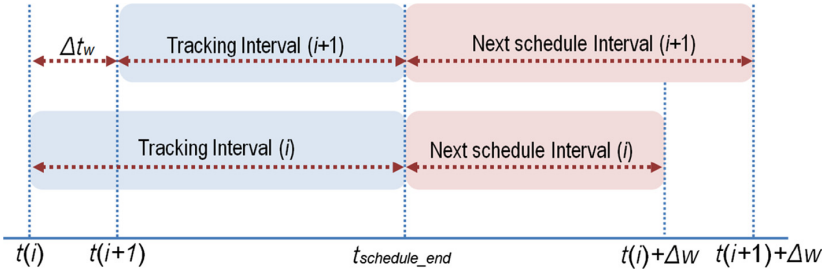

Fig. 1. Sliding window of the economic MPC.

length (Δw) can be between $24 - t_{schedule\_del}$+24 h (one-day strategy) and $24 - t_{schedule\_del}$+48 h (two-day strategy).

Fig. 2 shows the block diagram of the MPC approach. MPC control receives the following information at each sliding window position i:

1. Current continuous state of the CSP plant ($x_c(t(i))$), e.g., the TES energy level and thermal state in the SF.
2. Current discrete state of the plant ($x_d(t(i))$), e.g., active operating phases in the SF, TES or turbine.
3. Electricity price forecast made at time $t(i)$ ($p(j/i)$, for $j = 1,\ldots,N$), where j indicates each step in the MPC model, $N = \Delta w/\Delta t_o$ is the number of steps in the sliding window, and Δt_o is the time step of the MPC model expressed in hours.
4. Predictions of the average value of the maximum thermal power available from the SF ($P_{SFmax}(j/i)$, for $j = 1,\ldots,N$) made at time $t(i)$. The qualifying term 'maximum' is introduced to indicate that a partial defocus in the SF can result in a decrease in the available thermal power. A CSP plant model, DNI and other meteorological variables forecasts and initial conditions for $x_c(t(i))$ and $x_d(t(i))$ are used to generate these predictions.
5. Committed generation schedule still to be met ($P_{eref}(j/i)$, for $j = 1,\ldots,N_{TI}$), expressed in average gross electric power, where $N_{TI} = (t_{schedule\_end} - t(i))/\Delta t_o$ is the number of steps in the TI interval.

The outputs indicated below are generated as a result of the optimization at the sliding window position i:

1. Decision variables at time $t(i)$ ($u(j/i)$, for $j = 1,\ldots,N$). Only the decision variables $u(1/i)$ are applied to the plant as common in MPC approaches.
2. Average values of turbine-generated gross electric power calculated at time $t(i)$ ($P_e(j/i)$, for $j = 1,\ldots,N$). When $t(i) = t_{schedule\_del}$, values inside the NSI interval until 24.0 h of the next day are given as the new generation schedule for this day ($P_{eref}(j/i) = P_e(j/i)$, for $j = N_{TI}+1,\ldots,N'_{TI}$, where $N'_{TI} = N_{TI} + 24/\Delta t_o$ is the new number of steps in the TI interval).

The objective function to minimize is expressed by Eq. (1)

$$J(i) = -\Delta t_o \sum_{j=1}^{N_{TI}} \left[p(j/i)P_{enet}(j/i) - \phi(j/i)\left(P_{erefnet}(j/i) - P_{enet}(j/i)\right) - f_{cost}(\cdot)\right] - \Delta t_o \sum_{j=N_{TI}+1}^{N} \left(p(j/i)P_{enet}(j/i) - f_{cost}(\cdot)\right) - s(E(N+1/i)) \quad (1)$$

where $\phi(j/i)$ is an estimation of the penalty cost per kW h of deviation at hour j, $P_{enet}(j/i)$ is the turbine-generated net electric power, $P_{erefnet}(j/i)$ is the committed net electric power, $f_{cost}(.)$ represents generation costs, and $s(E(N+1/i))$ is a terminal value term applied to the final TES energy level. It is worth noting that function $-J(i)$ represents the profits along the sliding window. In this paper, it is assumed that the electricity production does not exceed the committed schedule and therefore, the term $\phi(j/i)$ refers to *falling* penalty.

According to the general proposal seen in Vasallo and Bravo (2016a), the MPC optimization model is an MIP model which includes technical and physical constraints and the dynamic model of the plant. Given that a generation scheduling problem is being addressed and that control is assumed to be efficiently resolved, fast dynamics must be removed. The MPC optimization model (hereinafter referred to as the MIP-MPC model) is proposed to

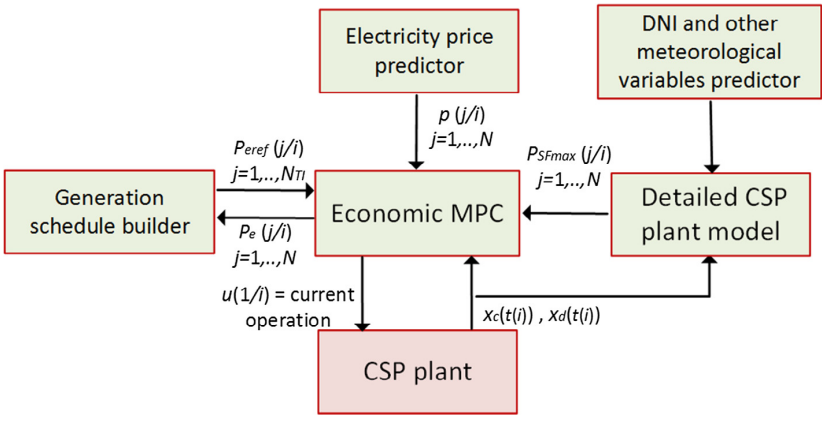

Fig. 2. Block diagram of the economic MPC.

adjust to the features of the CSP plant model (much more detailed) as much as possible yet preserving enough simplicity to avoid increasing the computational burden in a prohibitive way. Futhermore, the time step in the MIP-MPC model should be higher than that in the detailed CSP plant model to avoid high computation times.

3. Description of the case study

The economic MPC approach proposed by this paper is applied, in a simulation context, to a 50 MW PTC-based CSP plant with molten-salt-based TES. The CSP plant is based on the model presented in García et al. (2011) and also used in Vasallo and Bravo (2016a), which describes the plant *Andasol* 2 in Granada, Spain. Some characteristics of this model (adapted to this case study) are shown in Table 1.

The simulation scenario developed for this case study has the following features:

1. A sufficient time period is considered (from 01/01/2013 to 30/06/2013) with the purpose of testing several meteorological conditions.
2. The Spanish day-ahead energy market and the producer's price-taking property are considered. Price forecasts are assumed to be perfect and obtained from data of the Iberian market operator (OMIE, 2017). No premium per MW h is considered. Penalty costs per MW h are also obtained from OMIE. In order to keep things simple, generation costs are not taken into consideration.
3. The generation schedule and MIP-MPC model resolutions are hourly. The frequency of the rescheduling is also hourly. Therefore, $\Delta t_o = \Delta t_w = 1.0$ h (see Fig. 1). Parameter $t_{schedule\_del}$ is set to 10.0 h (Spanish market in 2013). Parameter Δw is set to 48 h to reach a compromise between computation time of the MIP-MPC model and the possibility of conserving energy for its sale after the end of the following day. Therefore, the length of the NSI interval at 10.0 h is 34 h, and the scheduling problem for the following day is based on the next 1 + 5/12 days (i.e., an intermediate scheme between the one-day and two-day strategies).
4. The detailed CSP plant model from Vasallo and Bravo (2016a) is used to generate predictions $P_{SFmax}(j/i)$ (see Fig. 2). DNI and ambient temperature are the only meteorological variables considered, and ambient temperature forecasts are assumed to be perfect and created from TMY2 data (TMY, 2017).
5. The CSP plant is represented by a one-hour-resolution model to avoid very high simulation times, as is common in literature, e.g. (Kraas et al., 2013; Law et al., 2016a). Specifically, a MIP model derived from the MIP-MPC model itself is employed and, therefore, performance differences between the optimization model and the plant are only due to DNI forecast errors. This model is referred to in this work as the MIP-plant model.
6. In order to address a realistic scenario, authors have used day-ahead global solar radiation forecasts, obtained from the Integrated Forecast System model (IFS) of the European Centre for Medium-range Weather Forecasts (ECMWF) and a set of solar radiation measures provided from a photovoltaic solar plant. These data sets are used to obtain forecasted and measured DNI profiles by means of statistical processing. This processing aims to develop a measured DNI profile coherent with the studied location and a realistic forecasted DNI profile (similar forecasting metrics to those found in (Marquez and Coimbra, 2011)). Finally, both sets are converted to maximum thermal power available from the SF by simulation with the detailed CSP plant model (see point 4).
7. Short-term DNI forecasts are also taken into account in this study. Several methods can be consulted in Law et al. (2014). A parameterized model is used to emulate the short-term predictor and to overcome the lack of short-term DNI forecast data for this study. One of its parameters, ω, is a value between 0 and 1, and represents the accuracy of the forecasts (from ideally perfect short-term DNI forecast to day-ahead DNI forecast, respectively). This range allows analyzing the influence of short-term DNI forecasts. Moreover, the developed predictor model works directly with the variable $P_{SFmax}(j/i)$ to avoid conversion from DNI values.

Table 1
Characteristics of the CSP plant.

Turbine capacity (gross)	52.5 MW-e
Solar field capacity	250 MW-t
Thermal capacity of the powerblock in solar-only mode	140 MW-t
Thermal capacity of the powerblock in TES-only mode	119 MW-t
Solar multiple	1.8
TES capacity (TES-only mode)	8 h
Turbine efficiency (full load)	38%
Fossil backup	only to prevent HTF freezing

The economic MPC strategy proposed in this paper is tested against the traditional day-ahead scheduling strategy (DAS strategy). This strategy is characterized by the following features:

1. The schedule for day D + 1 is generated at $t_{schedule\_del}$ of day D. At this moment, initial conditions for day D + 1 are estimated using the current status of the plant, the day-ahead forecast and the schedule still to be met.
2. Its time horizon is 34 h, i.e., the length of the NSI interval at $t_{schedule\_del}$ in the MPC approach. This election is made for a fair comparison between strategies.
3. The generation schedule is tracked without any rescheduling. Then, the hourly generation is the maximum that can be reached according to the committed value.

The optimization model used to generate the schedule in the DAS strategy is also derived from the MIP-MPC model. This optimization model is referred to as the MIP-DAS model in this paper. Tables 2 and 3 summarizes all information about the scheduling strategies and the models used.

Section 3.1 describes the synthetic short-term predictor. MIP-MPC, MIP-DAS and MIP-plant models are explained in Section 3.2. Section 3.3 describes the characteristics of the following input data: solar resource, its day-ahead forecast, electricity prices and the penalty costs per MW h of deviation. Finally, the results and discussion are shown in Section 4.

3.1. Synthetic short-term predictor

A synthetic short-term predictor is used to analyze the influence of short-term DNI forecasts. It is assumed that short-term forecasts are never worse than day-ahead forecasts. Eq. (2) describes the predictor:

$$P_{SFmax\_STF}(k/i) = P_{SFmax\_actual}(k/i) + r(k)\omega(P_{SFmax\_DA}(k/i) - P_{SFmax\_actual}(k/i)) \quad (2)$$

for $k = 1$ to $N_{STF} + 1$; where N_{STF} is the horizon (hours) of the short-term forecast; $r(k)$ is a linear function of index $k, r(1) = 1, r(N_{STF} + 1) = 1/(\omega + \epsilon), \epsilon$ is a very small amount to avoid division by zero; $P_{SFmax\_STF}(k/i), P_{SFmax\_actual}(k/i)$ and $P_{SFmax\_DA}(k/i)$ are

Table 2
Information about the scheduling strategies used.

Model	Strategy	Rescheduling	Short-term forecast	Feedback of the status of the plant
MIP-MPC	MPC	Hourly	Hourly	Hourly
MIP-DAS	DAS	No	No	Daily

Table 3
Information about the models used.

Model	Function
MIP-MPC	MPC strategy
MIP-DAS	DAS strategy
MIP-plant	To represent the plant
detailed model	To convert DNI to $P_{SFmax}(j)$

the short-term forecasted, actual and day-ahead forecasted maximum thermal powers available from SF; and ω is a parameter between 0 and 1, which represents the accuracy of the short-term forecast (from ideally perfect short-term DNI forecast to day-ahead DNI forecast, respectively). It is also worth noting that ω is the percentage of day-ahead forecast error to be added to the actual value to generate the short-term forecast of the first hour. This percentage grows linearly over time (with a non-null value of ω) and reaches 100% when $k = N_{STF} + 1$ (i.e., out of the horizon of the short-term forecast). Typical values for N_{STF} are 5 or 6 h (Law et al., 2014, 2016a). The objective of the synthetic predictor is to enable the approximate analysis of short-term DNI forecasts influence, overcoming the lack of such data for this case study. Therefore, it is not the focus of this paper to develop a more realistic short-term predictor. With the variation of parameter ω, the two extreme cases (ideally perfect short-term DNI forecast and lack of short-term forecast) and other intermediate cases are simulated. In this regard, the variable $P_{SFmax\_STF}(k/i)$ could represent the mathematical expectation of the short-term forecast.

3.2. MIP models

This subsection describes briefly the three one-hour-resolution MIP models. The MIP-DAS and MIP-plant models are derived from the MIP-MPC model. The formulation of the three MIP models for this case study was carried out without any non-linear element, except for binary variables. Thus, they are MILP models.

At this stage, it is important to clarify the following: The plant operator and control systems of the plant under study are supposed to take decisions based on two goals albeit with different priorities (Vasallo and Bravo, 2016a). The high-priority goal is to minimize the generation error. Once this objective is met, the low-priority goal can be applied, which consists of minimizing the defocused thermal power in the SF (thus maximizing the TES energy level). Therefore, the plant under study only has one independent decision variable in relation to power sharing, e.g., the setpoint for electricity generation. Then, the MPC action $u(1/i) = P_{e\_SP}(1/i)$. Equation $P_{e\_SP}(1/i) = P_e(1/i)$ is used to obtain the setpoint, where $P_e(1/i)$ is a value generated by the MPC control.

3.2.1. MIP-MPC model

Most MIP-MPC model constraints are derived from a linear one-hour-resolution simplification of the detailed CSP plant model (excluding the SF). The set of equations and inequalities comprising the MIP-MPC model and the values for its parameters are described in Vasallo and Bravo (2016a). Moreover, the synthetic predictor is added in order to generate the short-term predictions of $P_{SFmax}(j/i)$. The objective function to minimize is expressed in Eq. (3), which is a specific case of the objective function in Section 2.

$$J(i) = -\Delta t_o \sum_{j=1}^{N_{\eta}} \left[p(j/i) P_{enet}(j/i) - \phi(j/i)(P_{erefnet}(j/i) - P_{enet}(j/i)) \right] - \Delta t_o \sum_{j=N_{\eta}+1}^{N} (p(j/i) P_{enet}(j/i)) - KE(N+1/i) \quad (3)$$

In this objective function, generation costs are not taken into consideration and $KE(N+1/i)$ is the terminal value term formed by a value proportional to the final TES energy level, with constant K defined by equation $K = \eta p_{vlow}$, where η is an efficiency factor for the conversion of stored energy to net electric energy, and p_{vlow} is a value much lower than the minimum electricity price in the simulation period. This way, the terminal value term of the objective function makes the defocused thermal energy be as low as possible once the maximum economic profits (without terminal value term) have been obtained.

In the Spanish market, deviation from the scheduled generation produces penalty costs if it requires the intervention of the transmission system operator. These penalties are associated with the costs incurred to stabilize the system, and do not follow any pregiven function. Therefore, these costs are difficult to estimate. An average value for $\phi(j/i)$ is assumed in Section 3.3. An analysis is conducted on the performance of the MPC strategy when this average value varies in Section 4.

3.2.2. MIP-DAS model

The MIP-DAS model is an optimization model which generates the generation schedule for day D + 1 when $t(i) = t_{schedule\_del}$ at day D in case of the DAS strategy. The MIP-DAS model is derived from the MIP-MPC model in the following manner: the TI interval is removed and the NSI interval begins the hour 0 of day D + 1. Initial values for the moment before hour 0 of day D + 1 are estimated at $t_{schedule\_del}$ of day D using the current status of the plant, the day-ahead forecast and the schedule still to be met.

3.2.3. MIP-plant model

The MIP-plant model is a one-hour-resolution model used to represent the plant in the several-month-long simulation, and it prevents high simulation times. It is composed of two consecutive optimization models derived from the MIP-MPC model. The two goals with different priorities that guide the decisions of the plant operator and control systems (see the beginning of Section 3.2) explain this scheme. The MIP-plant model incorporates the constraints included in the MIP-MPC model but, unlike the latter, its time horizon is a one-hour step in order to represent the plant in the evolution of the simulation.

3.3. Input data description

The characteristics of the solar resource, its day-ahead forecast, electricity prices and the penalty costs per MW h of deviation for the studied time period are described in this subsection. Fig. 3 shows the hourly average values of the maximum thermal power available from the SF, $P_{SFmax\_actual}(j)$, which have been obtained using solar radiation data and the detailed CSP plant model. As can be seen in the figure, as the days advance, the $P_{SFmax\_actual}(j)$ profile increases in intensity and length. Furthermore, approximately

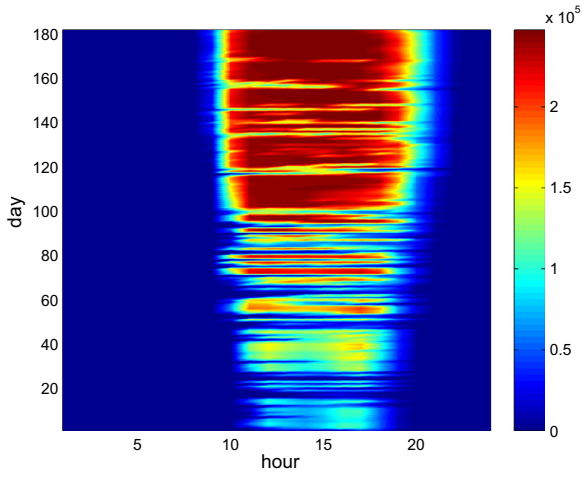

Fig. 3. Hourly average values for maximum thermal power available from the SF (kW).

the first one hundred days present a high meteorological variability, while the stability increases in the last eighty days.

An important variable that can influence the performance of scheduling strategies is, obviously, the day-ahead forecast error of the maximum thermal power available from the SF. In general, the forecast error increases with the meteorology variability, that is, winter days present higher prediction errors than clear summer days. In order to characterize the day-ahead forecast error on a monthly basis, some metrics are shown in Table 4. It is worth noting that only daylight hours are used to obtain the metrics, as the prediction error is absent during night hours. The mean of the maximum thermal power available from SF is denoted by $\overline{P}_{SFmax\_actual}$. The Relative Root Mean Squared Error and the Relative Mean Bias Error are denoted by *rRMSE* and *rMBE* respectively, (see Kraas et al., 2013 for expressions of these metrics). Some observations may be useful. The mean of the maximum thermal power available from the SF increases by 237% from January to June. The relative error is higher in winter months. In fact, March has been particularly bad in the studied period. Finally, the monthly bias error can vary widely.

Fig. 4 shows the difference between daily maximum thermal energy available from the SF and its day-ahead forecast. Red[1] is used if the predicted value is higher and black if it is lower. The width of the line is proportional to the forecast error. The figure shows days with little error and days with a very high forecast error. Roughly, the relative prediction error is higher in the first one hundred days and decreases in the last eighty days. Fig. 5 shows three example days for day-ahead forecast of P_{SFmax_actual}: May 26, 27 and 28. The three days present examples of underestimated, overestimated and accurate forecasts, respectively.

The electricity prices are shown in Fig. 6. Prices reach higher values during the first two months of the year (winter). Smaller values are found in the second two months of the year (moderate temperatures of the spring).

Fig. 7 shows an hourly boxplot of the penalty costs per MW h of deviation from the scheduled generation (falling penalties in this case study). Fig. 8 shows the autocorrelation of the penalty costs time series. There is no significant 24-h autocorrelation, so, it is no easy task to use autoregressive models to predict the penalty

[1] For interpretation of color in Fig. 4, the reader is referred to the web version of this article.

Table 4
Metrics of day-ahead forecast error for maximum thermal power from the SF.

Month	$\overline{P}_{SFmax\_actual}$ (MW)	*rRMSE* (%)	*rMBE* (%)
1	52.6	51.6	17.5
2	82.5	45.4	3.8
3	87.6	70.0	8.4
4	152.4	40.8	−5.3
5	164.4	28.2	10.6
6	177.5	13.4	−7.8

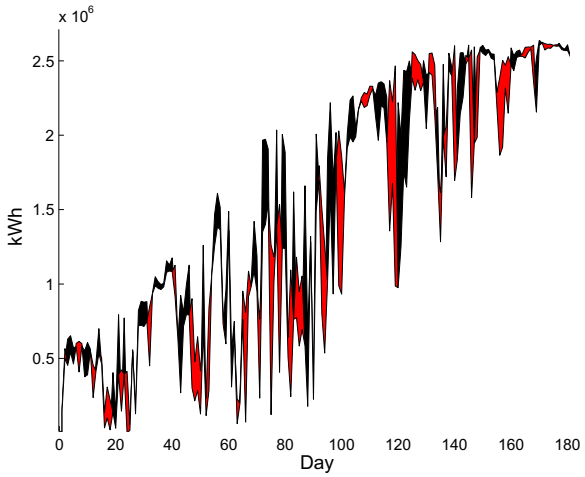

Fig. 4. Daily maximum thermal energy available from the SF and its day-ahead forecast.

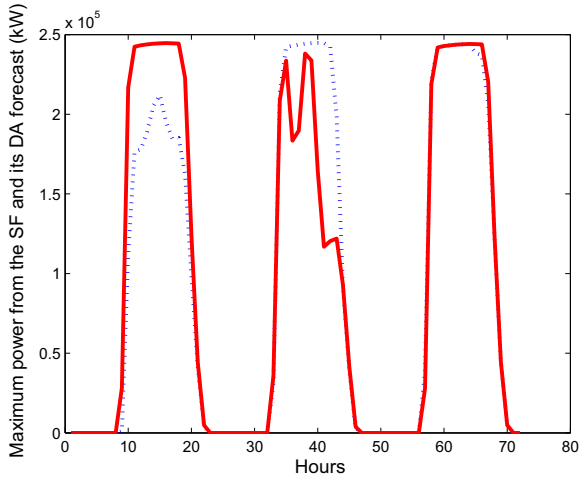

Fig. 5. Three example days for day-ahead forecast. Actual value: solid, red line; forecasted value: dotted, blue line. (For interpretation of the references to color in this figure legend, the reader is referred to the web version of this article.)

costs per MW h of deviation. For this reason, the proposed economic MPC approach uses an estimation $\phi(j,i)$ for this value. This estimation $\phi(j,i) = \phi = \gamma\bar{\phi}$, where $\bar{\phi} = 7.69$ Euros/MW h is the mean value for the penalty costs per MW h during the simulation period and $\gamma \geqslant 0$ is a parameter to be defined by the user. It is worth noting that γ defines the relative importance of the penaliza-

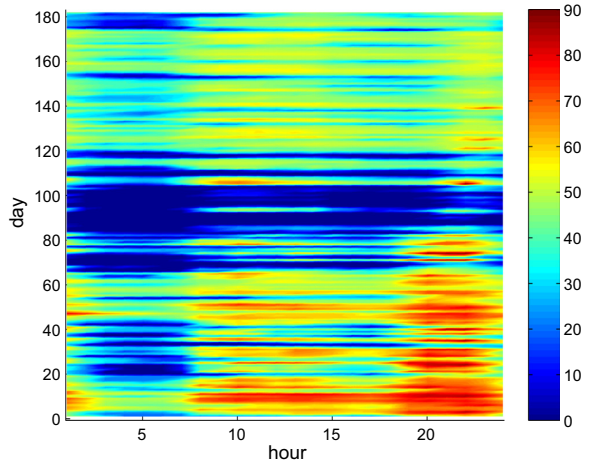

Fig. 6. Electricty prices (Euros/MW h).

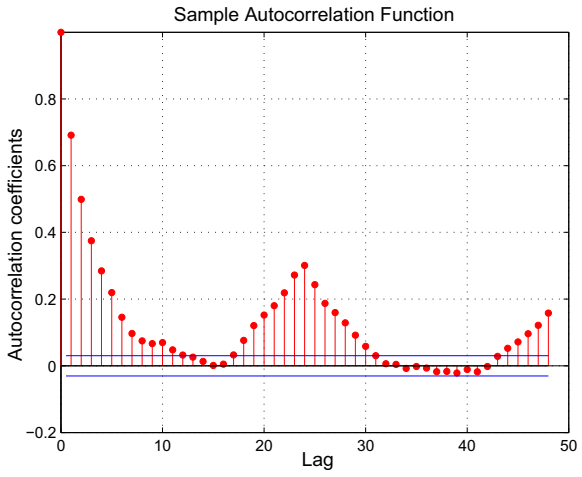

Fig. 8. Autocorrelation of penalty costs per MW h.

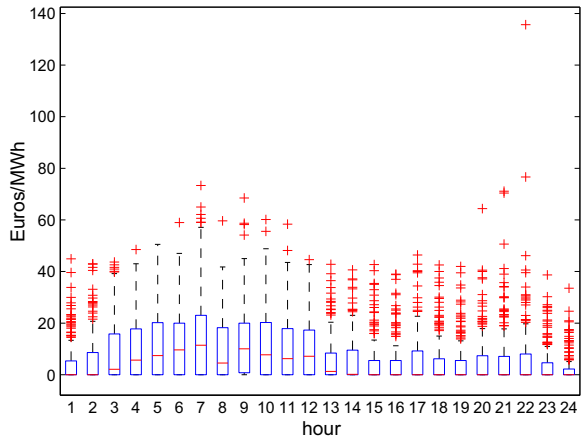

Fig. 7. Hourly boxplot for penalty costs per MW h of deviation. In each box, the central mark is the median; the edges of the box are the 25th and 75th percentiles. The whiskers extending to the most extreme datapoints (black bars) are not considered to be outliers. The outliers are plotted individually (red marks). (For interpretation of the references to color in this figure legend, the reader is referred to the web version of this article.)

tion term in the economic MPC approach. Since $\bar{\phi}$ is an unknown value a priori, several simulations with different values of γ have been conducted in this paper. This allows studying the economic impact of constant γ and analyzing the importance of an accurate estimation of $\bar{\phi}$.

4. Results and discussion

Simulation results are shown and discussed in this section. It is important to stress that there are many factors that affect the economic results of scheduling strategies, e.g., electricity market regulations, the local climate of the plant site, forecast quality, plant design, simplification hypothesis and models used (Law et al., 2016a). Therefore, the conclusions drawn from this case study could be different in other scenarios. Several configurations of the MPC strategy are compared to the reference strategy, that is, the day-ahead scheduling strategy. The configuration of the MPC strategy is set by two parameters. In this regard, $MPC_{\omega}(\gamma)$ denotes a configuration where the penalty cost per MW h is $\gamma\bar{\phi}$ (see Section 3.3) and the accuracy of the synthetic short-term predictor is ω (see Section 3.1). It is worth noting that while parameter γ is a tuning parameter of the MPC strategy, parameter ω characterizes the accuracy of the synthetic short-term predictor considered. $\gamma = 0.1, 0.5, 1, 2, 2.5, 3$ and $\omega = 0, 0.001, 0.5, 1$ values are used, so, 24 simulations have been carried out to study the different scenarios. Moreover, the horizon of the synthetic short-term predictor, N_{STF}, is set to 5 h in all scenarios, and the initial conditions for the simulation are turbine shut-down and zero TES energy level. Next, the following analysis are described: (1) economic comparison between MPC and DAS strategies varying γ and ω; (2) calculation of the percentage of improvement in profits of the MPC strategy with respect to the DAS strategy on a monthly basis; (3) study of the influence of the horizon of the short-term predictor on the profits; (4) economic comparison between MPC and DAS strategies considering the maximum room for improvement; and (5) energy analysis of both strategies. Finally, the conclusions drawn from the results are exposed.

4.1. Economic comparison between MPC and DAS strategies varying γ and ω

Total results in the six-month period are studied in this subsection. Figs. 9–11 show, respectively, the gross revenues, the penalty costs and the final profits obtained by several configurations of the MPC strategy and by the DAS strategy. Revenues decrease as the value of parameter ω increases, that is, as the short-term prediction worsens (see Fig. 9). Moreover, as the value of parameter γ increases, the obtained gross revenues decrease. This is coherent because an increase of the penalty cost makes the scheduler sacrifice revenues in order to meet the committed schedule. The higher revenues of the MPC strategy over the DAS strategy are explained by its rescheduling capacity. The penalty costs decrease as parameter γ increases (see Fig. 10). At first, a decrease of costs is convenient. However, as revenues decrease too, it is necessary to study the profits in order to evaluate the results. The higher penalty costs of the MPC strategy over the DAS strategy are justified in Section 4.5.

In relation to total profits (see Fig. 11), three conclusions are worth mentioning. Firstly, it should be underlined that the results obtained by the MPC scheduler outperform the profits obtained by

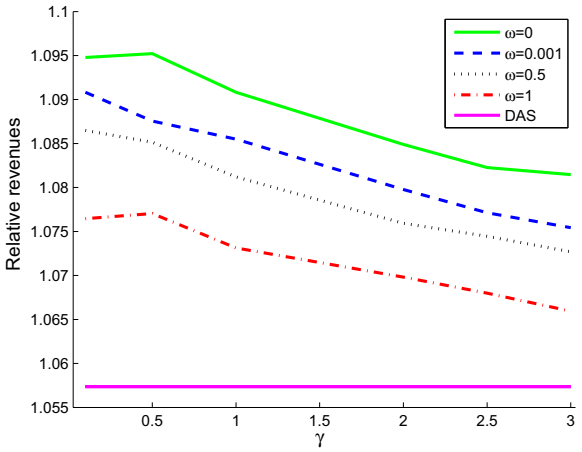

Fig. 9. Revenues obtained during the six-month period by the DAS strategy and by the MPC strategy for different values of penalty parameter (γ) and of parameter of short-term forecast accuracy (ω). The revenues are expressed in relative values with respect to a reference value. This latter value is defined as $\bar{p}N_H P_{enetmax} F_C$, where $\bar{p}$ is the mean energy price during the six-month period, N_H is the number of hours, $P_{enetmax}$ is the plant net capacity (50 MW) and F_C is the plant capacity factor (0.41, *Andasol* 2).

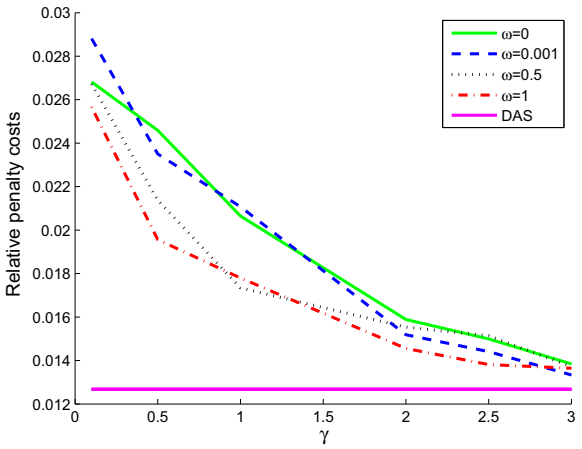

Fig. 10. Penalty costs charged during the six-month period when the DAS strategy and the MPC strategy are applied. The latter is applied for different values of penalty parameter (γ) and of parameter of short-term forecast accuracy (ω). The penalty costs are expressed in relative values with respect to a reference value (see the caption of Fig. 9).

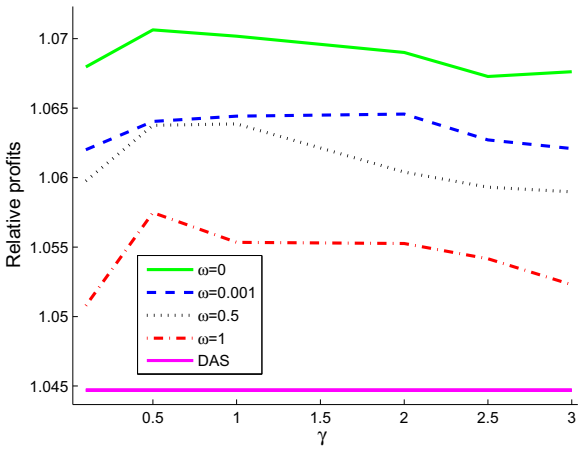

Fig. 11. Profits obtained during the six-month period by the DAS strategy and by the MPC strategy for different values of penalty parameter (γ) and of parameter of short-term forecast accuracy (ω). The profits are expressed in relative values with respect to a reference value (see the caption of Fig. 9).

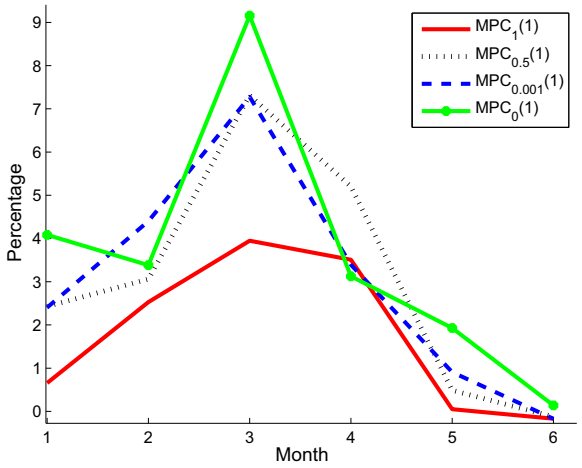

Fig. 12. Percentage of improvement in profits for $MPC_\omega(1)$ strategy with respect to the DAS strategy for each month and for different values of short-term forecast accuracy parameter (ω).

the reference scheduler in all cases. In fact, the MPC strategy without short-term forecast ($\omega = 1$) also overcomes the reference strategy. Secondly, it is also noted that improvements in the parameter ω increase the profits. This point confirms the importance of having a good short-term predictor. Finally, a value for the tuning parameter γ is proposed. It can be observed that when γ is within the interval (0.5–2) total profits are higher and they do not vary significantly. Then, a $\gamma = 1$ value can be a good option, that is, to use the mean $\bar{\phi}$ as an estimation for the penalty cost per MW h of deviation. Moreover, the existence of this interval causes the accuracy of this estimation not to be critical. In this regard, the following values represent the ratio between mean values (during the first six months) for penalty cost per MW h in consecutive years from 2012 to 2015: 2.06, 1.32, 0.85 and 1.09. It can be observed that these values are within the identified interval (except value 2.06 by very little). Therefore, the mean value from the previous year is proposed as an estimation of the penalty cost per MW h for the current year, assuming that the validity of the identified interval is maintained over the years.

4.2. Calculation of the percentage of improvement in profits of the MPC strategy with respect to the DAS strategy on a monthly basis

Fig. 12 shows the percentage of improvement for each month in profits of the $MPC_\omega(1)$ strategy with $\omega = 1, 0.5, 0.001$ and 0 with respect to the reference strategy. As can be seen, the MPC strategy obtains substantial improvements in the first four months, when the meteorological instability is present. In fact, the best result is obtained in March, that is, the month with the worse forecast for the maximum thermal power available from the SF. Therefore, the MPC strategy can compensate bad forecast situations.

4.3. Study of the influence of the horizon of the short-term predictor on the profits

As mentioned above, the horizon of the synthetic short-term predictor, N_{STF}, is set to 5 h. However, it may be interesting to study the evolution of the profits when a higher time horizon is used. Fig. 13 shows the profits obtained using $N_{STF} = 5, 6, 7, 8, 10$ and 12 applying a $MPC_{0.001}(2)$ scheduler. A slight increase in profits can be observed as the value of N_{STF} increases. In fact, the profits for $N_{STF} = 12$ almost reaches the profits of the $MPC_0(2)$ scheduler with $N_{STF} = 5$, that is, using perfect short-term forecast (see Fig. 11). The test was also performed with the $MPC_{0.001}(1)$ strategy and the resulting overall trend of profits was also incremental to the N_{STF} value. Nevertheless, some fluctuations arose. Theses fluctuations are possibly due to the higher penalty risk level with $\gamma = 1$ (see Section 4.5 for clarification of this point).

4.4. Economic comparison between MPC and DAS strategies considering the maximum room for improvement

A final economic analysis of the $MPC_{\omega}(1)$ strategy is carried out in comparison with the reference strategy. To partially overcome the dependence of results with the studied scenario, the maximum ideal profits (using perfect solar resource forecast) for the specifications of this case study are taken into account. Fig. 14 shows total profits in the six-month period of the following strategies: (1) MPC strategy with perfect day-ahead forecast; (2) DAS strategy with perfect day-ahead forecast; (3) $MPC_{\omega}(1)$ strategy with $\omega = 0, 0.001, 0.5$ and 1; and (4) DAS strategy. It is worth noting that perfect day-ahead forecast means perfect short-term forecast in this case study. The profits of these strategies decrease according to the order in which they are cited. With perfect day-ahead forecasts, the MPC strategy outperforms the DAS strategy thanks to the hourly rescheduling, which allows having information about the energy prices for the hours immediately after the end of the time horizon of the DAS strategy. Then, the MPC strategy could reserve energy for future high-price hours and, consequently, accept some deviation at the moment of the decision. Considering the profits of the MPC strategy with the perfect day-ahead forecast as the maximum ideal profits, the percentage difference in profits between MPC and DAS strategies in relation to the maximum ideal gain is 33.3%, 25,7%, 25.0% and 13.9% for $\omega = 0, 0.001, 0.5$ and 1. Since a perfect forecast is an idealized situation, it could be said that profits obtained by the MPC strategy are remarkable.

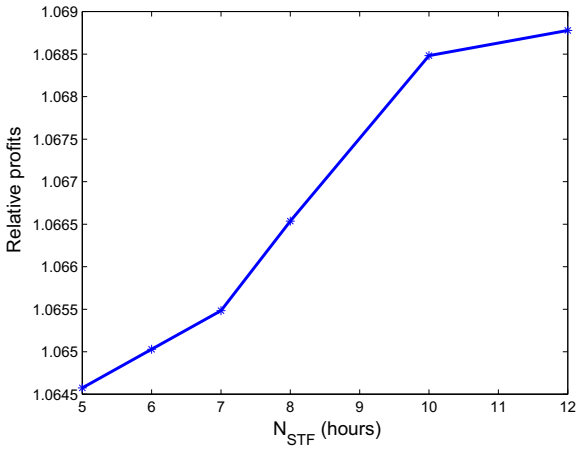

Fig. 13. Profits vs horizon of short-term forecast for strategy $MPC_{0.001}(2)$. Profits are expressed in relative values with respect to a reference value (see the caption of Fig. 9).

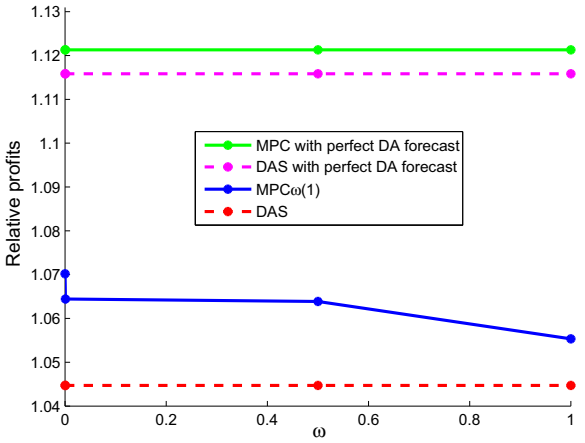

Fig. 14. Comparison between MPC and DAS strategies considering maximum ideal profits. The comparison is based on total values during the six-month period. Different values of short-term forecast accuracy parameter (ω) are used. Penalty parameter (γ) is set to 1. Profits are expressed in relative values with respect to a reference value (see the caption of Fig. 9).

4.5. Energy analysis of both strategies

Next, some energy results of DAS and $MPC_{0.001}(1)$ strategies are shown in Table 5. The amount of thermal energy available from the SF which is not transferred to the turbine and/or TES must be eliminated by means of a partial/total solar collector defocusing. This amount of energy is referred to as defocused energy (see Table 5). We can see that generation is slightly lower with the $MPC_{0.001}(1)$ strategy. Moreover, values for deviation and defocused energy with MPC strategy are also worse. The economic improvement of MPC strategy is shown in parameter *equivalent sale price*. This parameter is defined as the ratio between total profits and total generation. The worse energy results of the MPC strategy are explained by its capability to admit deviation in order to reserve energy to potentially attain higher future revenues, as its higher mean TES energy level confirms. As mentioned above, this capability is based on the hourly slide of the MPC window, which incorporates new information (precise or not). The parameter γ allows reducing this capability and can be used to regulate the risk level. In any case, while total deviation can be higher with the MPC strategy, this approach distributes it by taking advantage of the most favorable hours (see Figs. 6, 15(a) and (b)). The DAS deviations are concentrated around some concrete hours. However, MPC deviations are expanded along the day as a result of the search for high prices (see the example in Fig. 16 for better clarity). Finally, Fig. 17 shows the distribution of electric generation with price intervals for both strategies. The displacement of the generation to higher prices in the MPC strategy compared to the DAS strategy can be observed.

Table 5
Energy results of DAS and $MPC_{0.001}(1)$ strategies during the six-month period.

Hourly mean value	DAS	$MPC_{0.001}(1)$	Inc. ($MPC_{0.001}(1)$ over DAS)
Generation (MW h-e)	18.87	18.84	−0.18%
Deviation (MW h-e)	1.73	2.16	25.18%
Defocused energy (MW h-t)	4.83	4.96	2.75%
TES energy level (%)	33.4	39.6	18.71 %
Equivalent sale price (Euros/MW h-e)	42.13	43	2.07%

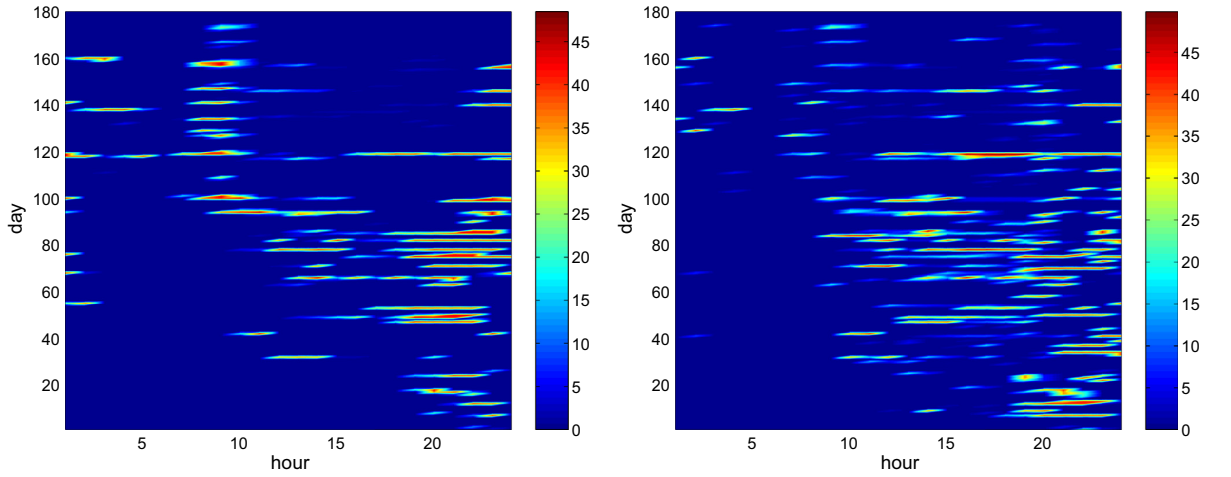

(a) Deviation with DAS strategy (MWh-e) (b) Deviation with MPC strategy (MWh-e)

Fig. 15. Deviation (MW h-e).

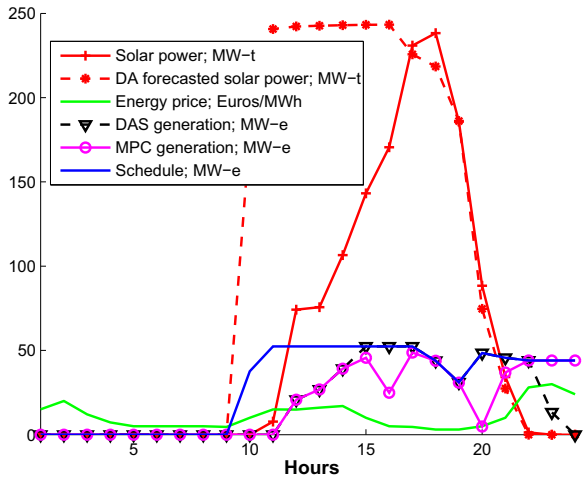

Fig. 16. Example of generation displacement to higher prices in the MPC strategy in comparison to the DAS strategy during a day with overestimated solar resource.

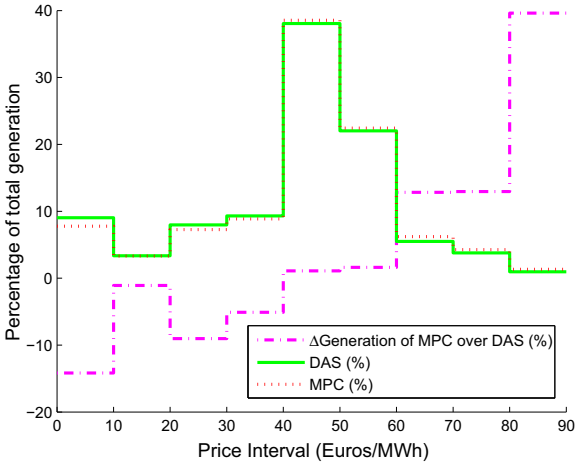

Fig. 17. Distribution of generation with price intervals for DAS and MPC strategies (%).

4.6. Conclusions drawn from the results

In summary, the following conclusions can be drawn after analyzing the results:

1. The MPC strategy obtains higher total profits than the DAS strategy during the period of six months, including the case without short-term forecasts. Moreover, improvements in short-term forecasts increase the profits. These results are expected because of the capabilities of MPC approaches.
2. To estimate the penalty cost per MW h of deviation, its mean value (during the studied period) from the previous year is proposed (see the last paragraph of Section 4.1)
3. The improvement in profits of the MPC strategy in relation to the reference strategy is higher in periods with a bad forecast. For example, the percentage of improvement during March is higher than 7% in cases with short-term forecasts ($\omega < 1$).
4. A higher horizon of the short-term forecast achieves slightly better results (assuming that the behavior of the short-term forecast is described by the developed synthetic predictor).
5. The MPC strategy reaches an improvement in total profits during the six months period between 13.9% and 33.3% of the maximum room for improvement in this case study. This maximum ideal improvement is defined as the difference in profits between the MPC strategy with perfect day-ahead forecasts and the DAS strategy.
6. The γ parameter allows regulating the risk level of the tracking in the MPC strategy. This strategy tends to admit certain deviation in order to store more energy. The stored energy is then used to potentially achieve higher future revenues, although this performance increases the penalties. This behavior leads to, in addition to a higher deviation, a higher mean TES energy level and, consequently, higher defocused energy. A high enough value of γ can reduce this performance, but it could

adversely affect profits. The ideal value of γ compensates the penalties and the worse energy behavior with higher profits.

In the opinion of the authors, the proposed economic MPC could reach better results in the following situations:

1. In the real case of an imperfect forecast of energy price (a perfect price forecast is supposed in this case study), the economic MPC could outperform the DAS strategy more clearly due to the perfect knowledge of the prices of the current day. Notice that the DAS strategy always uses forecasted prices. Nevertheless, the MPC strategy can utilize exact prices of the current day for its tracking function once the prices were cleared on the market the day before.
2. In scenarios with a higher level of penalty costs per MW h of deviation, the economic MPC could also overcome the DAS strategy more clearly because this high level of penalties could be reduced significantly.

Some improvements for the method are indicated next:

1. More complex models to form the penalization term in the optimization function can be evaluated. For example, the estimation of the penalty cost per MW h of deviation could be supposed to be time-varying. This value could be calculated using a weighted mean of a sliding window along previous values.
2. It is interesting to explore other aspects, such as analyzing the effect of the sliding window length on the results, or including robust terms in the optimization problem. The purpose of these robust terms is to achieve a more conservative generation schedule for the next day, thus avoiding hight deviation due to poor DNI forecast.

5. Conclusion

An economic MPC approach is proposed to address the optimal generation scheduling in CSP plants with TES. One of the main obstacles tackled in this type of problems is the penalty cost charged by the electricity market when deviation from the committed generation schedule arises due to the limited accuracy of the solar resource forecast. The proposed approach addresses this pitfall with two actions: (1) the economically advantageous, regular update of the generation schedule to track the committed schedule using the most recent forecast and the current status of the plant and (2) the generation, at the appropriative time, of a more feasible schedule for the following day thanks to the use of a better estimation for the initial conditions based on short-term forecasts. In order to achieve the proposed aims, the objective function of the MPC consists of economic terms, that uses forecasted electricity prices and estimations of penalty costs. The proposed approach is applied, in a simulation context, to a 50 MW parabolic trough collector based CSP plant with TES under the assumptions of a participation in the Spanish day-ahead energy market and perfect price forecasts. A time period of six months is taken into account in this case study to test several meteorological conditions. The proposed approach is then compared with a reference strategy based on a traditional day-ahead scheduling. The comparative analysis covers economic and energy results. A significant economic improvement is observed, especially in periods with bad forecast of solar resource. Several future research lines are indicated: (1) the analysis of scenarios with imperfect forecast of electricity prices or higher level of penalty costs, (2) the development of more complex methods to estimate the penalty cost per MW h of deviation, and (3) the provision of robustness for the proposed approach. It is also important to highlight that the proposed approach can be translated to another renewable energy source with energy storage system.

Acknowledgements

This research has been supported by DPI2016-76493-C3-2-R Project of *Ministerio de Economía y Competitividad* (Spain). The authors would like to thank Acciona Energa S.A. for expressing interest in the project.

References

Channon, S., Eames, P., 2014. The cost of balancing a parabolic trough concentrated solar power plant in the Spanish electricity spot markets. Sol. Energy 110 (0), 83–95.
Dieulot, J.Y., Colas, F., Chalal, L., Dauphin-Tanguy, G., 2015. Economic supervisory predictive control of a hybrid power generation plant. Electr. Power Syst. Res. 127, 221–229.
Dinter, F., Gonzalez, D.M., 2014. Operability, reliability and economic benefits of CSP with thermal energy storage: first year of operation of ANDASOL 3. Energy Procedia 49 (0), 2472–2481. Proceedings of the SolarPACES 2013 International Conference.
Domínguez, R., Baringo, L., Conejo, A., 2012. Optimal offering strategy for a concentrating solar power plant. Appl. Energy 98 (0), 316–325.
García, I.L., Álvarez, J.L., Blanco, D., 2011. Performance model for parabolic trough solar thermal power plants with thermal storage: comparison to operating plant data. Sol. Energy 85 (10), 2443–2460.
He, G., Chen, Q., Kang, C., Xia, Q., 2016. Optimal offering strategy for concentrating solar power plants in joint energy, reserve and regulation markets. IEEE Trans. Sustain. Energy 7 (3), 1245–1254.
Kost, C., Flath, C.M., Most, D., 2013. Concentrating solar power plant investment and operation decisions under different price and support mechanisms. Energy Policy 61 (0), 238–248.
Kraas, B., Schroedter-Homscheidt, M., Madlener, R., 2013. Economic merits of a state-of-the-art concentrating solar power forecasting system for participation in the Spanish electricity market. Sol. Energy 93 (0), 244–255.
Kuravi, S., Trahan, J., Goswami, D.Y., Rahman, M.M., Stefanakos, E.K., 2013. Thermal energy storage technologies and systems for concentrating solar power plants. Prog. Energy Combust. Sci. 39 (4), 285–319.
Law, E.W., Prasad, A.A., Kay, M., Taylor, R.A., 2014. Direct normal irradiance forecasting and its application to concentrated solar thermal output forecasting — a review. Sol. Energy 108 (0), 287–307.
Law, E.W., Kay, M., Taylor, R.A., 2016a. Calculating the financial value of a concentrated solar thermal plant operated using direct normal irradiance forecasts. Sol. Energy 125, 267–281.
Law, E.W., Kay, M., Taylor, R.A., 2016b. Evaluating the benefits of using short-term direct normal irradiance forecasts to operate a concentrated solar thermal plant. Sol. Energy 140, 93–108.
Lizarraga-Garcia, E., Ghobeity, A., Totten, M., Mitsos, A., 2013. Optimal operation of a solar-thermal power plant with energy storage and electricity buy-back from grid. Energy 51 (0), 61–70.
Madaeni, S., Sioshansi, R., Denholm, P., 2012. How thermal energy storage enhances the economic viability of concentrating solar power. Proc. IEEE 100 (2), 335–347.
Marquez, R., Coimbra, C.F., 2011. Forecasting of global and direct solar irradiance using stochastic learning methods, ground experiments and the {NWS} database. Sol. Energy 85 (5), 746–756.
OMIE, 2017. <http://www.omie.es/> (last access: 28.04.17).
Petrollese, M., Valverde, L., Cocco, D., Cau, G., Guerra, J., 2016. Real-time integration of optimal generation scheduling with MPC for the energy management of a renewable hydrogen-based microgrid. Appl. Energy 166, 96–106.
Pousinho, H., Silva, H., Mendes, V., Collares-Pereira, M., Cabrita, C.P., 2014. Self-scheduling for energy and spinning reserve of wind/CSP plants by a MILP approach. Energy 78, 524–534.
Pousinho, H., Contreras, J., Pinson, P., Mendes, V., 2015. Robust optimisation for self-scheduling and bidding strategies of hybrid cspfossil power plants. Int. J. Electr. Power Energy Syst. 67 (0), 639–650.
Pousinho, H., Esteves, J., Mendes, V., Collares-Pereira, M., Cabrita, C.P., 2016. Bilevel approach to wind-CSP day-ahead scheduling with spinning reserve under controllable degree of trust. Renew. Energy 85, 917–927.
Powell, K.M., Hedengren, J.D., Edgar, T.F., 2014. Dynamic optimization of a hybrid solar thermal and fossil fuel system. Sol. Energy 108 (0), 210–218.
Purohit, I., Purohit, P., Shekhar, S., 2013. Evaluating the potential of concentrating solar power generation in Northwestern India. Energy Policy 62 (0), 157–175.
The SAM website, 2017. <https://sam.nrel.gov/> (last access: 28.04.17).
Simoglou, C.K., Biskas, P.N., Bakirtzis, A.G., 2012. Optimal self-scheduling of a dominant power company in electricity markets. Int. J. Electr. Power Energy Syst. 43 (1), 640–649.
Sioshansi, R., Denholm, P., 2010. The value of concentrating solar power and thermal energy storage. IEEE Trans. Sustain. Energy 1 (3), 173–183.

Sokoler, L.E., Dinesen, P.J., Jrgensen, J.B., 2016. A hierarchical algorithm for integrated scheduling and control with applications to power systems. IEEE Trans. Control Syst. Technol. PP (99), 1–10.

User's manual for TMY2s, 2017. <http://rredc.nrel.gov/solar/pubs/tmy2/> (last access: 28.04.17).

Touretzky, C.R., Baldea, M., 2014. Integrating scheduling and control for economic MPC of buildings with energy storage. J. Process Control 24 (8), 1292–1300.

Usaola, J., 2012. Operation of concentrating solar power plants with storage in spot electricity markets. IET Renew. Power Gener. 6 (1), 59–66.

Vasallo, M.J., Bravo, J.M., 2016a. A MPC approach for optimal generation scheduling in CSP plants. Appl. Energy 165, 357–370.

Vasallo, M.J., Bravo, J.M., 2016b. A novel two-model based approach for optimal scheduling in CSP plants. Sol. Energy 126, 73–92.

Wittmann, M., Eck, M., Pitz-Paal, R., Mller-Steinhagen, H., 2011. Methodology for optimized operation strategies of solar thermal power plants with integrated heat storage. Sol. Energy 85 (4), 653–659. SolarPACES 2009..

Zhang, H., Baeyens, J., Degréve, J., Cacéres, G., 2013. Concentrated solar power plants: review and design methodology. Renew. Sustain. Energy Rev. 22 (0), 466–481.

Renewable Energy 135 (2019) 789–799

Contents lists available at ScienceDirect

Renewable Energy

journal homepage: www.elsevier.com/locate/renene

Optimal scheduling in concentrating solar power plants oriented to low generation cycling

Emilian Gelu Cojocaru, José Manuel Bravo, Manuel Jesús Vasallo*, Diego Marín Santos

Department of Electronic Engineering, Computer Systems, and Automatics, University of Huelva, Carretera Palos de La Frontera s/n, 21819, Palos de La Frontera, Huelva, Spain

ARTICLE INFO

Article history:
Received 25 June 2018
Received in revised form
18 October 2018
Accepted 6 December 2018
Available online 11 December 2018

Keywords:
Concentrating solar power plant
Thermal energy storage
Electricity market
Optimized operation strategy
Generation cycling
Mixed-integer programming

ABSTRACT

In a one-day ahead energy market, power plant owners have to provide a generation schedule in advance. A scheduling strategy for concentrating solar power plants with thermal energy storage is studied in this paper. The strategy is based on a mixed-integer linear programming model which approximates the plant operation. The main novelty of the method is the inclusion in the optimization model of a penalty term for generation variation (cycling) with different intensities depending on the power block situation, i.e., normal operation, startup or shutdown. This distinction increases the search space for schedules with reduced cycling and high energy sale profits. Cycling reduction leads to higher lifetimes of the power block elements, lower maintenance costs, and easier plant operability. A simulation case study, based on a 50 MW plant participating in the Spanish market, is included. The main conclusion of this study is that an important reduction of the generation cycling can be achieved without reducing profits. Other advantages of the method are also shown. By means of historical data, it is possible to estimate the lowest level of generation cycling which maintains profits. Moreover, lower generation deviations are obtained, facilitating the tasks of the electric system operator.

1. Introduction

Concentrating solar power (CSP) can be considered an emerging technology that has attracted great interest in countries such as Spain and the USA thanks to the support of local governments. In CSP plants, the incoming sunlight is concentrated on a relatively small target area by mirrors or lenses, and thus produces medium to high temperatures. This thermal power is converted to electrical power using heat exchangers and a steam turbine connected to an electric power generator. The most commercially-attractive [1] and widely installed CSP technology [2] is based on parabolic trough collector (PTC) which uses synthetic or organic oil as the heat transfer fluid (HTF). Energy storage has proven to be a useful element to address the problem of the variability of renewable energy generation [3–5]. Specifically, the addition of thermal energy storage (TES) to CSP plants allows them to generate electricity at times of little or no solar irradiance, and to rearrange production from lower to higher price periods. The possibility of scheduling the electricity production (also called *self-scheduling*) encourages CSP plants to participate in electricity markets, where the aim of electricity producers is to maximize profits from the sale of energy. Moreover, forecasts of weather and electricity price must be considered because in electricity markets power plant owners have to offer a daily schedule ahead of time [6].

As detailed in the seminal work [7], mixed-integer linear programming (MILP) is a modeling method that can be used to schedule the generation plan of several types of power plants. Furthermore, it is possibly the most widely-used modeling method to obtain an optimal scheduling in CSP plants [8–14]. In this regard, the scheduling method used in this paper is based on MILP. However, different approaches to MILP can be found in literature, e.g. Refs. [15–17], where Nonlinear Programming is used to optimize the operation, and [6,18], where Dynamic Programming is employed.

It is important to remark that MILP approaches use approximated models to solve the scheduling problem. The simplifications commonly applied are: 1) hourly resolution, 2) linear relations between variables, and 3) simple operating constraints. In this context [13], proposes the use of a detailed model and a MILP model

* Corresponding author.
E-mail addresses: emilian-gelu.cojocaru@alu.uhu.es (E.G. Cojocaru), caro@diesia.uhu.es (J.M. Bravo), manuel.vasallo@diesia.uhu.es (M.J. Vasallo), diego.marin@diesia.uhu.es (D.M. Santos).

https://doi.org/10.1016/j.renene.2018.12.026
0960-1481/

to combine accuracy and MILP capabilities.

The accuracy of direct normal irradiance (DNI) forecasts limits the predictability of the electricity production in CSP plants. This point can be a problem when participating in day-ahead electricity markets due to the risk of being penalized for deviating from the committed generation schedule. Such penalties depend on the size of the deviation, so the accuracy of DNI forecasts is undoubtedly an important aspect [19]. In this regard [20,21], analyze the financial value of CSP plants based on DNI forecasts. Moreover, robust and stochastic approaches are applied to deal with the uncertainty of CSP production and energy price forecasts in the CSP scheduling problem [22–25]. Another alternative to face the problem of uncertainty is found in Refs. [26,27], where a generation rescheduling mechanism based on a model-based predictive control (MPC) approach was suggested and studied. All the above papers also use mixed-integer programming.

Because of energy prices and DNI variability, a scheduling method based solely on maximizing profits can result in numerous high intensity cycling operations. Cycling refers to changing the power output of plants by means of switching (starting up and shutting down) and load variation. The excessive thermal stress during cycling harms the lifetime of the elements of the power block, such as the steam generator and the turbine [28]. In this regard, the penalization for generation changes can result in an increase in power block lifetime and a reduction of maintenance costs, as well as an easier plant operability [14]. Several works have tackled the problem of the power block lifetime of CSP plants from the standpoint of design and low-level operation [29–33]. In the context of the generation scheduling problem, few studies have carried out a deep analysis about the impact of penalization for generation changes to the plant performance. It is common to find in literature hard operation constraints, such as ramp limits for charging/discharging power from TES [22,25] and for electricity generation [34,35]. Penalties for generation changes included in the objective function can be found in Refs. [9,14]. This last paper studies the economic impact when these penalties vary. The study is based on annual simulations and perfect forecast, and concluded that a significant reduction of generation variability is possible with little impact on economic results.

This paper proposes a MILP-based scheduling scheme for CSP plants with TES, oriented towards reducing the generation cycling, in the context of a day-ahead strategy. In this regard, the main novelty is the inclusion of a binary-regularization term that penalizes for generation cycling and encompasses some of the previously mentioned penalization terms, such as the one in Ref. [36]. This binary-regularization term is inspired in trimmed lasso [37], and combines binary variables with fussed lasso [38]. Binary variables are used to modulate the penalization intensity applied to generation cycling in different situations of the power block: normal operation, startup, and shutdown. This distinction increases the degree of freedom when searching for better economic solutions, and could allow for a more efficient use of the information about the power block damage under different situations. A simulation case study that carries out a sensibility analysis over the penalization parameters is included in this paper, studying the impact on the economic profits derived from energy sales. Unlike the work in Ref. [14], the economic study considers imperfect forecast for energy prices and solar resource, and therefore penalties for deviation from the committed generation schedule. Solutions with significantly reduced cycling and which maintain the energy sale profits were found. In summary, the main contributions of this work are: (1) a binary-regularization term is proposed to penalize generation changes in a day-ahead scheduling strategy for a CSP plant in order to increase the power block lifetime, to reduce maintenance costs, and to simplify the plant operability; and (2) its economical impact has been studied, in a simulation context, considering imperfect forecast for energy prices and solar resource, and penalties for deviation from the committed generation schedule. Other benefits of the method have been studied in this work: (1) the possibility of tuning the suitable level of cycling penalization based on historical data; and (2) a gain in robustness in relation to the DNI forecast uncertainty, which leads to lower generation deviations. Fig. 1 outlines the idea of cycling reduction that is studied in this paper.

The problem formulation is given in Section 2. The generation scheduling strategy and its optimization model are described in Sections 3 and 4, respectively. A case study is explained in Section 5. Finally, some conclusions are drawn in Section 6.

2. Problem formulation

This section starts with a description of the CSP plant. Next, the generation problem to be solved is described.

2.1. Concentrating solar power plant description

The type of plant considered in this work is a PTC-based CSP plant with TES. Fig. 2 shows a simplified diagram of this plant, which consist of three main blocks: the Solar Field (SF), the TES system, and the Power Block (PB). A fossil fuel backup is also common in this type of plants, but in this work it is not considered for electricity generation. The liquids circulating in the SF, TES and PB are HTF; HTF and molten salt; and HTF, water and steam, respectively. A heat-exchanger system allows for a bidirectional exchange of energy between the HTF and the molten salt, and another exchanger system allows for an energy transfer from the SF and/or TES to the PB.

The SF is composed of a number of PTC loops connected in parallel to each other. The collectors are formed by reflective parabolic mirrors and receiver tubes installed at the focal line of the parabolic surface. The circulating HTF runs through the receiver tubes. Insulated pipes distribute the HTF to the loops. A single-axis tracking mechanism enables the collectors to follow the sun. A large portion of the incident solar power is consequently concentrated onto the receiver tubes and transferred to the HTF, increasing its temperature.

Power flows between the different elements are also shown in

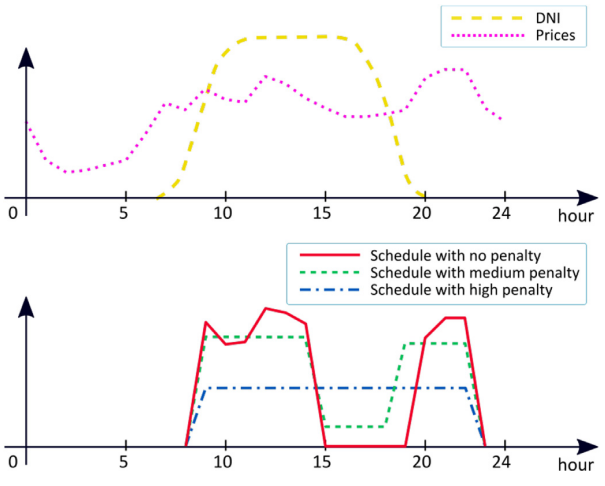

Fig. 1. Reduction in generation cycling.

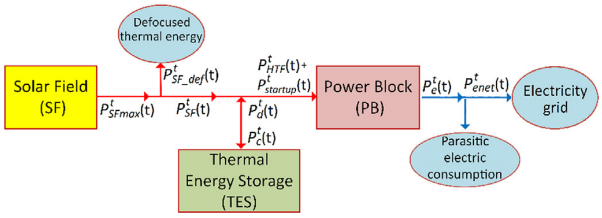

Fig. 2. Simplified diagram of a CSP plant with TES.

Fig. 2. The maximum thermal power available from the SF on the HTF side at daily time t is denoted as $P^t_{SFmax}(t)$. With $P^t_{SF_{def}}(t)$ we denote the part of this power that can be lost due to a partial or total defocus of the parabolic mirrors, which is sometimes necessary to avoid excessive HTF heating due to a low power demand. As such, the difference between the previous two variables is the thermal power actually transferred from the SF on the HTF side, denoted as $P^t_{SF}(t)$.

The TES system is an indirect two-tank molten salt system [39]. Molten salt circulates from the hot (cold) tank to the cold (hot) tank in energy discharging (charging) modes. As described above, a bidirectional heat exchanger system allows for energy transfer between the HTF and the molten salt. The discharging and charging thermal power on the HTF side in instant t are denoted $P^t_d(t)$ and $P^t_c(t)$, respectively.

The PB is made up of a heat exchanger train, a steam turbine that is coupled to an electricity generator, a condenser, a cooling system and other auxiliary elements. $P^t_{HTF}(t)$ is the thermal power in the PB inlet used to generate electricity. Note that $P^t_{HTF}(t)$ is equal to $P^t_{SF}(t) + P^t_d(t) - P^t_c(t) - P^t_{startup}(t)$, where $P^t_{startup}(t)$ is the fraction of thermal power used to increase the PB thermal state during startup. Finally $P^t_{enet}(t)$ is the electrical power transferred to the grid, which is a fraction of the generated electric power $P^t_e(t)$ in order to account for the parasitic electricity consumption by the plant.

Several power operating modes can be run at CSP plants (e.g., SF → PB, SF → TES, SF → PB + TES, SF + TES → PB, TES → PB). Moreover, the plant is operated by following a sequence of phases. Typical operating phases in the SF include nocturnal recirculation, freezing protection, HTF warm-up period, and sunlight period, among others.

2.2. The power generation problem

In this paper, the participation in a day-ahead energy market and the producer's price-taking property (i.e. its production schedules do not influence market prices) are assumed. The power generation problem is based on the following points:

- The problem is focused on high-level power sharing, with an hourly time scale, disregarding the low level control.
- The day D at instant $t = t_{subm}$ the CSP plant's owners must provide to the market an hourly generation profile for the next day ($D+1$). This profile, which represents the hourly mean values of the net power generation, is a commitment for the next day and therefore has to be considered as generation setpoints by the CSP plant.
- Moreover, each hour j of the current day (D), the mean net power generated by the CSP plant should be equal to the mean net power committed to the market the previous day (the generation setpoint). If this equality is not accomplished, the market applies some economic penalties associated to the difference.

For the sake of clarity, hereafter the name of the hourly mean-values power variables matches the names of the instantaneous variables except for the superscript t.

3. Power generation scheduling strategy

This section describes the scheduling strategy used to solve the power generation problem formulated in Subsection 2.2 and the building blocks of a potential implementation.

3.1. The day-ahead scheduling strategy

In order to solve the power generation problem, a MILP-based model is considered. A general description of this optimization model is presented in Section 4. The solution of this MILP problem is the hourly generation profile for the next day ($D+1$).

Fig. 3 shows the flowchart followed by the day-ahead scheduling (DAS) strategy used in this paper. At hour t of day D, the DAS scheduler provides the committed generation setpoint to the CSP plant. We assume that the CSP plant hourly generation is the maximum that can be reached while limited by the committed generation setpoint and the energy really available. If hour t is equal to t_{subm}, the generation schedule setpoints for day $D+1$ are obtained solving the MILP model with a time horizon length Δw (see Fig. 4). At this moment, the initial conditions for day $D+1$ are estimated using the current status of the plant, the day-ahead DNI forecast and the schedule still to be met. The time horizon Δw is set to a value higher than 24 h in order to consider the day $D+2$ (partially or totally) in the optimization problem.

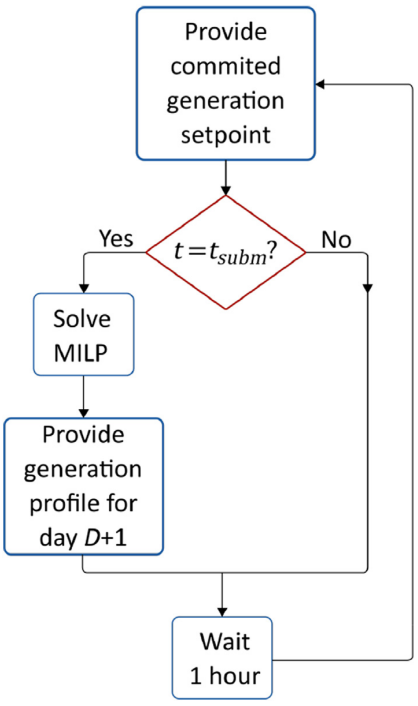

Fig. 3. Flowchart of the DAS strategy at hour t of day D.

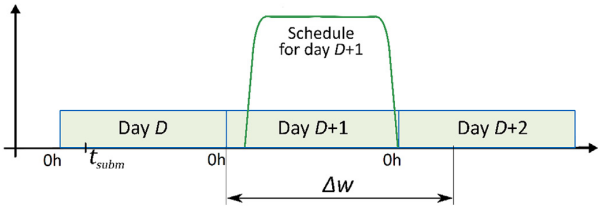

Fig. 4. Scheduling window of the DAS strategy.

3.2. The day-ahead scheduling strategy implementation

In order to implement the DAS strategy, a set of blocks is proposed (see Fig. 5):

- MILP-based scheduler. Considering that t denotes the daily time, as mentioned above, this block provides a day-ahead generation profile at time $t = t_{subm}$. This set of generation setpoints is obtained solving the MILP model.
- Setpoint provider. This block stores the day-ahead generation profile and provides the current setpoint for electricity generation.
- Initial condition estimator. At daily time $t = t_{subm}$, this block provides to the scheduler an estimation of the next day initial state of the CSP plant.
- Detailed SF model. This block is used to obtain predictions of the hourly mean value of the maximum thermal power available from the SF. DNI and other meteorological variables forecasts, and the state of CSP plant, are used to make these predictions.
- Electricity price predictor. Provides energy price forecasts.

Summarizing, at instant t_{subm} of day D the MILP-based scheduler block receives the following information:

1. An estimation of the initial state of the CSP plant at the beginning of day $D+1$.
2. Energy price forecasts made at time t_{subm} for days $D+1$ and $D+2$.
3. Predictions for the hourly mean value of the maximum thermal power available from the SF for days $D+1$ and $D+2$.

With this information the scheduler block solves the MILP problem and obtains the generation schedule profile. This profile is stored, as it will be applied during the next day (see block *Setpoint provider* in Fig. 5).

4. MILP model for generation scheduling

The optimization model presented in this paper is a one-hour-resolution extension of the one developed in Ref. [13]. The MILP model is composed of energy variables, binary variables, input data and parameters. The model parameters reflect the structural characteristics of the plant, or are mechanisms for adjustments in the optimization process. Input data are known variables (forecasts for maximum thermal power from the SF and electricity price) and initial conditions estimations. The energy variables represent the thermal energy in the TES, and hourly mean values for thermal or electrical energy flows among the distinct elements of the plant. The binary variables are necessary to formulate operating constraints.

Next, only the novel elements with respect to the original model are explained in detail. The set of constraints are described briefly. The reader is invited to consult [13] and the references included in it for a more detailed explanation.

4.1. Objective function

The objective function (expression 1) is a sum of economic revenues, costs, and a terminal value term. It combines several goals and therefore K, C_{Δ}, C_{Δ_β} and C_{Δ_λ} can be considered trade-off parameters.

$$\begin{aligned}\text{Maximize}\quad & KE(\Delta w+1)+\sum_{j=1}^{\Delta w}p(j)P_{enet}(j)\\ & -C_{\Delta}\sum_{j=1}^{\Delta w}\left|\Delta P_e(j)\right|(1-\beta(j)-\lambda(j))\\ & -C_{\Delta_\beta}\sum_{j=1}^{\Delta w}\left|\Delta P_e(j)\right|\beta(j)\\ & -C_{\Delta_\lambda}\sum_{j=1}^{\Delta w}\left|\Delta P_e(j)\right|\lambda(j)\end{aligned} \tag{1}$$

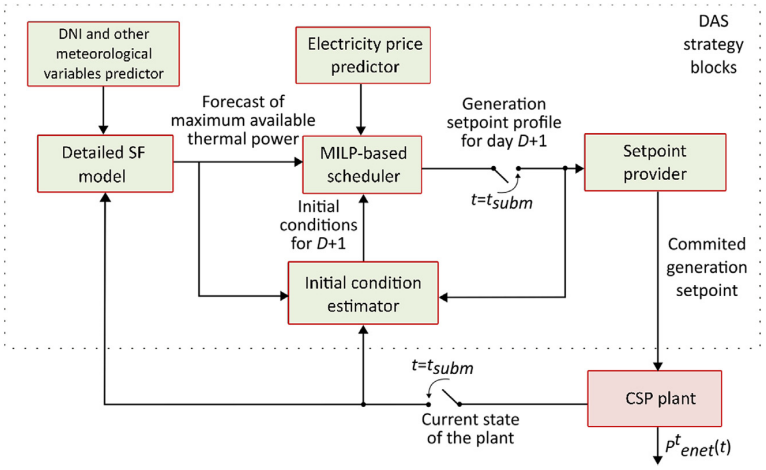

Fig. 5. Block diagram of the DAS strategy.

In the above expression, index j indicates the hour in the optimization window (the value $j = 0$ is associated to the last hour of day D, and $j = 1$ to the first hour of day $D + 1$); $P_e(j)$ and $P_{enet}(j)$ are turbine-generated gross and net electric power; $|\Delta P_e(j)|$ is the absolute value of the gradient of $P_e(j)$, with $\Delta P_e(j) = P_e(j) - P_e(j-1)$; $KE(\Delta w + 1)$ is the terminal value term formed by a value proportional to the final TES energy level; $\beta(j)$ and $\lambda(j)$ are binary variables with value equal to 1 if during hour j the turbine is in a startup or shutdown operation, respectively; and $p(j)$ are electricity price forecasts. Constant K is set to a small enough value to make the defocused thermal energy be as low as possible once the maximum economic profits (achieved without terminal value term) have been obtained. Note that minimizing the defocused thermal energy leads to the increase of the final TES energy. Lastly, the cycling penalization term includes parameters C_{Δ_β}, C_{Δ_λ} and C_Δ. They are the unit cost of the power gradient when the turbine is in startup, in shutdown, or is working in normal operation, respectively.

Although the objective function is nonlinear, $|\Delta P_e(j)|$ can be linearized by means of slack variables [40] and the products of binary and continuous variables using the method described in Appendix A of [13]. Since all constraints are also linear, or can be replaced by equivalent linear expressions, a MILP problem is formulated. In summary, expression (1) provides a tradeoff between the economic profit and the cycling level of the power block, being the maximization of the final TES energy level a secondary goal because of the small value selected for parameter K. Therefore, the only tuning parameters are C_{Δ_β}, C_{Δ_λ} and C_Δ (see Subsection 4.3 for a detailed explanation).

4.2. Constraints

A brief description of the set of constraints included in the MILP model is commented below.

- Energy balance constraints. These constraints express how thermal and electrical power is distributed and transformed among the elements of the plant, and also illustrate the dynamic behavior of the plant.
- Initial conditions constraints. These constraints indicate the TES energy and the turbine state at the initial instant of day $D + 1$.
- Operational constraints. Most of the operational constraints reflect the various physical characteristics of the plant, such as bounds for power values in the different elements of the plant, or limitations depending on the current operation in the plant (eg., stronger limitations during startup).
- Binary variables constraints. These constraints establish the logical relations between the binary variables.

4.3. Cycling penalization mechanism

The main contribution of this work is to study the impact of a cycling penalization mechanism included in the day-ahead scheduling strategy. This subsection explains the idea. Constraint (2) is included in order to force a generation schedule with a maximum of one power block start per day. Notice that this constraint is removed when $C_\Delta = 0$.

$$C_\Delta \sum_{j=1}^{24} \beta(j) \leq C_\Delta. \tag{2}$$

The objective function defined in expression (1) includes a cycling penalization term. The assumption made in this work about the power block damage is that lower values for $|\Delta P_e(j)|$ mean lower degradation. The tuning parameters $C_{\Delta_\beta}, C_{\Delta_\lambda}, C_\Delta \geq 0$ define the intensities of the cycling penalization. Parameter C_{Δ_β} is associated with the power gradient in the turbine startup, C_{Δ_λ} with the power gradient in the turbine shutdown, and C_Δ with the power gradient during the rest of the time when the turbine is working. Hereafter, in order to take into consideration the tuning parameters, the notation DAS(C_{Δ_β}, C_{Δ_λ}, C_Δ) indicates the values given to the parameters in the DAS strategy. Some interesting cases are enumerated below.

- Notice that DAS(0,0,0) implies a case without cycling penalization.
- In the DAS(C_Δ, C_Δ, C_Δ) strategy, with $C_\Delta > 0$, the cycling penalization term is reduced to

$$C_\Delta \sum_{j=1}^{\Delta w} \left| \Delta P_e(j) \right|.$$

The same level of penalization is applied to the generation variation during startup, shutdown or normal operation of the turbine. Similar penalization terms have been used in Refs. [9,14,36].

- On the other hand, with DAS(0,0, C_Δ) and $C_\Delta > 0$, the cycling penalization term is

$$C_\Delta \sum_{j=1}^{\Delta w} \left| \Delta P_e(j) \right| (1 - \beta(j) - \lambda(j)).$$

In order to generate electrical power we need to startup and shutdown the turbine. Therefore, in this case the penalization is not applied to startup and shutdown processes, considering they are necessary steps and the damage due to the intensity of both processes is not taken into account.

- Intermediate values of C_{Δ_β} and C_{Δ_λ}, i.e. DAS($\frac{1}{2}C_\Delta$, $\frac{1}{2}C_\Delta$, C_Δ), provide a combination between the two above cases.
- Other options can be considered with different values of C_{Δ_β}, C_{Δ_λ} and C_Δ, providing a wide range of cycling penalization strategies.

5. Case study

In this section, the DAS(C_{Δ_β}, C_{Δ_λ}, C_Δ) strategy is applied, in a simulation context, to a 50 MW PTC-based CSP plant with molten-salt-based TES. The CSP plant is based on the model presented in Ref. [41] and also used in Ref. [13], which describes the plant *Andasol 2* in Granada, Spain. Table 1 shows some characteristics of this model (adapted to this case study). The main objective of this study is to assess the economical impact on the energy sale profits of the cycling penalization method. With this purpose, a sensitivity study for the penalization parameters is carried out. Other advantages of the method are also found. Subsection 5.1 describes the

Table 1
Characteristics of the CSP plant.

Turbine capacity (gross)	52.5 MW-e
Solar field capacity	250 MW-t
Thermal capacity in solar-only mode	140 MW-t
Thermal capacity in TES-only mode	119 MW-t
Solar multiple	1.8
TES capacity (TES-only mode)	8 h
Power block efficiency (full load)	38%
Fossil backup only for preventing HTF freezing	

main features of the simulation scenario developed for this case study. Results and discussion are presented in Subsection 5.2.

5.1. Features of the simulation scenario

A time period of one year is considered (from 01/01/2013 to 31/12/2013). The Spanish day-ahead energy market and the producer's price-taking property are considered. Parameter t_{subm} is set to 10.0 h (Spanish market in 2013). Parameter Δw is set to 34 h. The values for the rest of parameters can be consulted in Ref. [13]. The hourly electricity price is obtained from the Iberian market operator OMIE [42] and can be seen in Fig. 6. A synthetic scenario for energy price forecast is generated using the persistent method and actual values of prices, with the goal of obtaining an annual mean for the metric RMSE (root mean square error) of 2.7 €/MW h [43] for the day-ahead forecast. Annual mean values for the metric RMSE are 3.3 €/MW h and 3.5 €/MW h for the two day-ahead and three-day ahead price forecasts, respectively. Penalty costs per MWh of deviation are obtained from the Spanish electric system operator [44]. No premium per MWh is considered. To generate predictions of the maximum thermal power available from the SF (see Fig. 5), the detailed SF submodel from Ref. [13] is used. DNI and ambient temperature are the only meteorological variables considered, and ambient temperature forecasts are assumed to be perfect and created from TMY2 data [45]. A set of solar radiation measures is available. In the same way as for prices, a synthetic scenario for DNI forecast is created using the persistent method and the actual values, with the purpose of achieving an annual mean for the metric nRMSE (normalized root mean square error) of 32% [19] for the day-ahead forecast. The DNI forecasts are supposed to be provided at 0.0 h every day. The persistent method is considered for the two-day-ahead and three-day-ahead DNI forecasts (see Fig. 4), obtaining annual values for nRMSE of 43% and 45%, respectively.

In the proposed simulation context, the CSP plant (see Fig. 5) is represented by the combination of two models. On the one hand, the detailed SF submodel characterizes the evolution of temperatures and operating phases in the SF, and generates the hourly mean values of the maximum thermal power available from the SF using the actual DNI data (see Fig. 7). On the other hand, a one-hour-resolution model is used to represent the energy balances in the rest of the plant's blocks. This structure avoids very high simulation times, as in Refs. [20,21]. Specifically, a second MILP model derived from the MILP model used for generation scheduling

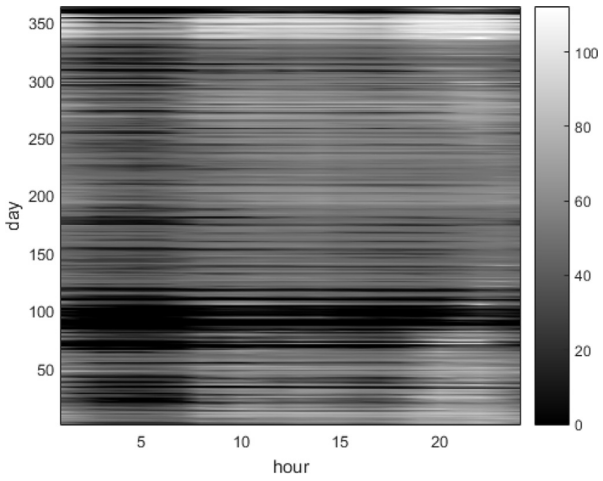

Fig. 6. Electricity prices during 2013 in the Spanish energy market (€/MW h).

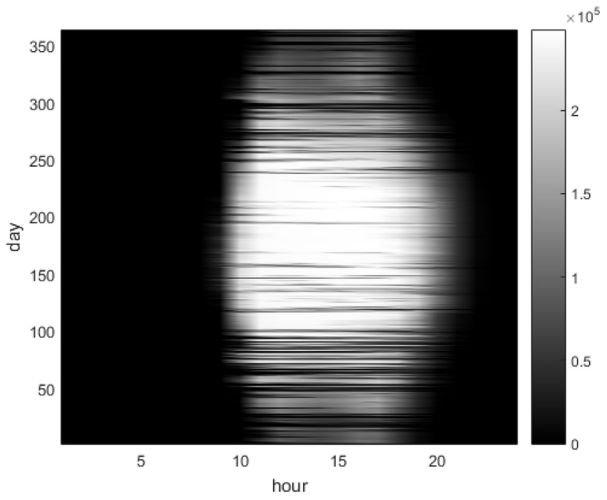

Fig. 7. Hourly average values for maximum thermal power available from the SF (P_{SFmax}, kW) for the case study.

is applied. This model receives each hour the generation power setpoint and the maximum available thermal power, and resolves the energy balance considering all the operating constraints. Among its outputs are the generated electric power and the plant's state (TES energy level and turbine ON/OFF state). It is composed of two consecutive optimization models. The first optimization goal is to minimize the generation error. Once this objective is met, the second optimization goal is to minimize the defocused thermal power in the SF. It is supposed that control systems and operator decisions comply with these operating rules. Fig. 8 shows the scheme for simulation.

MATLAB [46]; 0000) and a desktop computer was used as simulation platform. The MILP models were generated in YALMIP [47], a free toolbox for MATLAB, and solved by SCIP (v3.0.2) [48], a free solver for mixed integer problems. The size of the optimization problem for generation scheduling is 511 continuous variables, 272 binary variables and 1293 constraints. The approximate required computation times are: 1) generation and resolution of the MILP model for generation scheduling: 2 s, 2) one-day simulation of the detailed SF model: 12 s, and 3) annual simulation of the whole system: 2 h 50 min.

5.2. Results and discussion

The economic impact on energy sale profits when the level of

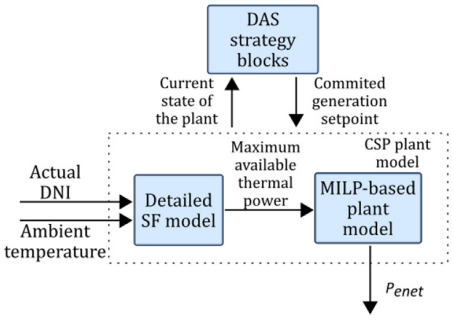

Fig. 8. CSP plant simulation by the combination of two models.

cycling penalty increases is studied first. The cycling reduction preserves the power block lifetime and reduces the maintenance costs, therefore it involves an economic benefit in the long term, although this aspect has not been studied quantitatively. Moreover, other benefits provided by the method are analyzed, such as the possibility of tuning the suitable level of cycling penalization based on historical data, and the reduction of generation deviation due to DNI forecast uncertainty.

5.2.1. Economic impact on energy sale profits

When the DAS(0,0,0) strategy (without cycling penalization) is applied to the considered time period, the total results are: profits = 7.854 millions €; revenues = 7.995 millions €; deviation penalties = 141 thousands €; the mean of the absolute value of the hourly gradient in the power block output $\overline{|\Delta P_e|} = 4.87$ MW; and the mean of the absolute value of the hourly gradient in the power block output when calculated removing gradients in startups and shutdowns $\overline{|\Delta P_e^B|} = 2.35$ MW. This is the reference case on which the bellow comparisons are based. Note that these two metrics aim to reflect the power block damage according to the assumption that lower values for $|\Delta P_e|$ mean lower damage. The second metric does not include damage during startups and shutdowns.

The strategies DAS(0,0, C_Δ), DAS($\frac{1}{2}C_\Delta$, $\frac{1}{2}C_\Delta$, C_Δ), and DAS(C_Δ, C_Δ, C_Δ) with $C_\Delta \in \{5, 30, 50, 100, 200, 1000\}$ €/MW h were simulated. Notice that the DAS($\frac{1}{2}C_\Delta$, $\frac{1}{2}C_\Delta$, C_Δ) strategy is an intermediate case between the other two. In order to illustrate the influence of the considered cycling penalization method on generation scheduling, Figs. 9 and 10 are included. Some generation profiles for the next day, obtained in the 14^{th} week of the simulated time period, have been represented. Fig. 9 shows the electricity prices and the generation profiles for the next day obtained by the reference case (without cycling penalization). It is important to remark the high variability observed in the scheduled profiles in order to follow the electricity prices and, therefore, to maximize economic profits. A next day profile with high variability is converted into a generation profile with high gradients, reducing the power block lifetime, and increasing the maintenance cost and the difficulty of the plant operation. The main goal of this work is to obtain generation profiles with an important reduction of this variability, but with a low economic impact. Fig. 10 shows the scheduled profiles obtained by the DAS(0,0, C_Δ), DAS($\frac{1}{2}C_\Delta$, $\frac{1}{2}C_\Delta$, C_Δ), and DAS(C_Δ, C_Δ, C_Δ) strategies

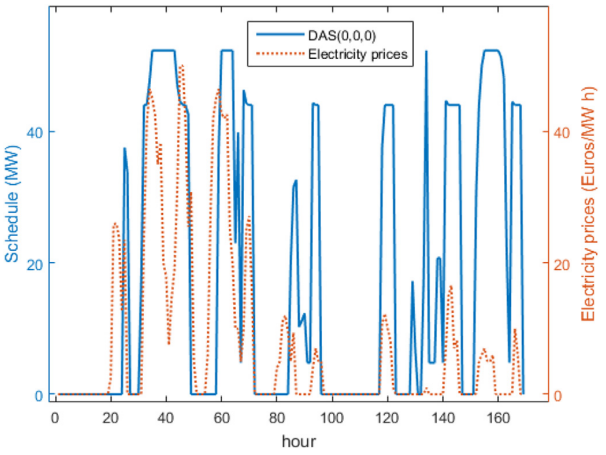

Fig. 9. Generation scheduling profile obtained in the 14^{th} week of the simulated time period.

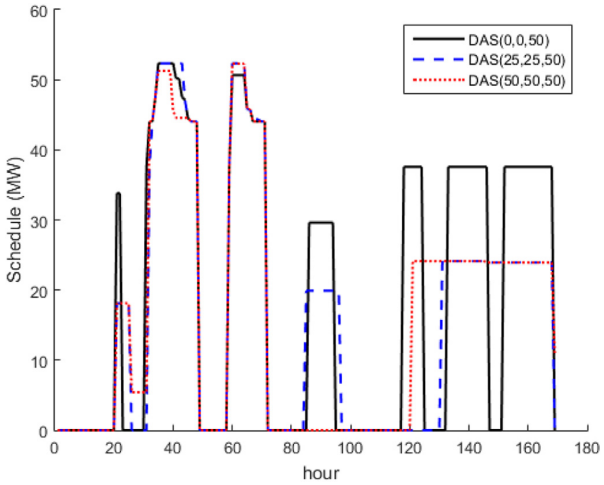

Fig. 10. Generation scheduling profiles obtained in the 14^{th} week of the simulated time period.

with $C_\Delta = 50$. In all cases, the high variability of the scheduled profiles is reduced in comparison to the reference case. As can be seen, the DAS(C_Δ, C_Δ, C_Δ) strategy reduces the number of startups and shutdowns due to the penalization in these processes but, as a consequence, it sometimes bounds the maximum electricity production in order to generate in an uninterrupted mode during a higher time period. Alternatively, the DAS(0,0, C_Δ) strategy presents startups and shutdowns every day of the example, therefore generally reaching higher generation levels than the DAS(C_Δ, C_Δ, C_Δ). On the other hand, DAS($\frac{1}{2}C_\Delta$, $\frac{1}{2}C_\Delta$, C_Δ) provides a compromise between the previous generation profiles.

Figs. 11 and 12 provide a study of the cycling penalization method in terms of obtained economic profits and generation variability. Simulations with cycling penalty parameter $C_\Delta > 0$ are compared with the reference case ($C_\Delta = 0$, i.e., without cycling penalization). For example, in Fig. 11, considering only the cases

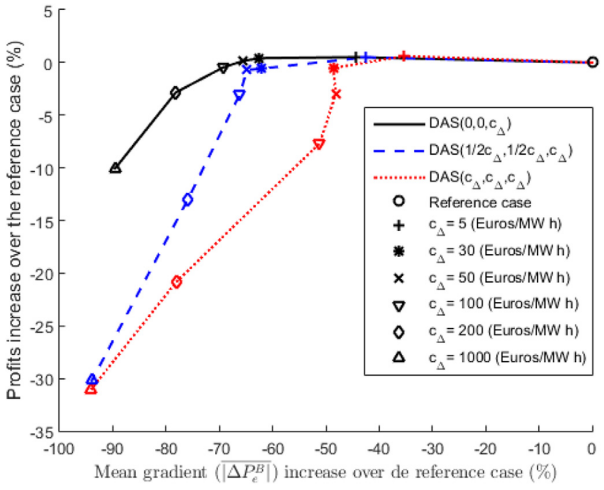

Fig. 11. Percentage increment of profits compared with the reference case (without cycling penalization) against percentage increment of $\overline{|\Delta P_e^B|}$ also compared with the reference case.

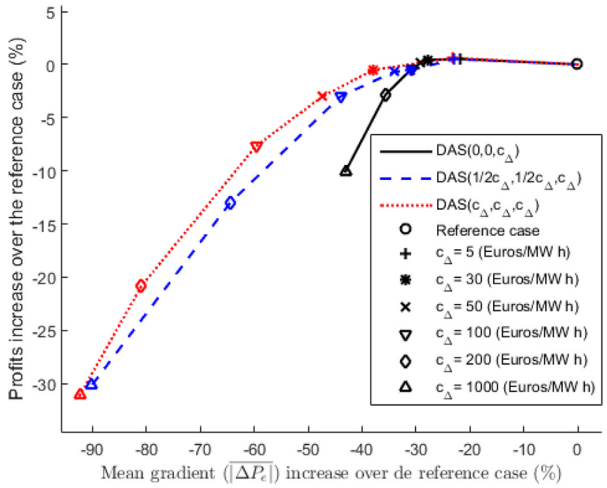

Fig. 12. Percentage increment of profits compared with the reference case (without cycling penalization) against percentage increment of $|\overline{\Delta P_e}|$ also compared with the reference case.

with $C_\Delta = 100$ €/MW h, the DAS(C_Δ, C_Δ, C_Δ) strategy (dotted line) obtains more than 50% reduction of $\left|\overline{\Delta P_e^B}\right|$, with a decrease of profits close to 8% compared to the reference case. The DAS(0,0, C_Δ) (solid line) and DAS($\frac{1}{2}C_\Delta$, $\frac{1}{2}C_\Delta$, C_Δ) (dashed line) strategies obtain a next to 70% decrease of $\left|\overline{\Delta P_e^B}\right|$. However, the DAS(0,0, C_Δ) strategy obtains a slight reduction of profits close to 0.5%, while DAS($\frac{1}{2}C_\Delta$, $\frac{1}{2}C_\Delta$, C_Δ) obtains a decrease of profits next to 3%.

The conclusions drawn from Figs. 11 and 12 are the following:

- The studied method obtains a significant reduction of $|\overline{\Delta P_e}|$ and $\left|\overline{\Delta P_e^B}\right|$ as C_Δ increases.
- The method improves the results obtained by the reference case ($C_\Delta = 0$) in the considered scenario. That is, there is a set of values of C_Δ where the strategies obtain the same or a slight increment of profits with respect to the reference case, and a significant reduction of gradients $|\overline{\Delta P_e}|$ and $\left|\overline{\Delta P_e^B}\right|$.
- As expected, the DAS(0,0, C_Δ) strategy improves the results obtained by the DAS(C_Δ, C_Δ, C_Δ) strategy if metric $\left|\overline{\Delta P_e^B}\right|$ is considered (see Fig. 11). In this case, the DAS(0,0, C_Δ) strategy obtains a next to 70% decrease of $\left|\overline{\Delta P_e^B}\right|$, while maintaining the profits at the same level as the reference case (see $C_\Delta = 100$ €/MW h). However, reaching a decrease of 70% of $\left|\overline{\Delta P_e^B}\right|$ with the DAS(C_Δ, C_Δ, C_Δ) strategy implies a severe decrease of profits (more than 10%).
- On the other hand, the DAS(C_Δ, C_Δ, C_Δ) strategy improves the results obtained by the DAS(0,0, C_Δ) strategy if metric $|\overline{\Delta P_e}|$ is considered (see Fig. 12), as would be expected.
- A compromise between the previous cases can be obtained if intermediate values of C_{Δ_β} and C_{Δ_λ}, that is, $0 < C_{\Delta_\beta} < C_\Delta$ and $0 < C_{\Delta_\lambda} < C_\Delta$, are considered.

As a conclusion we can say that the economically optimal solution is not very sensitive to the shape of the generation profile. More rigid generation profiles do not significantly worsen the economic profits, in fact, a slight improvement of profits is observed. This is an aspect in favor of using the cycling penalization mechanism studied in this work. An explanation of this slight improvement of profits could be found in the regular profiles obtained by the strategy with $C_\Delta > 0$, and its apparent ability to compensate the uncertainty present in the DNI and prices forecasts.

In order to study the influence of the uncertainty present in the DNI forecast, Figs. 13 and 14 are included. Simulations with perfect DNI forecast of the extreme cases DAS(0,0, C_Δ) and DAS(C_Δ, C_Δ, C_Δ), with $C_\Delta \geq 0$, are compared with the reference case ($C_\Delta = 0$ and imperfect DNI forecast). As can be seen, an expected increase in the obtained profits is observed due to the perfect DNI forecast. Except for this point, Figs. 13 and 14 are quite similar to Figs. 11 and 12, respectively. Therefore, the general conclusions drawn before are not altered by the uncertainty present in the DNI forecast, and thus they could be maintained for other forecasted DNI data.

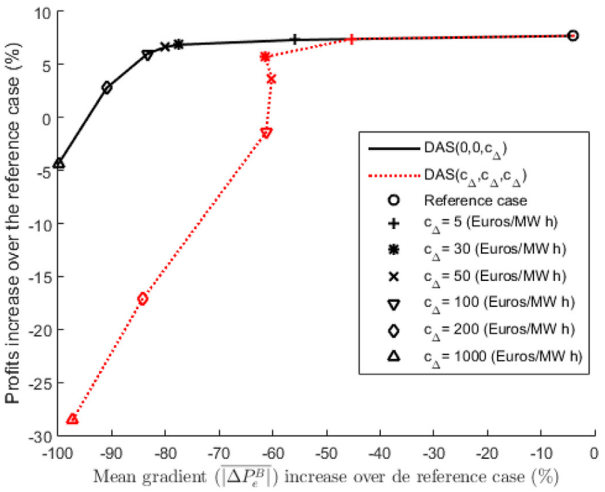

Fig. 13. Percentage increment of profits compared with the reference case (without cycling penalization) against percentage increment of $\left|\overline{\Delta P_e^B}\right|$ also compared with the reference case. Perfect DNI forecast case.

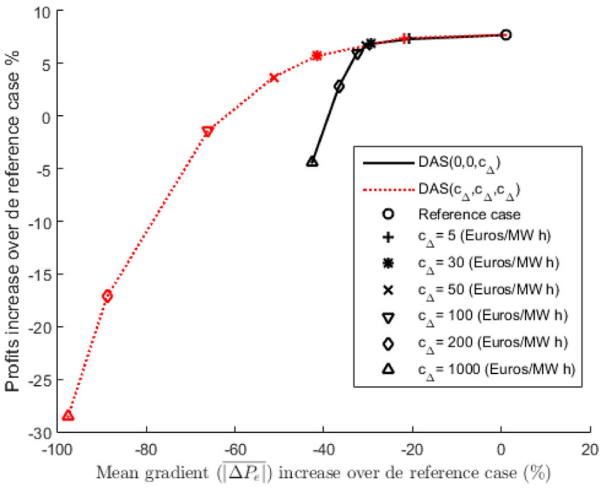

Fig. 14. Percentage increment of profits compared with the reference case (without cycling penalization) against percentage increment of $|\overline{\Delta P_e}|$ also compared with the reference case. Perfect DNI forecast case.

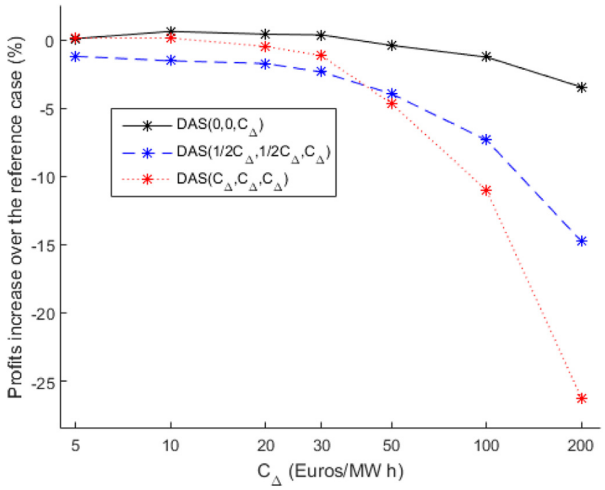

Fig. 15. Percentage increment of profits compared with the reference case (without cycling penalization) against C_Δ during the first four months.

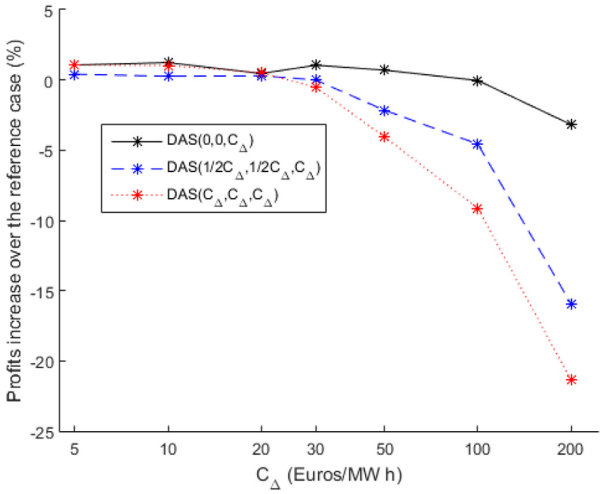

Fig. 17. Percentage increment of profits compared with the reference case (without cycling penalization) against C_Δ during the first six-month period.

5.2.2. *Tuning of penalization intensity*

An interesting issue is the estimation of a suitable C_Δ value. Of course, an obvious choice is the maximum value of C_Δ such that the obtained profits are similar to the profits obtained by the reference case ($C_\Delta = 0$). However, this value is not known in advance. A method to obtain an estimation of a suitable C_Δ value is by means of simulation using data from previous months. In this sense, Fig. 15 shows percentage increment of profits compared with the reference case for the DAS(0,0, C_Δ), DAS($\frac{1}{2}C_\Delta$, $\frac{1}{2}C_\Delta$, C_Δ), and DAS(C_Δ, C_Δ, C_Δ) strategies. These results are restricted to the first four months of the simulated time period. As can be seen, the level of profits is quite stable if $C_\Delta \leq 30$ is considered. This stability can be extended to values of $C_\Delta \leq 100$ in the DAS(0,0, C_Δ) strategy. Fig. 16, focused on the following two months, shows results similar to Fig. 15. Therefore, the results from the first four months of the simulated scenario could be used to infer a suitable C_Δ to be used in the two following months. Fig. 17 shows the overall percentage increment of profits compared with the reference case for the six-month period. This example illustrates the possibility of tuning the suitable level of penalization by means of simulations, using historical data (real and forecasted DNI and energy prices, and penalty costs). As a future line of research it is mentioned that more precise damage models could allow for the improvement of the penalization term, while the intensity of this penalization could be obtained by using historical data, as illustrated in the previous example.

5.2.3. *Reduction of generation deviation*

Another important issue to study is the deviation from the committed generation schedule obtained by the cycling penalization method. A minimal deviation is desired in order to avoid economic penalties, and to facilitate the solution to the imbalance problem of the grid with high renewable penetration [19]. Fig. 18 shows the percentage increment of profits compared with the reference case (without cycling penalization) against percentage

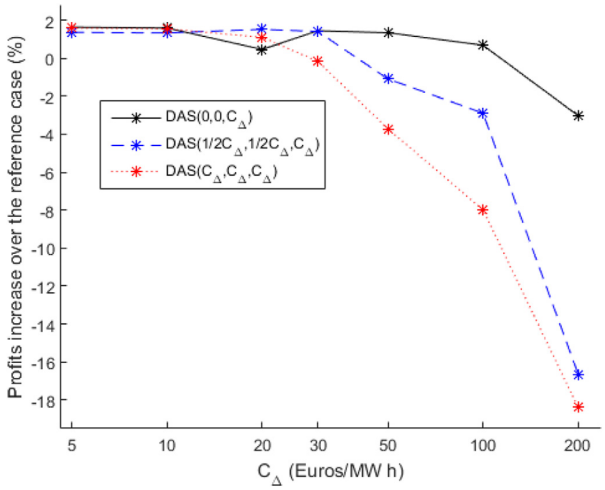

Fig. 16. Percentage increment of profits compared with the reference case (without cycling penalization) against C_Δ during the fifth and sixth months.

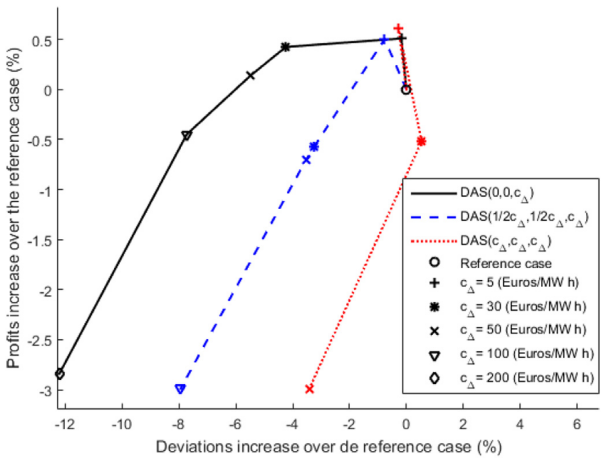

Fig. 18. Percentage increment of profits compared with the reference case (without cycling penalization) against percentage increment of generation deviation also compared with the reference case.

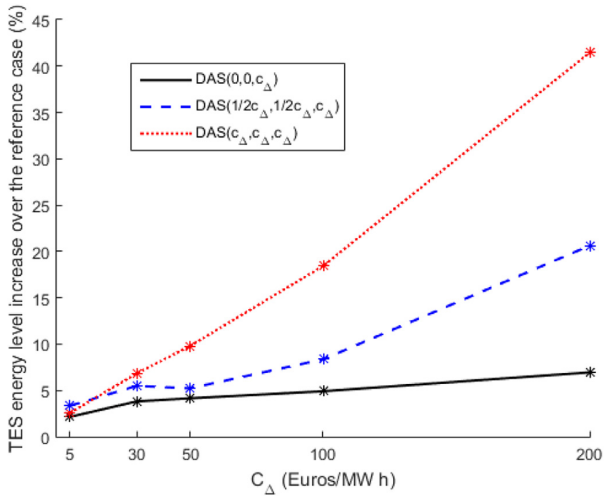

Fig. 19. Percentage increment of mean TES energy level compared with the reference case (without cycling penalization) against C_Δ.

increment of deviation also compared with the reference case. As can be seen, as C_Δ increases the deviation in all strategies tends to decrease. In fact, the DAS(0,0, C_Δ) strategy obtains next to 6% reduction (see $C_\Delta = 100$) in the resulting deviation compared to the reference case, with the same level of profits. However the reduction obtained by the strategies DAS($\frac{1}{2}C_\Delta$, $\frac{1}{2}C_\Delta$, C_Δ) and DAS(C_Δ, C_Δ, C_Δ) is considerably lower in the case with the same level of profits. In this respect, the DAS(0,0, C_Δ) strategy obtains better results in the simulated scenario.

Fig. 19 compares the percentage increment of mean TES energy level with the reference case (without cycling penalization) against C_Δ. In all strategies, the mean TES energy level increases as parameter C_Δ increases. This relation can explain the reduction of deviations commented before since, on average, more stored energy is available to avoid deviations. In this regard, C_Δ could be considered a robustness parameter from the deviation point of view.

6. Conclusions

A binary-regularization term is proposed to penalize generation changes in a day-ahead scheduling strategy for CSP plants. The search space for generation schedules with reduced cycling and high energy sale profits is increased in this method thanks to the application of different penalization intensities to the generation variation under distinct power block situations: normal operation, startup and shutdown. The method is applied, in a simulation context, to a 50 MW parabolic-trough-collector-based CSP plant with TES, under the assumption of participation in the Spanish day-ahead energy market, and of imperfect forecast of solar resource and energy prices. It could be observed in this study that the optimal solution is not very sensitive to the shape of the generation profile. Moreover, an important reduction of the generation cycling can be obtained without diminishing energy sale profits. The best result presents a next to 70% decrease in the mean of the absolute value of the hourly gradient in the turbine output when calculated only in normal operation. A significant cycling reduction is also achieved when the solar resource forecast is assumed perfect, which indicates a certain independence from the forecast accuracy. The advantages of a reduced cycling are higher lifetime for the power block elements, lower maintenance costs and easier plant operability. The possibility of adjusting the generation scheduling method in order to maintain energy profits while minimizing generation cycling is also analyzed in the case study. Historical data is used for this purpose. Another benefit of the reduced cycling is the decrease of deviation from the generation schedule submitted to the market, which facilities the functions of the electric system operator. A next to 6% reduction in deviation is obtained using the cycling penalization method. Finally, it is interesting to remark that the proposed approach could be applied to other renewable energy sources with energy storage systems.

Acknowledgements

This research has been supported by DPI2016-76493-C3-2-R Project of Ministerio de Economía y Competitividad (Spain). The authors would like to thank Acciona Energía S.A. for expressing interest in the project.

References

[1] I. Purohit, P. Purohit, S. Shekhar, Evaluating the potential of concentrating solar power generation in Northwestern India, Energy Pol. 62 (0) (2013) 157–175.
[2] H. Zhang, J. Baeyens, J. Degréve, G. Cacéres, Concentrated solar power plants: review and design methodology, Renew. Sustain. Energy Rev. 22 (0) (2013) 466–481.
[3] Y. Li, W. Gao, Y. Ruan, Performance investigation of grid-connected residential pv-battery system focusing on enhancing self-consumption and peak shaving in kyushu, Japan, Renew. Energy 127 (2018) 514–523.
[4] S.S. Reddy, Optimal scheduling of thermal-wind-solar power system with storage, Renew. Energy 101 (2017) 1357–1368.
[5] O. Talent, H. Du, Optimal sizing and energy scheduling of photovoltaic-battery systems under different tariff structures, Renew. Energy 129 (2018) 513–526.
[6] M. Wittmann, M. Eck, R. Pitz-Paal, H. Müller-Steinhagen, Methodology for optimized operation strategies of solar thermal power plants with integrated heat storage, Sol. Energy 85 (4) (2011) 653–659. SolarPACES 2009.
[7] A. Turgeon, Optimal scheduling of thermal generating units, IEEE Trans. Automat. Contr. 23 (6) (1978) 1000–1005.
[8] R. Sioshansi, P. Denholm, The value of concentrating solar power and thermal energy storage, Sustain. Energy, IEEE Trans. 1 (3) (2010) 173–183.
[9] J. Usaola, Operation of concentrating solar power plants with storage in spot electricity markets, Renew. Power Generat., IET 6 (1) (2012) 59–66.
[10] C. Kost, C.M. Flath, D. Most, Concentrating solar power plant investment and operation decisions under different price and support mechanisms, Energy Pol. 61 (0) (2013) 238–248.
[11] H. Pousinho, J. Esteves, V. Mendes, M. Collares-Pereira, C.P. Cabrita, Bilevel approach to wind-CSP day-ahead scheduling with spinning reserve under controllable degree of trust, Renew. Energy 85 (2016) 917–927.
[12] H. Pousinho, H. Silva, V. Mendes, M. Collares-Pereira, C.P. Cabrita, Self-scheduling for energy and spinning reserve of wind/CSP plants by a MILP approach, Energy 78 (2014) 524–534.
[13] M.J. Vasallo, J.M. Bravo, A novel two-model based approach for optimal scheduling in CSP plants, Sol. Energy 126 (2016b) 73–92.
[14] M.J. Wagner, A.M. Newman, W.T. Hamilton, R.J. Braun, Optimized dispatch in a first-principles concentrating solar power production model, Appl. Energy 203 (2017) 959–971.
[15] A. Ghobeity, C.J. Noone, C.N. Papanicolas, A. Mitsos, Optimal time-invariant operation of a power and water cogeneration solar-thermal plant, Sol. Energy 85 (9) (2011) 2295–2320.
[16] E. Lizarraga-Garcia, A. Ghobeity, M. Totten, A. Mitsos, Optimal operation of a solar-thermal power plant with energy storage and electricity buy-back from grid, Energy 51 (0) (2013) 61–70.
[17] K.M. Powell, J.D. Hedengren, T.F. Edgar, Dynamic optimization of a hybrid solar thermal and fossil fuel system, Sol. Energy 108 (0) (2014) 210–218.
[18] S. Channon, P. Eames, The cost of balancing a parabolic trough concentrated solar power plant in the Spanish electricity spot markets, Sol. Energy 110 (0) (2014) 83–95.
[19] E.W. Law, A.A. Prasad, M. Kay, R.A. Taylor, Direct normal irradiance forecasting and its application to concentrated solar thermal output forecasting — a review, Sol. Energy 108 (0) (2014) 287–307.
[20] B. Kraas, M. Schroedter-Homscheidt, R. Madlener, Economic merits of a state-of-the-art concentrating solar power forecasting system for participation in the Spanish electricity market, Sol. Energy 93 (0) (2013) 244–255.
[21] E.W. Law, M. Kay, R.A. Taylor, Calculating the financial value of a concentrated solar thermal plant operated using direct normal irradiance forecasts, Sol. Energy 125 (2016) 267–281.
[22] R. Domínguez, L. Baringo, A. Conejo, Optimal offering strategy for a

concentrating solar power plant, Appl. Energy 98 (0) (2012) 316–325.
[23] G. He, Q. Chen, C. Kang, Q. Xia, Optimal offering strategy for concentrating solar power plants in joint energy, reserve and regulation markets, IEEE Trans. Sustain. Energy 7 (3) (2016) 1245–1254, https://doi.org/10.1109/TSTE.2016.2533637.
[24] M. Petrollese, D. Cocco, G. Cau, E. Cogliani, Comparison of three different approaches for the optimization of the csp plant scheduling, Sol. Energy 150 (2017) 463–476.
[25] H. Pousinho, J. Contreras, P. Pinson, V. Mendes, Robust optimisation for self-scheduling and bidding strategies of hybrid csp-fossil power plants, Int. J. Electr. Power Energy Syst. 67 (0) (2015) 639–650.
[26] M.J. Vasallo, J.M. Bravo, A MPC approach for optimal generation scheduling in CSP plants, Appl. Energy 165 (2016a) 357–370.
[27] M.J. Vasallo, J.M. Bravo, E.G. Cojocaru, M.E. Gegúndez, Calculating the profits of an economic MPC applied to CSP plants with thermal storage system, Sol. Energy 155 (Supplement C) (2017) 1165–1177.
[28] P. González-Gómez, J. Gómez-Hernández, J. Briongos, D. Santana, Transient thermo-mechanical analysis of steam generators for solar tower plants, Appl. Energy 212 (2018) 1051–1068.
[29] S. Dettori, V. Iannino, V. Colla, A. Signorini, An adaptive fuzzy logic-based approach to PID control of steam turbines in solar applications, Appl. Energy 227 (2018) 655–664.
[30] D. Ferruzza, M. Topel, B. Laumert, F. Haglind, Impact of steam generator start-up limitations on the performance of a parabolic trough solar power plant, Sol. Energy 169 (2018) 255–263.
[31] M. Topel, B. Laumert, Improving concentrating solar power plant performance by increasing steam turbine flexibility at start-up, Sol. Energy 165 (2018) 10–18.
[32] M. Topel, M. Genrup, M. Jocker, J. Spelling, B. Laumert, Operational improvements for startup time reduction in solar steam turbines, ASME J. Eng. Gas Turbines Power 137 (4) (2015).
[33] J. Spelling, M. Jcker, A. Martin, Annual performance improvement for solar steam turbines through the use of temperature-maintaining modifications, Sol. Energy 86 (1) (2012) 496–504.
[34] T. Xu, N. Zhang, Coordinated operation of concentrated solar power and wind resources for the provision of energy and reserve services, IEEE Trans. Power Syst. 32 (2) (2017) 1260–1271.
[35] Y. Yang, S. Guo, D. Liu, R. Li, Y. Chu, Operation optimization strategy for wind-concentrated solar power hybrid power generation system, Energy Convers. Manag. 160 (2018) 243–250.
[36] E.G. Cojocaru, M.J. Vasallo, J.M. Bravo, D. Marn, A lifetime-extending model-based predictive control for scheduling in concentrating solar power plants, in: 2018 IEEE International Conference on Industrial Technology (ICIT), 2018, pp. 1732–1737.
[37] D. Bertsimas, M.S. Copenhaver, R. Mazumder, The Trimmed Lasso: Sparsity and Robustness, 2017.
[38] R. Tibshirani, M. Saunders, S. Rosset, J. Zhu, K. Knight, Sparsity and smoothness via the fused lasso, J. R. Stat. Soc. B (2005) 91–108.
[39] G. Peir, C. Prieto, J. Gasia, A. Jov, L. Mir, L.F. Cabeza, Two-tank molten salts thermal energy storage system for solar power plants at pilot plant scale: lessons learnt and recommendations for its design, start-up and operation, Renew. Energy 121 (2018) 236–248.
[40] S. Boyd, L. Vandenberghe, Convex Optimization, Cambridge University Press, United Kingdom, 2004.
[41] I.L. García, J.L. Álvarez, D. Blanco, Performance model for parabolic trough solar thermal power plants with thermal storage: comparison to operating plant data, Sol. Energy 85 (10) (2011) 2443–2460.
[42] OMIE. Last access: 25.05.18. http://www.omie.es/; 2018.
[43] Z. Yang, L. Ce, L. Lian, Electricity price forecasting by a hybrid model, combining wavelet transform, ARMA and kernel-based extreme learning machine methods, Appl. Energy 190 (Supplement C) (2017) 291–305.
[44] Red Eléctrica de España. Last access: 16.05.18. http://www.esios.ree.es/; 2018.
[45] User's manual for TMY2s. Last access: 25.05.18. http://rredc.nrel.gov/solar/pubs/tmy2/; 2018.
[46] MATLAB . Natick, Massachusetts: The MathWorks Inc., .
[47] J. Löfberg, YALMIP : a toolbox for modeling and optimization in MATLAB, in: Proceedings of the CACSD Conference. Taipei, Taiwan, 2004. http://users.isy.liu.se/johanl/yalmip.
[48] T. Achterberg, SCIP: solving constraint integer programs, Math. Program. Comput. 1 (1) (2009) 1–41.

Received: 13 September 2018 | Revised: 7 February 2019 | Accepted: 3 March 2019
DOI: 10.1002/oca.2498

SPECIAL ISSUE ARTICLE

WILEY

A binary-regularization-based model predictive control applied to generation scheduling in concentrating solar power plants

Emilian G. Cojocaru | José M. Bravo | Manuel J. Vasallo | Diego Marín

Departamento de Ingeniería Electrónica, de Sistemas Informáticos y Automática, Universidad de Huelva, Huelva, Spain

Correspondence
José M. Bravo, Departamento de Ingeniería Electrónica, de Sistemas Informáticos y Automática, Universidad de Huelva, Huelva 21819, Spain.
Email: caro@uhu.es

Funding information
Ministerio de Economía y Competitividad (Spain), Grant/Award Number: DPI2016-76493-C3-2-R

Summary

This paper proposes the use of model predictive control (MPC) with binary-regularization to manage the electric power generation problem in concentrating solar power plants with thermal energy storage. The main advantage of the of MPC with binary-regularization formulation is the inclusion of a power block protection method based on a binary-regularization term that penalizes power generation variation (also called generation *cycling*) differently according to the power block situation, ie, normal operation, startup, or shutdown. This distinction simplifies the choice of schedules with reduced variation and high energy sale profits. The interest in this reduction is the achievement of a higher lifetime of the power block elements, lower maintenance costs, and easier plant operability. A benefit of the generation scheduling based on MPC is the capacity of rescheduling the power generation at regular periods, taking advantage of the most recent energy prices and weather forecast, and of the plant's current state. An interesting question is if the proposed protection mechanism affects the economic results of the MPC black strategy. In this regard, an economic study based on a realistic simulation of a 50 MW parabolic trough collector-based concentrating solar power plant with thermal energy storage, under the assumption of participation in the Spanish day-ahead energy market scenario, is included. Realistic values for actual and forecasted solar resource and for energy price are used, and for penalties for deviation from the committed generation schedule. The economic study shows that the proposed scheduling method provides an important reduction of the generation cycling without decreasing energy sales profits. Another advantage of the proposed method is the possibility of estimating the highest level of power block protection, which maintains the profits by means of historical data, which favors its practical implementation.

KEYWORDS

energy system, power generation, predictive control application

1 | INTRODUCTION

As an emerging technology, the expansion of concentrating solar power (CSP) plants has been possible in countries such as Spain and the USA thanks to the support of local goverments. The most commercially attractive[1] and widely installed CSP technology[2] is based on parabolic trough collectors (PTCs), and uses synthetic or organic oil as the heat transfer fluid (HTF). The addition of thermal energy storage (TES) allows CPS plants to generate electricity during periods with little or no solar irradiance, and also to rearrange production and displace it from lower to higher price periods. The ability to schedule the plant's electricity production (also called *self-scheduling*) encourages the participation of CSP plants in electricity markets, where the aim of electricity producers is the maximization of profits from the sale of energy.

Model predictive control (MPC) is a well-known control technique[3] that uses a model to represent the plant in order to predict its future behavior, and has been used as a low-level control strategy in CSP plants.[4,5] This control approach is based on a sliding-window strategy where a cost function is optimized over a moving time horizon, allowing real-time optimization. Vasallo and Bravo[6] suggested to use a generation rescheduling mechanism based on an MPC approach in CSP plants with TES. Mixed-integer programming (MIP) was used as modeling tool. Mixed-integer programming allows to obtain the generation plan for several types of electrical plants, or to integrate scheduling and control.[7,8] Furthermore, it is possibly the most widely used modeling method in optimal scheduling for CSP plants.[9-11] The MIP approach allows for the implementation of practical hybrid MPC.[12] Taking into consideration the aforementioned, the formulation of the MPC with binary-regularization (MPC^{BR}) optimization problem proposed in this paper has been carried out using MIP. Basically, MPC^{BR} takes direct energy prices, direct normal irradiance (DNI), and other meteorological variables forecasts, and provides a generation scheduling profile solving a MIP.

In order to maximize profits from the sale of energy (tracking volatile energy prices), the MPC scheme proposed in the work of Vasallo and Bravo[6] can suggest an overactuated generation scheduling, ie, a schedule with numerous cycling operations of high intensity. The concept of cycling refers to the modification of the power output of a plant by means of switching (plant start-up and shutdown), and load variation. Cycling has a detrimental effect on the plant, as the excessive thermal stress from these actions reduces the lifetime of the elements of the power block, such as the steam generator and the turbine.[13] In this regard, the penalization for generation changes can result in an increase in power block lifetime and a reduction of maintenance costs, and an easier plant operability.[14] Considering an energy generation context with mixed energy sources, reducing the power generation variability from renewable sources has another indirect benefit worth mentioning, ie, a reduction in cycling of the fossil power plants in charge of meeting the challenge of ramping and providing reserve requirements,[15] resulting in a twofold effect. The problem of the power block lifetime of CSP plants has been tackled in several works, from the standpoint of design and low-level operation.[16-20] From the perspective of the generation scheduling problem, few studies have carried out a deep analysis concerning how the penalization of generation changes affects the plant performance. A common approach that is found in literature is the use of operation constraints, such as ramp limits for the TES charge and discharge power,[21,22] and for the electricity generation.[23,24] The penalization of generation changes included in the objective function can be found in the works of Usaola[10] and Wagner et al.[14] This last paper studies the economic impact resulting from the variation of these penalties. The study used annual simulations and a perfect forecast scenario, and concluded that the generation variability can be significantly reduced with little impact on economic results. Cojocaru et al[25] proposed to include in the MPC formulation an operational constraint to limit the number of turbine startups, and an ℓ_1-norm term, based on fused lasso,[26] to penalize the changes in the electricity generation. The ℓ_1-norm is an approximation of the sparsity-inducing ℓ_0-norm and can be used to reduce the variability of the operating point.[27] However, it has the negative effect of reducing the economic profits derived from the sale of energy.

This paper proposes a new extension of previous MPC approaches oriented to increase the lifetime of the power block. A power block protection method based on a new binary-regularization term that penalizes the generation variation is included. This new binary-regularization term is inspired in trimmed lasso,[28] and combines binary variables with fussed lasso.[26] The key idea is to reduce the changes in the electricity generation while improving the economic results obtained in the work of Cojocaru et al.[25] As a means of evaluating the penalization intensity applied to the generation cycling under different power block situations, ie, normal operation, startup, and shutdown, binary variables are used. In order to evaluate the impact of these parameters over the economic profits from energy sales, a simulation case study based on the Spanish day-ahead market, which carries out a sensibility analysis over the penalization parameters, is included in this paper.

The proposed MPC^{BR} approach is described in Section 3. A case study that verifies the economic improvement is included in Section 4. Finally, the conclusions are presented in Section 5, and a summary of the nomenclature in Appendix.

2 | PROBLEM FORMULATION

This section begins with a description of the CSP plant, followed by an explanation of the generation problem. Lastly, the proposed scheduling strategy and its optimization model are presented.

2.1 | Description of the CSP plant

The type of plant under consideration in this work is a PTC-based CSP plant with TES. A simplified diagram of the plant is given in Figure 1, showing three main blocks, ie, the solar field (SF), the power block (PB), and the TES system. In addition, common in this type of plant is a fossil fuel backup; yet, in this work, it is not considered for electricity generation. The liquid circulating in the SF is the HTF; with HTF, water, and steam circulating in the PB; and HTF and molten salt in the TES system. The bidirectional exchange of energy between the HTF and the molted salts of the TES is allowed for by a heat exchanger, with a second exchanger system providing the transfer from the SF and/or TES to the PB.

The SF is composed of a number of PTC loops connected in parallel to each other, with the collectors formed by reflective parabolic mirrors, and receiver tubes installed at the focal line of the parabolic surface. A single-axis tracking mechanism enables the collectors to follow the sun. A large portion of the incident solar power is consequently concentrated onto the receiver tubes and transferred to the HTF circulating through the receiver tubes, increasing its temperature. The distribution of HTF to the loops is made through insulated pipes.

The thermal power distribution between the various plant elements, and the electrical power generation, are also shown in Figure 1. The maximum thermal power available from the SF on the HTF side at daily time t is denoted as $P^t_{SF\,\max}(t)$. With $P^t_{\mathrm{SF\_def}}(t)$, we denote the part of this power that can be discarded due to a partial or total defocus of the parabolic mirrors, which is sometimes necessary to avoid HTF overheating due to a low power demand. As such, the difference between the previous two energy fluxes is the thermal power actually transferred from the SF on the HTF side, which is denoted as $P^t_{SF}(t)$.

The TES system is an indirect type, using two tanks of molten salt. TES energy charging involves molten salt circulation from the cold tank to the hot one, with a reversed flow in the discharge mode. As described above, a bidirectional heat exchanger system allows for the energy transfer between the HTF and the molten salt. The charging and discharging thermal power on the HTF side in instant t are denoted $P^t_c(t)$ and $P^t_d(t)$, respectively.

As for the PB, it is made up of a heat exchanger train, a steam turbine coupled to an electricity generator, a condenser, a cooling system, and other auxiliary elements. $P^t_{HTF}(t)$ is the thermal power in the PB inlet used to generate electricity. Note that $P^t_{HTF}(t)$ is equal to $P^t_{SF}(t)+P^t_d(t)-P^t_c(t)-P^t_{\mathrm{startup}}(t)$, where $P^t_{\mathrm{startup}}(t)$ represents the fraction of thermal power used to increase the PB thermal state during startup. Finally, $P^t_{enet}(t)$ is the net electrical power transferred to the electricity grid, which, in order to account for the parasitic electricity consumption by the plant, is a fraction of the generated electric power $P^t_e(t)$.

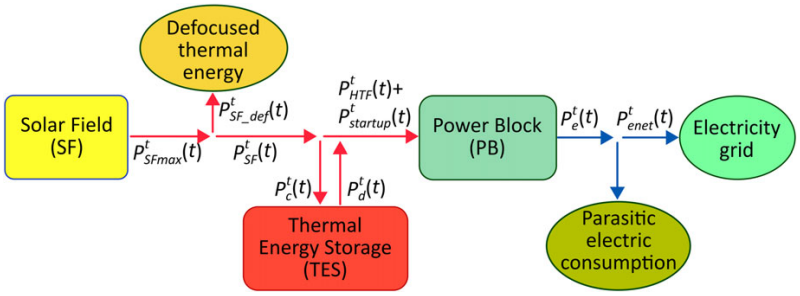

FIGURE 1 Simplified diagram of a concentrating solar power plant with thermal energy storage [Colour figure can be viewed at wileyonlinelibrary.com]

The CSP plants can be run in several power operating modes (eg, SF → PB, SF → TES, SF → PB + TES, SF + TES → PB, and TES → PB). Moreover, the plant is operated by following a sequence of phases. Concerning the SF, its specific operating phases include nocturnal recirculation, freezing protection, HTF warm-up period, and sunlight period, among others.

2.2 | The power generation problem

Concerning the power generation problem, it is assumed the participation in a day-ahead energy market, and the producer's price-taking property (ie, the generation schedule of a given producer does not influence market prices). The proposed problem is based on the following points.

- The focus is made on the high-level power sharing, with an hourly time scale, disregarding the low-level control.
- During day D at instant $t = t_{subm}$, the generation profile for the following day must be provided to the market by the CSP plant's owner. This profile, which consists of the hourly mean values of the net power generation, is denoted as $P^D_{eref}(j|D+1)$, with $j = 1, \dots, 24$. The generation schedule seeks to maximize economic benefits.
- Each hour j of the current day (D), the mean net power produced, denoted $P_{enet}(j|D)$, with $j = 1, \dots, 24$, should be equal to the mean net power committed the previous day, which is $P^D_{eref}(j|D)$ with $j = 1, \dots, 24$. Deviations from the scheduled generation result in some form of economic penalty applied by the market, which is asociated with the difference $P^D_{eref}(j|D) - P^D_{enet}(j|D)$, with $j = 1, \dots, 24$.

In summary, the power generation problem is two-fold, ie, to obtain a generation profile for the next day ($D + 1$), and to track the committed generation profile of the current day D. The CSP plant owners must solve the power generation problem in order to maximize the profits obtained from the electricity sales. For better clarity, hereafter, the name of the hourly mean value power variables will match the names of the instantaneous variables, except for the superscript t, which accompanies the instantaneous terms.

3 | MODEL PREDICTIVE CONTROL WITH BINARY-REGULARIZATION APPROACH

The MPC approach described in the works of Vasallo and Bravo[6] and Vasallo et al[29] is adopted for this work as starting point. Section 3.1 describes the sliding window on which the approach is based. The key ideas of the strategy are explained in Section 3.2. Section 3.3 makes a description of the functional blocks, which implement the strategy. A detailed description of the input and output data of the scheduler block is given in Section 3.4. The optimization model is described in Section 3.5. The PB protection mechanism included in the optimization model is explained in Section 3.6.

3.1 | Model predictive control sliding window

To address the power generation problem, the two goals of the MPC approach are as follows: (1) the economically optimal, regular tracking of the generation schedule that has been committed to and (2) the development of the optimal generation schedule for the next trading day at the appropriate time. These goals require the MPC sliding window to be divided into two intervals (see Figure 2), ie, the tracking interval (TI) and the next schedule interval (NSI). The generation schedule must then be updated to track the schedule that has been committed to within the TI interval, while the NSI interval is used to maximize future profits and generate the schedule for the following day at the appropriate time. Several variables and parameters related to the sliding window are defined as follows:

- $t(i) = i\Delta t_w$, where $i = 0, 1, \dots$ are the time instants when the MPC control generates its output. The beginning time of the sliding window when in position i is $t(i)$. Case $i = 0$ refers to instant 0.0 hours of the current day D. Δt_w is the time step for control update.
- t_{subm}, previously defined in Section 2.2, is the deadline hour in day D for the submission of the generation schedule for the next day $D + 1$. This deadline hour depends on each country's market.

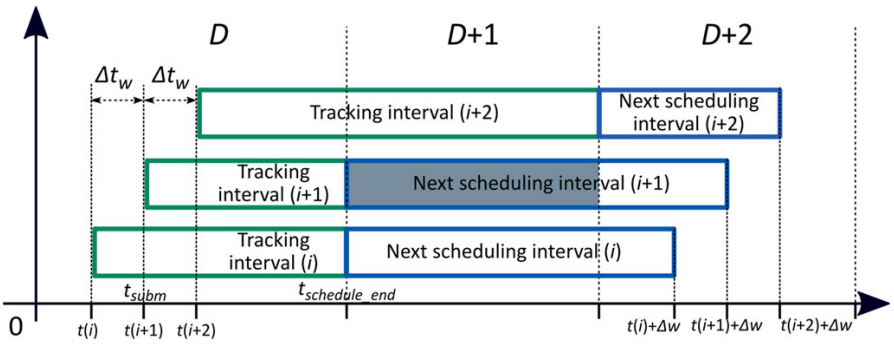

FIGURE 2 Sliding window of the model predictive control [Colour figure can be viewed at wileyonlinelibrary.com]

- $t_{schedule\_end}$ is the end time of the committed generation schedule. If the current time has not reached the time t_{subm}, $t_{schedule\_end}$ shall usually be 24.0 hour of day D. On the contrary, $t_{schedule\_end}$ shall be 24.0 hour of day $D + 1$ because the generation schedule for this day has already been delivered (see Figure 2).
- Δw is the constant length of the sliding window.

3.2 | Model predictive control with binary-regularization strategy

The MPC^{BR} strategy, which is proposed as the way to solve the power generation problem formulated in Section 2.2, is characterized by the following features.

- The optimization problem is modeled with mixed-integer linear programming (MILP), given that certain operational constraints have to be modeled with binary variables. A detailed description of this optimization model is presented in Section 3.5.
- The hourly generation along the sliding window is obtained at each time instant $t(i)$ by solving the MILP model. From this generation, only the first value is executed, as common in MPC approaches. This mechanism provides rescheduling capacity in order to take advantage of the most recent forecast information and the plant's state. The rescheduling aims to increase the economic profits, therefore compensating the penalty costs due to generation deviation.
- The schedule for day $D + 1$, $P^{D}_{eref}(j|D + 1)$, with $j = 1, \ldots, 24$, is generated using the solution returned by the MILP model at t_{subm}, specifically collecting the values into the time interval associated to day D+1. In Figure 2, the schedule for day $D + 1$ is shown by a shadowed interval.
- Parameter Δw is set to a value that will make the length of the NSI interval at t_{subm} of day D higher than 24 hours to partially or totally include day $D + 2$ in the optimization problem.

3.3 | Model predictive control with binary-regularization block diagram

In order to implement the MPC^{BR} strategy, a set of functional blocks is proposed (see Figure 3).

- MILP-MPC^{BR}–based scheduler. This block resolves the MILP model at each instant $t(i)$.
- Detailed SF model. The predictions of the hourly mean value of the maximum thermal power available from the SF are obtained using a detailed model of the SF, which is represented by this block. These predictions are made using DNI and other meteorological variables forecasts, and a set of continuous and binary variables obtained from the CSP plant, which characterize its current state, and depend on the model used to represent it. A description of the detailed CSP plant model and its distinct state variables is out of the scope of this work, but can be consulted in the work of Vasallo and Bravo.[11]
- Predictor blocks for DNI and other meteorological variables, and for electricity price. These blocks provide the input data for the scheduler block and the detailed SF model.
- Generation schedule builder. This block stores the generation schedule for day $D + 1$, when calculated at t_{subm} of day D, and sends the schedule still to be met to the MILP-MPC^{BR}–based scheduler.
- CSP plant. It is assumed that an integrated low-level control system is used to reach the generation set-point P_{e_SP}, while also minimizing the defocused thermal power in the SF through the use of TES.

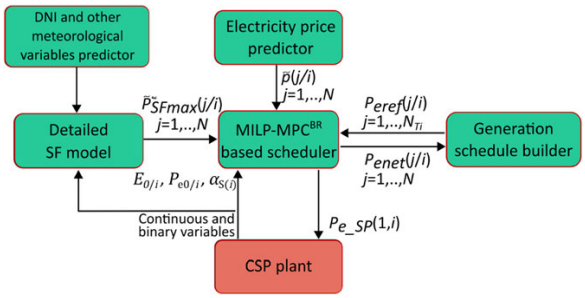

FIGURE 3 Block diagram of the model predictive control. CSP, concentrating solar power; DNI, direct normal irradiance; MILP, mixed-integer linear programming; MPC^{BR}, model predictive control with binary-regularization; SF, solar field [Colour figure can be viewed at wileyonlinelibrary.com]

3.4 | Mixed-integer linear programming–model predictive control with binary-regularization scheduler block

The MILP-MPC^{BR}–based scheduler block receives the following information at each sliding window position i (see Figure 3).

1. Updated continuous state of the CSP plant. The initial TES energy level ($E_{0/i}$) and the initial generated gross electric power ($P_{e0/i}$) are the only continuous variables considered in the MILP model developed in Section 3.5.
2. Updated discrete state of the plant. A set $\alpha_{\mathbb{S}(i)} = \{\alpha_{0/i}, \alpha_{-1/i}, \ldots, \alpha_{-\max(T_{\min\_u}, T_{\min\_d})/i}\}$ of past values for the binary variable, which indicates if the turbine is in operation, is the only information of this type required by the MILP model developed in Section 3.5. Parameters T_{min_u} and T_{min_d} are the minimum up time and minimum down time for the turbine. Several examples are shown to clarify the notation. $\alpha_{0/i}$ indicates the turbine ON/OFF state during the hour prior to the beginning of the sliding window, when the current position is i; $\alpha_{-1/i}$ refers to the penultimate hour prior to the beginning of the sliding window, and so on.
3. Energy price forecast made at time $t(i)$ ($\tilde{p}(j/i)$, for $j = 1, \ldots, N$), where j indicates each step in the MPC model, $N = \Delta w/\Delta t_o$ is the number of steps in the sliding window, and Δt_o is the time step of the MILP model expressed in hours. As the power generation problem has been defined with an hourly scale, parameter Δt_o is set to 1 hour. However, the general formulation for Δt_o will remain in the rest of this paper.
4. Predictions of the mean value of the maximum thermal power available from the SF ($\tilde{P}^{\omega}_{SF\,\max}(j/i)$, for $j = 1, .., N$) made at time $t(i)$.
5. Committed generation schedule still to be met ($P_{eref}(j/i)$, for $j = 1, .., N_{TI}$), expressed in average net electric power, where $N_{TI} = (t_{\text{schedule\_end}} - t(i))/\Delta t_o$ is the number of steps in the TI interval.

Next, the outputs generated as a result of the optimization at position i of the sliding window are indicated.

1. Mean values of turbine-generated net electric power calculated at time $t(i)$ ($P_{enet}(j/i)$, for $j = 1, .., N$). At instant $t(i) = t_{subm}$, the values inside the NSI interval until 24.0 hours of the following day are given as the new generation schedule for this day ($P_{eref}(j/i) = P^{D}_{eref}(j - N_{TI}|D + 1) = P_{enet}(j/i)$, for $j = N_{TI} + 1, .., N'_{TI}$, where $N'_{TI} = N_{TI} + 24/\Delta t_o$ is the new number of steps in the TI interval).
2. The generation setpoint $P_{e\_SP}(1, i) = P_{enet}(1/i)$. Note that only the first value is applied to the plant, as common in MPC approaches.

The MILP model, which resolves the optimization problem along the sliding window, is referred to in this paper as MILP-MPC^{BR} model in this paper. It must include technical and physical constraints, and the dynamic model of the plant. Section 3.5 describes this model.

3.5 | Mixed-integer linear programming–model predictive control with binary-regularization model

The optimization model presented in this paper is an extension of the one developed in the work of Vasallo and Bravo,[6] with the model presented there being a one-hour-resolution simplification of the detailed model also developed in that

paper. The detailed model is based on energy balances, except for the SF submodel, which makes use of a more detailed description of the temperature evolution. In the aforementioned paper, the MILP model excludes the SF submodel, considering the thermal power from the SF as input data. For the extended MILP model developed in this paper, the same structure is used, in coherence with what has already been mentioned in the previous sections.

For the set of equations and inequalities that compose the optimization model of the scheduler, the index j indicates the position in the optimization window (the value $j = 1$ is associated to the first interval). Negative and zero values of j refer to time intervals preceding the first one in the optimization window. The elements that compose the MILP model are energy variables, binary variables, input data, and parameters. The parameters in the model reflect the structural characteristics of the plant, or are mechanisms for adjustments in the optimization process. As input data, there are known variables (forecasts for maximum thermal power from the SF and for electricity prices, and generation schedule still to be met) and initial conditions. Energy variables are used to represent the thermal energy in the TES, and hourly mean values for thermal or electrical energy flows among the distinct elements of the plant. The operational constraints of the plant are formulated using binary variables. As an example, the binary variables α, β, and λ are equal to 1 if the turbine is in normal operation, in startup, or in shutdown, respectively. Note that the decision variables of the MILP-MPC^{BR} optimization problem are the energy and binary variables.

Next, a structured enumeration of the equations that form the MILP model is presented. A careful explanation of most of the constraints can be found in the work of Vasallo and Bravo.[6]

3.5.1 | Objective function

The objective function includes a set of terms that define economic revenues, costs, and a terminal value term. The distinct terms in this equation correspond to several goals, with the trade-off between them being modulated by means of various parameters accompanying the corresponding terms

$$\begin{aligned}\text{Maximize } J(i) = &\sum_{j=1}^{N} \tilde{p}(j/i) P_{enet}(j/i) - \sum_{j=1}^{N_{TI}} \phi(j/i)(P_{eref}(j/i) - P_{enet}(j/i)) - C_{\Delta_\beta} \sum_{j=1}^{N} |\Delta P_e(j/i)| \beta(j/i) \\ &- C_{\Delta_\lambda} \sum_{j=1}^{N} |\Delta P_e(j/i)| \lambda(j/i) - C_{\Delta} \sum_{j=1}^{N} |\Delta P_e(j/i)| \, (1 - \beta(j/i) - \lambda(j/i)) + KE(N+1/i).\end{aligned} \tag{1}$$

In the aforementioned expression, $\phi(j/i)$ is an estimation of the penalty cost per MW h of deviation at hour j; $KE(N+1/i)$ is the terminal value term, taking a value proportional to the final TES energy level, with constant K set to a small enough value as to obtain a minimum thermal energy defocus once the maximum economic profits (equal to the ones achieved without terminal value term) have been obtained (note that the effect of minimizing the defocused thermal energy results in the increase of the final TES energy); $|\Delta P_e(j/i)|$ is the absolute value of the increment of gross electric power generated in the PB, with $\Delta P_e(j/i) = P_e(j/i) - P_e(j-1/i)$; and lastly, C_{Δ_β}, C_{Δ_λ} and C_{Δ} are the unit cost of the power increment (see Section 3.6 for a detailed explanation of these terms). In this context, C_{Δ_β}, C_{Δ_λ} and C_{Δ} are tunable design parameters that penalize the generation variation.

Notice that the expression $J(i)$ represents the profits along the sliding window, and provides a tradeoff between the economic profit and the structural durability. In this paper, it is assumed that the electricity production does not exceed the committed schedule and, therefore, the term $\phi(j/i)$ refers to *falling* penalty. This point is assured by constraints (23).

In order to maintain a linear objective function, the nonlinear term $|\Delta P_e(j/i)|$ can be linearized by means of slack variables[30] and the products of binary and continuous variables, using the method described in appendix A of the work of Vasallo and Bravo.[11] Given that all the model constraints (shown as follows) are also linear, or allow their replacement by equivalent linear expressions, the problem is formulated as an MILP model. In summary, the terms in expression (1) correspond to the maximization of economic profits, of the PB protection, and of the final TES energy level, yet these are conflicting objectives. As such, expression (1) provides a trade-off between the economic profit and the protection level of the PB, with the maximization of the final TES energy level being a secondary goal, which is imposed by having a small value selected for parameter K. Therefore, the tuning parameters are reduced to $\phi(j/i)$, C_{Δ_β}, C_{Δ_λ}, and C_{Δ}.

3.5.2 | Energy balance constraints

These constraints model the distribution and transformation of thermal and electrical power among the elements of the plant, and illustrating the dynamic behavior of the plant (the only continuous state variable is the TES energy level).

For $j = 1, \ldots, N$

$$\tilde{P}^{\omega}_{SF\max}(j/i) = P_{SF}(j/i) + P_{SF\_def}(j/i) \tag{2}$$

$$P_{SF}(j/i) + P_d(j/i) = P_{HTF}(j/i) + P_c(j/i) + P_{\text{startup}}(j/i) \tag{3}$$

$$P_e(j/i) = \alpha(j/i)\left[aP_{HTF}(j/i) + b\right] \tag{4}$$

$$P_{enet}(j/i) = \eta_{\text{gross2net}} P_e(j/i) \tag{5}$$

$$E(j+1/i) = E(j/i) + Pc(j/i)\eta_{exch\_TES} - Pd(j/i)/\eta_{exch\_TES}. \tag{6}$$

The power balance on the HTF side is given by constraints (2) and (3). Constraints (4) and (5) reflect the conversion of thermal power $P_{HTF}(j/i)$ to electricity power $P_{enet}(j/i)$, where $\eta_{gross2net}$ is the ratio for the considered parasitic electric consumption, and a and b are two constants. The energy balance in the TES is reflected in expression (6) where $E(j/i)$ is the TES energy level at the beginning of the step j, and η_{exch_TES} is a constant related to the efficiency of the HTF-TES heat exchangers.

3.5.3 | Initial conditions constraints

These constraints impose the TES energy and the PB state at the initial instant of the sliding window, where $E_{0/i}$, $P_{e0/i}$ and $\alpha_{0/i}$ are the initial conditions previously defined in Section 3.4

$$E(1/i) = E_{0/i} \tag{7}$$

$$P_e(0/i) = P_{e0/i} \tag{8}$$

$$\alpha(0/i) = \alpha_{0/i}. \tag{9}$$

3.5.4 | Operational constraints

Most of the operational constraints define the various physical characteristics of the plant, such as bounds for power values in the different elements of the plant, or limitations specific to certain plant operations (eg, stronger limitations during startup). It is also possible to include constraints that strictly refer to a desired behavior, eg, to limit the number of daily turbine startups, as is the case of Equation (22). For $j = 1, \ldots, N$

$$P_{SF\_def}(j/i) \geq 0 \tag{10}$$

$$P_{SF}(j/i) \geq 0 \tag{11}$$

$$E_{\min} \leq E(j+1/i) \leq E_{\max} \tag{12}$$

$$\alpha(j/i)P_{HTF\min} \leq P_{HTF}(j/i) \leq \alpha(j/i)P_{HTF\max} \tag{13}$$

$$\mu(j/i)P_{c\min} \leq P_c(j/i) \leq \mu(j/i)P_{c\max\_exch} \tag{14}$$

$$\delta(j/i)P_{d\min} \leq P_d(j/i) \leq \delta(j/i)P_{d\max\_exch} \tag{15}$$

$$P_{d\max\_\text{mixed}}(j/i) = \delta(j/i)\left(1 - \frac{P_{SF}(j/i)}{P_{HTF\max}}\right)P_{d\max\_onlyTES} \tag{16}$$

$$P_d(j/i) \leq P_{d\max\_\text{mixed}}(j/i) \tag{17}$$

$$P_{\text{startup}}(j/i) = \beta(j/i)P_{\text{start\_up}} \tag{18}$$

$$P_{HTF}(j/i) \leq \beta(j/i)\Delta P_{HTF\_stu\_\max} + (1 - \beta(j/i))M \tag{19}$$

$$P_{HTF}(j/i) \geq \beta(j/i)pc\Delta P_{HTF\_stu\_\max} \tag{20}$$

$$S\left(T_{\min\_u}, T_{\min\_d}, \alpha_{\mathbb{S}(i)}\right) \tag{21}$$

$$C_{\Delta} \sum_{l=N_{TI}+1}^{\min(N_{TI}+24,\Delta w)} \beta(l/i) \leq C_{\Delta}. \tag{22}$$

For $j = 1, \ldots, N_{TI}$,

$$P_{enet}(j/i) \leq P_{eref}(j/i). \tag{23}$$

Parameters $E_{\min}, E_{\max}, P_{HTF\,\min}, P_{HTF\,\max}, P_{c\,\min}, P_{c\,\max\_exch}, P_{d\,\min}$, and $P_{d\,\max\_exch}$ define the lower and upper bounds of the energy in TES, and of the thermal power entering, charging, and discharging thermal power on the HTF side, respectively. These parameters are used in constraints (10) to (15) and reflect operational limits of the related variables. The binary variables $\mu(j/i)$ and $\delta(j/i)$ are equal to 1 if during hour j the TES is charging or discharging, respectively. Parameter $P_{d\,\max\_onlyTES}$ is the maximum value for discharging thermal power on the HTF side in the TES-only mode (TES → PB), and the variable $P_{d\,\max\_\mathrm{mixed}}(j/i)$ is the maximum value for discharging thermal power in mixed mode (SF + TES → PB) on the HTF side. Constraints (16) to (17) reflect an upper limit of discharging thermal power $P_d(j/i)$ in TES-only mode and mixed mode.

Energy constraints associated to the startup process are reflected in expressions (18) to (20), with only one type of startup curve being taken into account. From this curve, parameter $P_{\text{start\_up}}$ (approximated value for the fraction of thermal energy in the PB inlet used to increase the thermal state in the PB during an hour with startup) of expression (18) is obtained (see the work of Vasallo and Bravo[11]), with this energy being provided from either the SF, the TES, or as a mix from the two. It is assumed that the durations of the startup and shutdown processes are less than one hour. Expressions (19) and (20) set lower and upper bounds to $P_{HTF}(j/i)$ (see the work of Vasallo and Bravo[11]) during hours with startup. A ramp behavior is supposed for the startup process, so the upper bound for this process (parameter $\Delta P_{HTF\_stu\_\max}$) has a lower value than $P_{HTF\,\max}$. Parameter pc is the percentage to establish a minimum operating point when the turbine starts. The minimum time between consecutive turbine startups and shutdowns is established using the constraints (21), with the set of values $\alpha_{\mathbb{S}(i)}$ previously defined in Section 3.4. This set of constraints (21) can be consulted in the work of Domíngez et al.[21] Constraint (23) sets an upper bound for $P_{enet}(j/i)$ in the TI interval, equal to $P_{eref}(j/i)$. Constraint (22) is explained in Section 3.6.

3.5.5 | Binary variables constraints

These constraints establish the logical relations between the binary variables

$$\mu(j/i) + \delta(j/i) \leq 1 \tag{24}$$

$$\beta(j/i) - \lambda(j/i) = \alpha(j/i) - \alpha(j-1/i) \tag{25}$$

$$\beta(j/i) + \lambda(j/i) \leq 1. \tag{26}$$

Constraint (24) ensures that simultaneous TES charge and discharge is not allowed. The binary variables $\alpha(j/i)$, $\beta(j/i)$, and $\lambda(j/i)$ define turbine normal, startup, or shutdown operation by means of constraints (25) and (26). In turbine normal operation, the binary variables are defined by $\beta(j/i) = 0$, $\lambda(j/i) = 0$, and $\alpha(j/i) = \alpha(j-1/i) = 1$; in startup by $\beta(j/i) = 1$, $\lambda(j/i) = 0$, $\alpha(j/i) = 1$, and $\alpha(j-1/i) = 0$; and in shutdown by $\beta(j/i) = 0$, $\lambda(j/i) = 1$, $\alpha(j/i) = 0$, and $\alpha(j-1/i) = 1$. Note that when the turbine is stopped the values of the three binary variables are equal to 0. Constraint (26) ensures that simultaneous startup and shutdown is not allowed.

3.6 | Power block protection mechanism

The main contribution of this work is to study the impact of the double PB protection mechanism included in the MPC^{BR} scheduling strategy, whose goal is to reduce the generation cycling. The assumption made in this work about the PB damage is that lower values of $|\Delta P_e(j/i)|$ mean higher protection. The first protection mechanism is the term

$$-C_{\Delta_\beta} \sum_{j=1}^{N} |\Delta P_e(j/i)| \beta(j/i) - C_{\Delta_\lambda} \sum_{j=1}^{N} |\Delta P_e(j/i)| \lambda(j/i) - C_{\Delta} \sum_{j=1}^{N} |\Delta P_e(j/i)| \left(1 - \beta(j/i) - \lambda(j/i)\right),$$

of the objective function defined in expression (1). This penalization term is based on fused lasso,[26] which penalizes by ℓ_1-norm the differences of the decision variables. The penalization term tries to shrink to exactly zero the different

$\Delta P_e(j/i)$, providing high protection. However, the generation of electric power requires startup and shutdown operations of the PB. In order to take into account this point, the difference $|\Delta P_e(j/i)|$ is combined with the binary variables $\beta(j/i)$ and $\lambda(j/i)$, and expression $(1 - \beta(j/i) - \lambda(j/i))$. This point is inspired in trimmed lasso,[28] an extension of lasso that uses binary variables to control the shrinkage to towards sparse models. The tuning parameters $C_{\Delta_\beta}, C_{\Delta_\lambda}, C_\Delta \geq 0$ define the intensity of the PB protection. Parameter C_{Δ_β} is associated to the power increment during turbine startup, C_{Δ_λ} to the power increment during turbine shutdown, and C_Δ to the power increment during the rest of the time when the turbine is working.

Some cases of interest are enumerated as follows.

- Having values of $C_{\Delta_\beta} = 0$, $C_{\Delta_\lambda} = 0$, and $C_\Delta = 0$ corresponds to a case with no PB protection.
- Considering a strategy with $C_{\Delta_\beta} = C_{\Delta_\lambda}$ and $C_{\Delta_\lambda} = C_\Delta > 0$, the PB protection term is reduced to

$$-C_\Delta \sum_{j=1}^{N} |\Delta P_e(j/i)|.$$

  This translates to having the same level of penalization applied to the generation variation during startup, shutdown, or normal operation of the turbine. Similar penalization terms have been used in other works.[10,14,25]
- For a different case of interest, with $C_{\Delta_\beta} = 0$, $C_{\Delta_\lambda} = 0$, and $C_\Delta > 0$, the PB protection term is

$$-C_\Delta \sum_{j=1}^{N} |\Delta P_e(j/i)| \left(1 - \beta(j/i) - \lambda(j/i)\right).$$

  In this case, the penalization is not applied during startup and shutdown, considering that they are necessary processes, and the damage due to the intensity of both process is not taken into account.
- Intermediate values of C_{Δ_β} and C_{Δ_λ}, ie, $C_{\Delta_\beta} = \frac{1}{2}C_\Delta$, $C_{\Delta_\lambda} = \frac{1}{2}C_\Delta$, and $C_\Delta > 0$, provide a combination between the two aforementioned cases.
- Other options can be considered with different values of C_{Δ_β}, C_{Δ_λ}, and C_Δ, providing a wide range of PB protection strategies.

An additional protection mechanism is given by the inclusion of the constraint (22), which forces a generation schedule where only one PB start per day is allowed, as a maximum. It can be noticed that a value of $C_\Delta = 0$ removes this constraint.

4 | CASE STUDY

This section presents the application of the MPC^{BR} approach proposed by this paper, in a simulation context, to a 50 MW PTC-based CSP plant with molten-salt-based TES. The CSP plant is based on the model presented in the work of Llorente et al[31] and also used in the work of Vasallo and Bravo,[6] which describes the plant *Andasol* 2 in Granada, Spain. Some characteristics of this model (adapted to this case study) are shown in Table 1. Note that the solar multiple is the ratio between the SF thermal capacity and the PB thermal capacity. The main features of the simulation scenario developed for this case study are described in Section 4.1. Results and discussion are presented in Section 4.2.

TABLE 1 Characteristics of the concentrating solar power plant

Description	Value
Turbine capacity (gross)	52.5 MWe
Solar field thermal capacity	250 MWt
Thermal capacity in solar-only mode	140 MWt
Thermal capacity in TES-only mode	119 MWt
Solar multiple (SF thermal capacity/PB thermal capacity)	1.8
TES capacity (TES-only mode)	8 hours
Power block efficiency (full load)	38%
Fossil backup only for preventing HTF freezing	

Abbreviations: HTF, heat transfer fluid; PB, power block; SF, solar field; TES, thermal energy storage.

4.1 | Features of the simulation scenario

The simulations are performed considering a time period of six months (from January 1, 2013 to June 30, 2013). The context under consideration is the Spanish day-ahead energy market, with the producer's price-taking property. The penalty costs per MW h of deviation are obtained from the Spanish electric system operator.[32] No premium per MW h is considered in this study.

4.1.1 | Input data of the MILP-MPC^{BR} model

At instant $t_{subm} + 1$ of day D, it is supposed that the prices are cleared on the market; therefore, prices for the day $D + 1$ are known from this moment. Energy price forecasts are generated using a synthetic method based on the persistent method and actual values of prices (obtained from the Iberian market operator OMIE,[33] see Figure 4). At day D before t_{subm}, the last known energy prices are the prices of day D. A persisten predictor uses these prices to make the prediction of day D+1 (one-day-ahead forecast) and day D+2 (two-day-ahead forecast). Of course, this is a naive forecast method that can not compete with other forecast methods. In order to make the energy prices forecast more realistic, we have consulted in the literature the level of forecast error obtained by other methods, ie, based on regression methods with exogenous variables. In this paper, we use a synthetic scenario for energy prices forecast using a mix of the persistent method and the actual value of energy prices in order to obtain a root mean square error (RMSE) of 2.7 $euros/MWh$[34] for the day-ahead forecast and 3.3 $euros/MWh$ for the two-day-ahead price forecast. The RMSE is the error between the used energy prices forecast and the actual energy prices. A carefully explanation of the synthetic method used can be consulted in the Appendix.

To generate the predictions $\tilde{P}^{\omega}_{SF\,\max}(j/i)$ (see Figure 3), the detailed SF submodel from the work of Vasallo and Bravo[6] is used. The DNI and ambient temperature are the only meteorological variables considered, with the ambient temperature forecasts assumed to be perfect, and created from TMY2 data.[35] A set of solar radiation measures is available. In the same way as for prices, a synthetic scenario for DNI forecast is generated using the persistent method and the actual values, with the generated forecast having an annual mean value for the metric normalised RMSE of 32%[36] for the day-ahead forecast. The DNI forecasts are supposed to be provided at 0.0 hour every day. The persistent method is considered for the two-day-ahead and three-day-ahead DNI forecasts (see Figure 2), with these predictions obtaining annual values for normalized RMSE of 43% and 45%, respectively. In order to take into account fresh data, short-term DNI forecasts with a time horizon of 5 hours are also included in this study. Several methods to obtain this kind of forecast can be consulted in the work of Law et al.[36] A parameterized model is used to emulate the short-term predictor (see the work of Vasallo et al[29]) and to overcome the lack of short-term DNI forecast data for this study. One of its parameters, ω, is a value between 0 and 1, and represents the accuracy of the forecasts (from ideally perfect short-term DNI forecast to nonexisting short-term DNI forecast, respectively). This range allows analyzing the influence of short-term DNI forecasts in spite of the lack of this data.

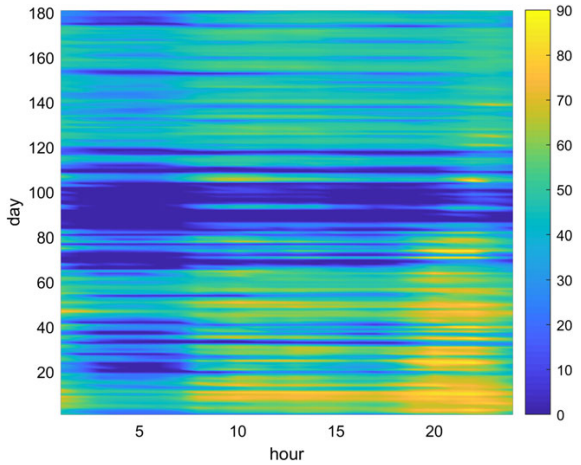

FIGURE 4 Electricity prices (€ /MW h) during the first six-month period of 2013 in the Spanish day-ahead energy market [Colour figure can be viewed at wileyonlinelibrary.com]

4.1.2 | Parameters of the MILP-MPC^{BR} model

Parameter Δt_w is set to 1.0 hour (see Figure 2). Parameter t_{subm} is set to 10.0 hours (Spanish market in 2013). Parameter Δw is set to 48 hours. As commented before, parameter K of the terminal value term in the objective function (expression (1)) is set to a small enough value so that, $K = 1e-7$ €/MW h, once the maximum economic profits (without terminal value term) have been obtained, the defocused thermal power may be as low as possible. Concerning the Spanish energy market, deviations from the scheduled generation produce penalty costs if they require the intervention of the transmission system operator. These penalties are associated with the costs incurred to stabilize the system, and do not follow any pregiven function. In this work, the estimation $\phi(j/i) = \gamma\bar{\phi}$ is used, where $\bar{\phi} = 6$ €/MW h is the mean value for the penalty costs in 2012 in the Spanish Market and $\gamma \geq 0$ is a tuning parameter. Parameter γ defines the relative importance of the deviation penalization term in the considered cost function of the MPC^{BR} strategy. An economic study for different appplied values of parameter γ is included in this paper to analyze the importance of an accurate estimation of $\bar{\phi}$.

In summary, the tuning parameters, which determine the MPC strategy, are the deviation penalization parameter γ, the short-term DNI accuracy parameter ω, and the cycling penalization parameters C_{Δ_β}, C_{Δ_λ}, and C_Δ. The notation $\text{MPC}^{BR}_{\omega,\gamma}(C_{\Delta_\beta}, C_{\Delta_\lambda}, C_\Delta)$ is used to refer to the values used for the tuning parameters.

4.1.3 | Simulation plant model

For the considered simulation context, the CSP plant (see Figure 3) is represented by the combination of two models. The first of them is the detailed SF submodel, which characterizes the evolution of temperatures and operating phases in the SF, and generates the hourly mean values of the maximum thermal power available from the SF using the actual DNI data (see Figure 5). A complete description of the detailed SF submodel is out of the scope of this paper but can be consulted in the work of Vasallo and Bravo.[11] The second model is a one-hour-resolution model used to represent the energy balances in the rest of the plant's blocks. This structure is used to avoid very high simulation times, as in the works of Kraas et al[37] and Law et al.[38] This model, referred in this work as the MILP-plant model, is derived from the MILP-MPC^{BR} model itself. The model receives each hour the power generation setpoint P_{e_SP} and the real value of $P_{SF\,\max}$, and resolves the energy balance considering all the operating constraints. Among its outputs are the generated electric power and the plant's state (TES energy level and turbine ON/OFF state). Two consecutive optimization models compose this model. The first one (see expression (27)) is used to reach the first optimization goal of minimizing the generation error

$$\begin{aligned} &\text{Minimize } P_{e\_SP}(1/i) - P_{enet}(1/i) \\ &\quad \text{s.t. } P_{SF\,\max}(1/i) = P_{SF}(1/i) + P_{SF\_def}(1/i) \\ &\qquad P_{e\_SP}(1/i) \geq P_{enet}(1/i) \\ &\qquad (3), (4), \ldots, (20) \\ &\qquad (24), \ldots, (26) \text{ for } j = 1. \end{aligned} \tag{27}$$

Once this objective is met, the second optimization model (see expression (28)) is used to reach the goal of minimizing the defocused thermal power in the SF. Note that $P^*_{enet}(1/i)$ is the optimal solution obtained solving (27). It is supposed that control systems and operator decisions comply with these operating rules

$$\begin{aligned} &\text{Minimize } P_{SF\_def}(1/i) \\ &\quad \text{s.t. } P_{SF\,\max}(1/i) = P_{SF}(1/i) + P_{SF\_def}(1/i) \\ &\qquad P_{enet}(1|i) = P^*_{enet}(1|i) \\ &\qquad (3), (4), \ldots, (20) \\ &\qquad (24), \ldots, (26) \text{ for } j = 1. \end{aligned} \tag{28}$$

Table 2 summarizes the functions of the three models used in this work. MATLAB[39] was used as simulation platform. The MILP models were generated in YALMIP,[40] a free toolbox for MATLAB, and solved by SCIP (v3.0.2),[41] a free solver for mixed integer problems. The formulated MILP problem includes 577 continuous variables, 240 binary variables, 387 equality constraints, and 1119 inequality constraints. The obtained average execution time of a simulation step in a standard personal computer is 18 seconds.

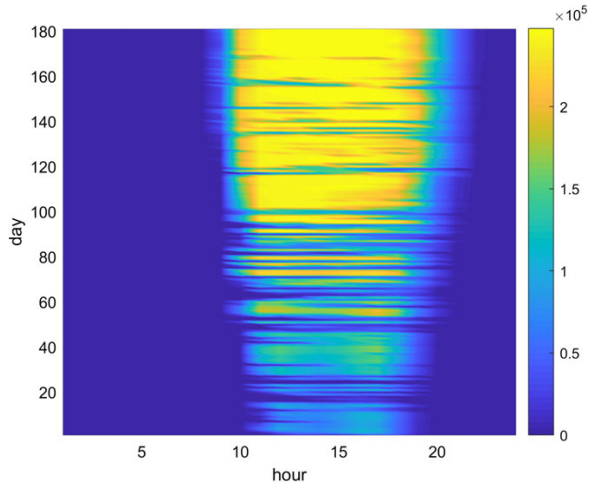

FIGURE 5 Hourly mean values for maximum thermal power available from solar field ($P_{SF\,\max}$, kW) [Colour figure can be viewed at wileyonlinelibrary.com]

TABLE 2 Information about the models used

Model	Function
MILP-MPC^{BR}	$\text{MPC}^{BR}_{\omega,\gamma}(C_{\Delta_\beta}, C_{\Delta_\lambda}, C_\Delta)$ strategy
MILP-plant + detailed SF submodel	to represent the plant
Detailed SF submodel	to convert DNI to $\tilde{P}^{\omega}_{SF\,\max}(j/i)$

Abbreviations: DNI, direct normal irradiance; MILP, mixed-integer linear programming; MPC^{BR}, model predictive control with binary-regularization; SF, solar field.

4.2 | Results and discussion

In order to illustrate the qualitative influence of the considered protection methods on generation scheduling, Figure 6 is included. Some normalized generation profiles for the next day (P_{eref}), obtained in the 14th week of the simulated time period, have been represented. Figure 6 shows the normalized real and forecasted electricity prices, the normalized TES level, and the normalized generation profiles for the next day obtained by $\text{MPC}^{BR}_{0,1}(0,0,0)$ (without PB protection) and $\text{MPC}^{BR}_{0,1}(0,0,20)$ strategy (with PB protection). It is important to remark the high variability observed in the scheduled profiles obtained by $\text{MPC}^{BR}_{0,1}(0,0,0)$ to follow the electricity prices and, therefore, to maximize economic profits. A scheduled next day profile with high variability is converted into a generation profile with high cycling, reducing the PB lifetime, and increasing the maintenance cost and the difficulty of the plant operability. The main goal of this work is to obtain scheduled generation profiles with an important reduction of this variability, but with a low economic impact. In the scheduled profiles obtained by the $\text{MPC}^{BR}_{0,1}(0,0,20)$ strategy, the high variability is reduced in comparison to the case without PB protection, presenting only one startup and shutdown per day in the given example.

Next, a quantitative study of the proposed power protection scheme is provided. The protection of the PB preserves its lifetime and reduces the maintenance costs; therefore, it involves an economic benefit in the long term, although this aspect has not been studied quantitatively. The simulation case to which all the calculations are referred is described in Section 4.2.1. Section 4.2.2 introduces some assumptions to simplify the study. The solutions of the $\text{MPC}^{BR}_{\omega,\gamma}(C_{\Delta_\beta}, C_{\Delta_\lambda}, C_\Delta)$ strategy are analyzed in Section 4.2.3. The idea to estimate the suitable level of cycling penalization is explored in Section 4.2.4. Finally, the main conclusions derived from all the results are drawn in Section 4.2.5.

4.2.1 | Definition of the reference case

The $\text{MPC}^{BR}_{0,1}(0,0,0)$ strategy, without PB protection and applied to the considered simulation scenario, is the reference case to which all the calculations are referred. The total results obtained by $\text{MPC}^{BR}_{0,1}(0,0,0)$ strategy are profits = 3 467 133 €, revenues = 3 575 250 €, penalties = 108 117 €, and the mean of the absolute value of the hourly increment of the generated

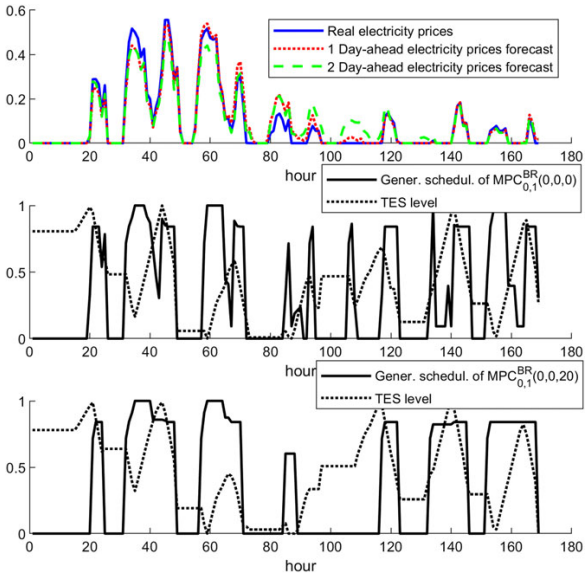

FIGURE 6 Generation scheduling profiles obtained in the 14th week of the simulated time period. TES, thermal energy storage [Colour figure can be viewed at wileyonlinelibrary.com]

electric power $\overline{|\Delta P_e^B|} = 2.54$ MW and $\overline{|\Delta P_e|} = 5.26$ MW (these metrics are calculated removing, and without removing, increments in startups and shutdowns, respectively).

4.2.2 | Assumptions to simplify the parameters tuning

Parameters ω and γ must be swept through a range of values in the simulations. In order to simplify the study, some assumptions about the values of these parameters are made, as will be explained next.

The accuracy of the short-term DNI predictor is given by parameter ω. The results obtained with the extreme cases $\omega = 0$ and $\omega = 1$ (perfect and nonexistent short-term DNI forecast, respectively) are going to be used as bounds of the behaviour with any predictor. In order to justify this assumption, a set of simulations were carried out. Figure 7 shows the energy sale profits of several simulations varying the values of parameters C_Δ and γ, with $\omega = 0$, 0.001, and 1, $C_{\Delta_\beta} = 0$, and $C_{\Delta_\lambda} = 0$. The value $\omega = 0.001$ indicates an almost perfect short-term DNI forecast during the first hour and no improvement over the day-ahead forecast during the sixth hour. Moreover, the forecast worsening is lineal over time (see the work of Vasallo et al[29]). It can be observed in Figure 7 that profits with $\omega = 0$ and 1 bound all results with $\omega = 0.001$. It is therefore assumed that the range formed by the results with $\omega = 0$ and $\omega = 1$ includes the behavior with any other predictor.

Figure 8 shows the profits in simulations with $\omega = 0$ and $\omega = 1$, with $C_\Delta = 0$, 1, and 30 €/MW h, $C_{\Delta_\beta} = 0$, $C_{\Delta_\lambda} = 0$, and with several values of γ. It is observed little sensitivity with this parameter, and a value of 1 is assumed to be a reasonable value.

4.2.3 | Analysis of the solutions of the MPC$^{BR}_{\omega,\gamma}(C_{\Delta_\beta}, C_{\Delta_\lambda}, C_\Delta)$ strategy

The MPC$^{BR}_{\omega,1}(0, 0, C_\Delta)$, MPC$^{BR}_{\omega,1}(0.5C_\Delta, 0.5C_\Delta, C_\Delta)$, and MPC$^{BR}_{\omega,1}(C_\Delta, C_\Delta, C_\Delta)$ strategies with parameter C_Δ=1, 5, 10, and 20 €/MW h and with $\omega = 0$ and $\omega = 1$ were simulated and compared with the reference case. The results are showed in Figures 9 and 10.

Black solid lines show the results obtained by the MPC$^{BR}_{\omega,1}(0, 0, C_\Delta)$ strategy with $\omega = 0$ and $\omega = 1$. Obviously, a perfect short-term DNI forecast ($\omega = 0$) is a much more favorable situation than non-existing short-term DNI forecast ($\omega = 1$), and therefore, a next to 2.25% decrement of profits is obtained with $\omega = 1$ compared the case with $\omega = 0$.

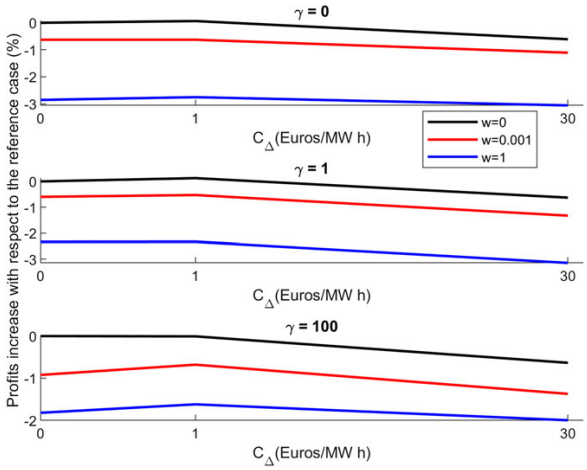

FIGURE 7 Justification to use the extreme cases of the short-term direct normal irradiance predictor as behaviour bounds [Colour figure can be viewed at wileyonlinelibrary.com]

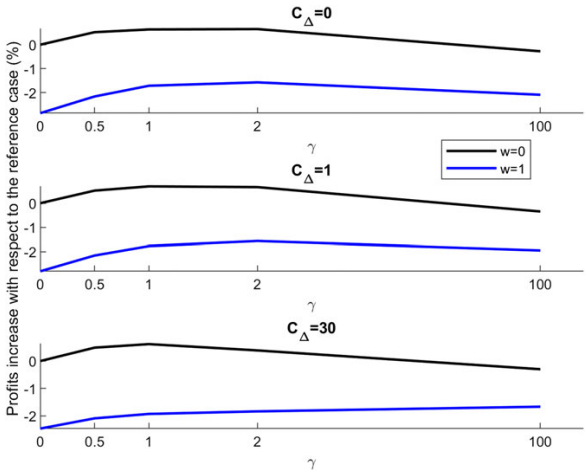

FIGURE 8 Justification to consider parameter $\gamma = 1$ as a reasonable value [Colour figure can be viewed at wileyonlinelibrary.com]

The results of the $\text{MPC}^{BR}_{\omega,1}(0.5C_\Delta, 0.5C_\Delta, C_\Delta)$ and $\text{MPC}^{BR}_{\omega,1}(C_\Delta, C_\Delta, C_\Delta)$ strategies are shown in red dashed and green dotted lines, respectively.

From Figures 9 and 10, the following conclusions can be drawn.

- The proposed method obtains a significant reduction of $\overline{|\Delta P^B_e|}$ and $\overline{|\Delta P_e|}$ as C_Δ, and therefore, the PB protection increases.
- The results obtained by the proposed strategy are better than the ones of the reference case ($C_\Delta = 0$) in the considered scenario. That is, there is a set of values of C_Δ for which the proposed strategy obtains profits similar to the reference case, and a significant reduction of the increments $\overline{|\Delta P_e|}$ and $\overline{|\Delta P^B_e|}$. For example, considering the case with $C_\Delta = 1$ in Figures 9 and 10, the reductions obtained by all strategies are close to 30% and 15% of $\overline{|\Delta P^B_e|}$ and $\overline{|\Delta P_e|}$, respectively, without a significant reduction of the profits.
- As expected, the proposed $\text{MPC}^{BR}_{\omega,\gamma}(0, 0, C_\Delta)$ obtains better results than the $\text{MPC}^{BR}_{\omega,\gamma}(C_\Delta, C_\Delta, C_\Delta)$ strategy if metric $\overline{|\Delta P^B_e|}$ is considered (see Figure 9). In this case, the $\text{MPC}^{BR}_{\omega,\gamma}(0, 0, C_\Delta)$ obtains a decrement of $\overline{|\Delta P^B_e|}$ close to 60%, while maintaining the same level of profits as the reference case (see C_Δ= 5 €/MW h). However, to reach a decrement of 60% of $\overline{|\Delta P^B_e|}$ with the $\text{MPC}^{BR}_{\omega,\gamma}(C_\Delta, C_\Delta, C_\Delta)$ method results in a decrement of profits (more than 1.5%).

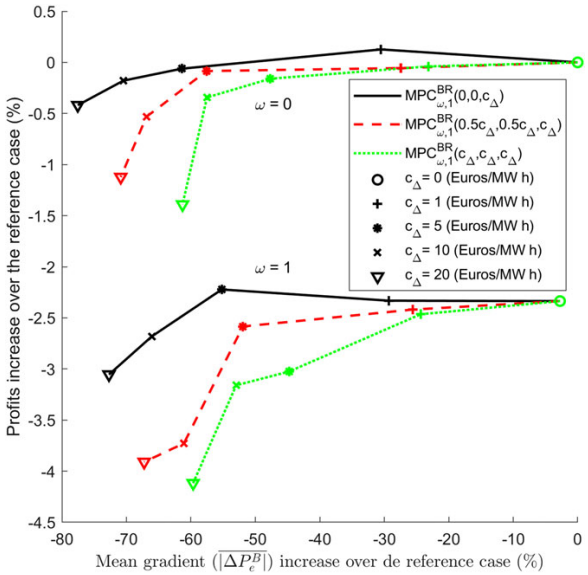

FIGURE 9 Percentage increment of energy sale profits compared with the reference case (without power block protection) against percentage increment of $\overline{|\Delta P_e^B|}$ also compared with the reference case [Colour figure can be viewed at wileyonlinelibrary.com]

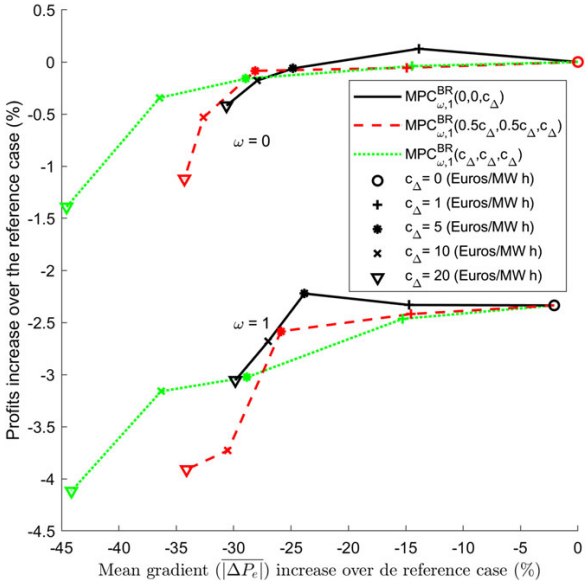

FIGURE 10 Percentage increment of energy sale profits compared with the reference case (without power block protection) against percentage increment of $\overline{|\Delta P_e|}$ also compared with the reference case [Colour figure can be viewed at wileyonlinelibrary.com]

- On the other hand, if metric $\overline{|\Delta P_e|}$ is considered (see Figure 10), the proposed $\text{MPC}^{BR}_{\omega,\gamma}(C_\Delta, C_\Delta, C_\Delta)$ method tends to improve the results obtained by the $\text{MPC}^{BR}_{\omega,\gamma}(0, 0, C_\Delta)$ method, as would be expected.
- Intermediate values of C_{Δ_β} and C_{Δ_λ}, ie, $0 < C_{\Delta_\beta} < C_\Delta$ and $0 < C_{\Delta_\lambda} < C_\Delta$, provide a compromise between the previous cases.

A conclusion that can be drawn from the above is that the economically optimal solution is not very sensitive to the shape of the generation profile. The use of more rigid generation profiles does not significantly worsen the economic profits, with a slight improvement of profits being sometimes observed. This aspect favours the use of the PB protection mechanism proposed in this work.

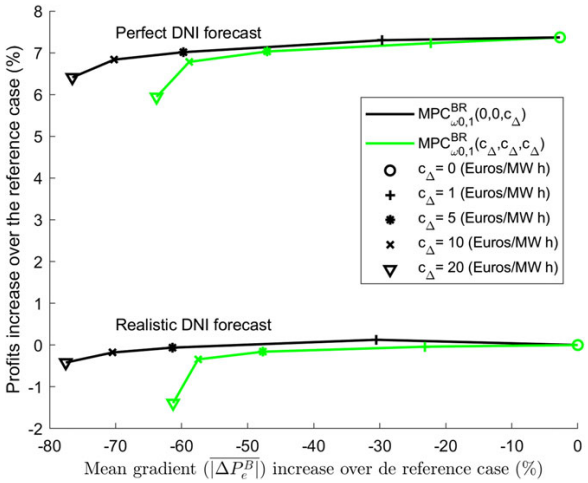

FIGURE 11 Percentage increment of energy sale profits compared with the reference case (without power block protection) against percentage increment of $|\overline{\Delta P_e^B}|$ also compared with the reference case, for perfect and imperfect direct normal irradiance (DNI) forecast [Colour figure can be viewed at wileyonlinelibrary.com]

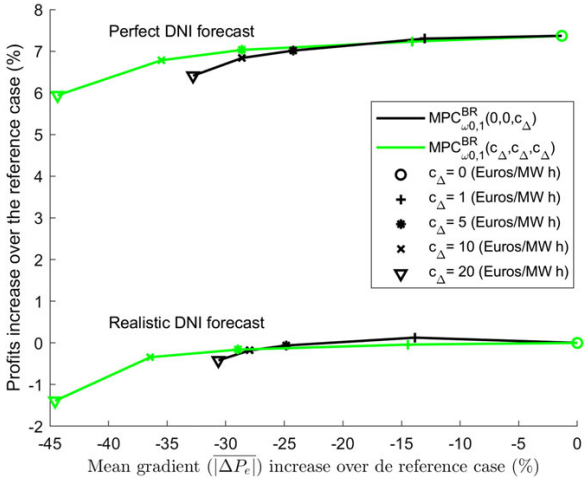

FIGURE 12 Percentage increment of energy sale profits compared with the reference case (without power block protection) against percentage increment of $|\overline{\Delta P_e}|$ also compared with the reference case, for perfect and imperfect direct normal irradiance (DNI) forecast [Colour figure can be viewed at wileyonlinelibrary.com]

The effect of the uncertainties present in the DNI forecast are also studied, with simulation results shown in Figures 11 and 12. This study compares simulations with perfect DNI forecast of the extreme strategies $MPC^{BR}_{0,1}(0,0,C_\Delta)$ and $MPC^{BR}_{0,1}(C_\Delta,C_\Delta,C_\Delta)$, with $C_\Delta > 0$, with the reference case ($C_\Delta = 0$), and also with imperfect DNI forecast. As can be seen, the perfect DNI forecast results in an expected increase in the obtained profits. Except for this point, the shape of the traces obtained using perfect DNI forecast is quite similar to the results obtained with imperfect DNI forecast. Therefore, the general conclusions that were drawn before are not altered by the uncertainty present in the DNI forecast, so it seems reasonable to assume that they could be maintained for other forecasted DNI data.

In order to make a comparison, an alternative day-ahead scheduling (DAS) strategy with PB protection (denoted as $DAS(C_{\Delta_\beta},C_{\Delta_\lambda},C_\Delta)$) is considered in this paper. This scheduling strategy has no feedback except for the moment in which the generation schedule for day D+1 is developed at t_{subm} of day D, when the plant's state and the forecasts are updated. Therefore, the associated MILP optimization problem is solved only once per day. Another feature of the $DAS(C_{\Delta_\beta},C_{\Delta_\lambda},C_\Delta)$ strategy is that each hour it tries to generate the committed power using the energy actually available,

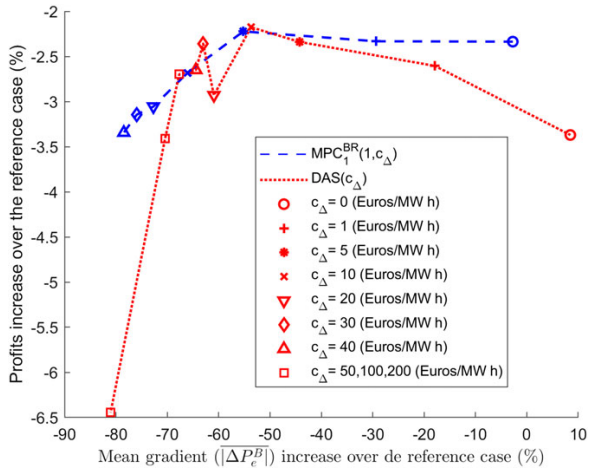

FIGURE 13 Percentage increment of energy sale profits compared with the reference case (without power block protection) against percentage increment of $|\overline{\Delta P_e^B}|$ also compared with the reference case [Colour figure can be viewed at wileyonlinelibrary.com]

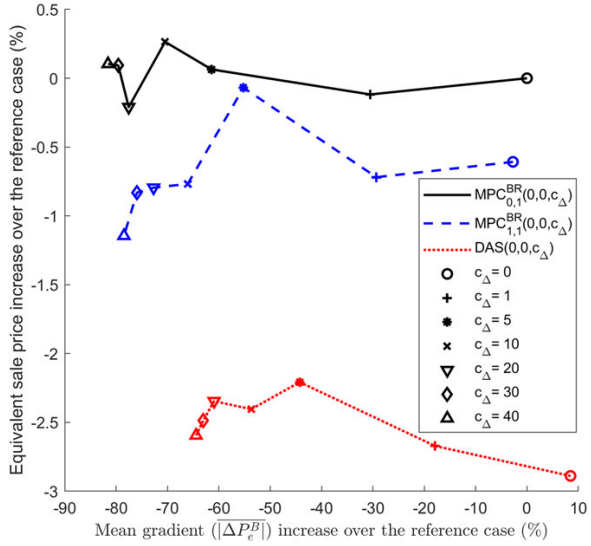

FIGURE 14 Percentage increment of the equivalent sale price compared with the reference case (without power block protection) against percentage increment of $|\overline{\Delta P_e^B}|$ also compared with the reference case [Colour figure can be viewed at wileyonlinelibrary.com]

without any rescheduling (due to the lack of new information). Figure 13 compares the results of the MPC$_{1,1}^{BR}(0,0,C_\Delta)$ strategy, ie, the lower bound of the range, with the alternative DAS(0,0,C_Δ) strategy. It can be observed that the DAS(0,0,C_Δ) strategy does not overcome the MPC$_{1,1}^{BR}(0,0,C_\Delta)$ strategy (except for one point). As a consequence, the MPC^{BR} strategy overcomes the DAS strategy, as expected, since the rescheduling with fresh information is a positive mechanism. Moreover, Figure 13 shows that the PB protection is also a useful element for the DAS(0,0, C_Δ) strategy because it reduces the generation variation, while the profits do not decrease. In fact, a slight increase in profits is found for the first values of parameter C_Δ.

In order to analyze the superiority of the MPC$_{\omega,1}^{BR}(0,0,C_\Delta)$ strategy over the DAS strategy, the equivalent sale price is defined. This metric is calculated dividing the energy sale profits between the whole amount of generated electric energy. Figure 14 shows the results of this metric for several simulations. It can be observed that the equivalent sale price is higher in the MPC$_{1,1}^{BR}(0,0,C_\Delta)$ strategy. This higher value is caused by the rescheduling, which displaces the generation towards high price periods.

4.2.4 | Tuning of cycling penalization intensity

An aspect of interest for this study is the estimation of a suitable value of C_Δ. The obvious choice would be to use the maximum value of C_Δ for which the obtained profits are similar to the profits obtained by the reference case ($C_\Delta = 0$). However, this value is not known in advance. An estimation of a suitable C_Δ value could be obtained by means of simulation using data from previous months. In this sense, Figure 15 shows percentage increment of profits compared with the reference case for the $\text{MPC}^{BR}_{0,1}(0, 0, C_\Delta)$ and $\text{MPC}^{BR}_{1,1}(0, 0, C_\Delta)$ strategies. These results are obtained considering only the first four months of the simulated time period. As can be seen, the variation level of profits is less than 1% if a value of $C_\Delta \leq 10$ €/MW h is considered. Figure 16, showing simulation results for the last 2 months of the simulated time period, confirms the stability of the profits if $C_\Delta \leq 10$ €/MW h is considered. Therefore, the information from the simulation results of the first four months of the simulated scenario provides a way to infer a suitable value of C_Δ to be used in the last 2 months. The overall percentage increments of profits compared with the reference case for the whole simulated scenario are shown in Figure 17. This example shows the possibility of tuning the suitable level of penalization by means of simulations, making use of historical data (real and forecasted values for DNI and energy prices, and penalty costs). As a future line of research, it is mentioned that more precise damage models could allow for the improvement of the penalization

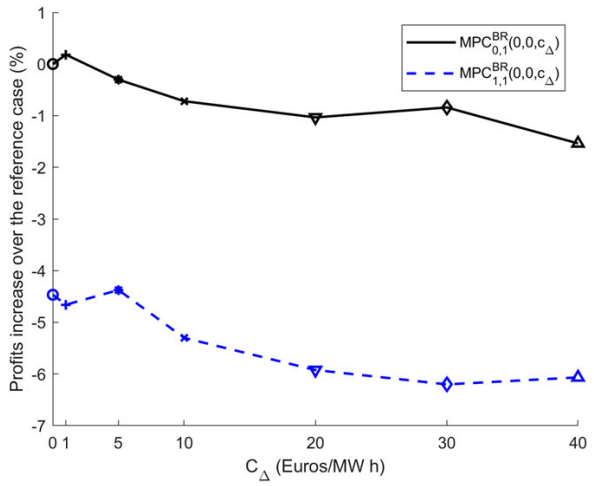

FIGURE 15 Percentage increment of profits compared with the reference case (without power block protection) against C_Δ during the first 4 months [Colour figure can be viewed at wileyonlinelibrary.com]

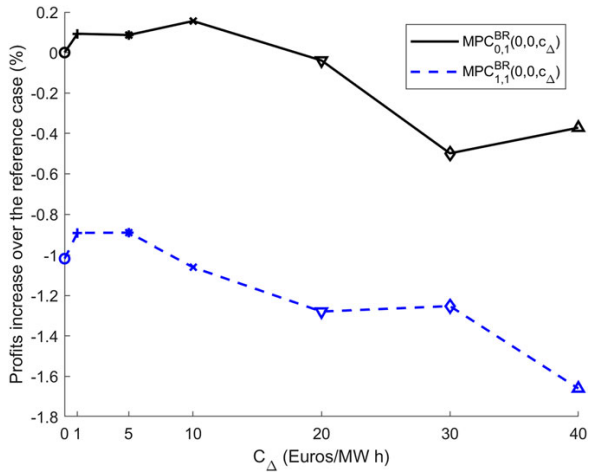

FIGURE 16 Percentage increment of profits compared with the reference case (without power block protection) against C_Δ during the last 2 months [Colour figure can be viewed at wileyonlinelibrary.com]

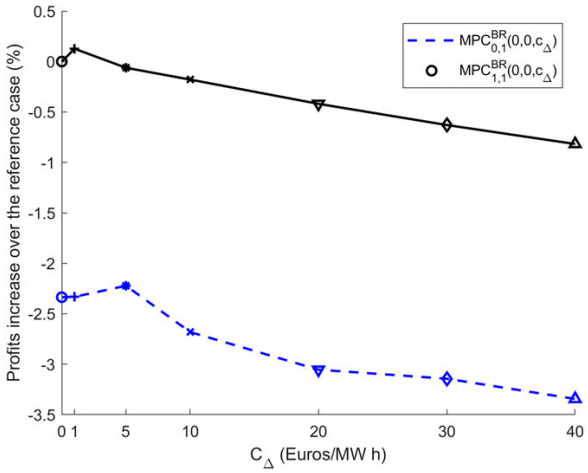

FIGURE 17 Percentage increment of profits compared with the reference case (without power block protection) against C_Δ during the 6-month period [Colour figure can be viewed at wileyonlinelibrary.com]

term, while the intensity of the applied penalization could be obtained using historical data, as illustrated in the previous example.

4.2.5 | Main conclusions from the results

A set of simulations covering a large number of reasonable cases has been done. The main conclusions obtained from the results are the following.

1. The proposed MPC^{BR} scheduling strategy obtains an important reduction of the cycling, with no impact on energy sale profits. The economically optimal solution is not very sensitive to the shape of the generation profile. Therefore, more rigid generation profiles do not significantly worsen the economic profits; in fact, a slight improvement of profits is observed in some cases.
2. When a perfect solar resource forecast is considered (forecast without error), the obtained results are quite similar, which indicates a certain independence from the DNI forecast accuracy.
3. The proposed MPC^{BR} scheduling strategy is also compared with a DAS strategy (without hourly rescheduling). In this case, MPC^{BR} provides a superior performance owing to the rescheduling capacity.
4. As discussed above, the proposed method obtains some results with a slight increment of economic profits with respect to the reference case (MPC without PB protection); thus, it overcomes the previous method presented in the work of Cojocaru et al.[25]
5. The possibility to estimate the highest level of cycling penalization, which maintains the economic profits, is also studied and validated.

5 | CONCLUSIONS

This work has presented a new scheduling method that can be applied in concentrated solar power plants in the context of an energy day-ahead market. A scheme based on MPC is proposed to allow rescheduling and developing the generation schedule for the next day at the required hour. A protection procedure for the PB is included as the main novelty. The new formulation includes a regularization term to penalize the variability of the PB output. However, binary variables are used to apply different penalization intensities in PB normal operation, startup, and shutdown situations. Furthermore, constraints to limit the daily startups are included. With the purpose of illustrating the new scheduler, a realistic case study based on the simulation of a 50 MW CSP plant with TES was included. A comparison with previous scheduling methods shows that the new proposal including PB protection provides better economic results. In fact, an important reduction of the generation cycling can be obtained without diminishing energy sale profits. The advantages of a reduced

cycling are higher lifetime for the PB elements, lower maintenance costs, and easier plant operability. The possibility of estimating the highest level of PB protection that maintains the energy sale profits is also analyzed in the case study.

ACKNOWLEDGEMENT

This research has been supported by DPI2016-76493-C3-2-R of Ministerio de Economía y Competitividad (Spain).

ORCID

José M. Bravo https://orcid.org/0000-0001-5321-8503

REFERENCES

1. Purohit I, Purohit P, Shekhar S. Evaluating the potential of concentrating solar power generation in Northwestern India. *Energy Policy*. 2013;62:157-175.
2. Zhang HL, Baeyens J, Degréve J, Cacéres G. Concentrated solar power plants: review and design methodology. *Renew Sustain Energy Rev*. 2013;22:466-481.
3. Camacho EF, Bordons Alba C. *Model Predictive Control*. 2nd ed. London, UK: Springer-Verlag London Limited; 2007.
4. Gil P, Henriques J, Cardoso A, Carvalho P, Dourado A. Affine neural network-based predictive control applied to a distributed solar collector field. *IEEE Trans Control Syst Technol*. 2014;22(2):585-596.
5. de la Parte MP, Cirre CM, Camacho EF, Berenguel M. Application of predictive sliding mode controllers to a solar plant. *IEEE Trans Control Syst Technol*. 2008;16(4):819-825.
6. Vasallo MJ, Bravo JM. A MPC approach for optimal generation scheduling in CSP plants. *Appl Energy*. 2016;165:357-370.
7. Turgeon A. Optimal scheduling of thermal generating units. *IEEE Trans Autom Control*. 1978;23(6):1000-1005.
8. Sokoler LE, Dinesen PJ, Jørgensen JB. A hierarchical algorithm for integrated scheduling and control with applications to power systems. *IEEE Trans Control Syst Technol*. 2017;25(2):590-599.
9. Sioshansi R, Denholm P. The value of concentrating solar power and thermal energy storage. *IEEE Trans Sustain Energy*. 2010;1(3):173-183.
10. Usaola J. Operation of concentrating solar power plants with storage in spot electricity markets. *IET Renew Power Gener*. 2012;6(1):59-66.
11. Vasallo MJ, Bravo JM. A novel two-model based approach for optimal scheduling in CSP plants. *Sol Energy*. 2016;126:73-92.
12. Álvarez JD, Pasamontes M, Guzmán JL, Camacho EF. A practical hybrid predictive control algorithm for a low-temperature thermosolar plant. *Optim Control Appl Methods*. 2016;37(3):508-520.
13. González-Gómez PA, Gómez-Hernández J, Briongos JV, Santana D. Transient thermo-mechanical analysis of steam generators for solar tower plants. *Appl Energy*. 2018;212:1051-1068.
14. Wagner MJ, Newman AM, Hamilton WT, Braun RJ. Optimized dispatch in a first-principles concentrating solar power production model. *Appl Energy*. 2017;203:959-971.
15. Kumar N, Besuner P, Lefton S, Agan D, Hilleman D. *Power Plant Cycling Costs*. Technical report. Denver, CO: Intertek APTECH for the USA National Renewable Energy Laboratory; 2012.
16. Dettori S, Iannino V, Colla V, Signorini A. An adaptive fuzzy logic-based approach to PID control of steam turbines in solar applications. *Appl Energy*. 2018;227:655-664.
17. Ferruzza D, Topel M, Laumert B, Haglind F. Impact of steam generator start-up limitations on the performance of a parabolic trough solar power plant. *Sol Energy*. 2018;169:255-263.
18. Topel M, Laumert B. Improving concentrating solar power plant performance by increasing steam turbine flexibility at start-up. *Sol Energy*. 2018;165:10-18.
19. Topel M, Genrup M, Jöcker M, Spelling J, Laumert B. Operational improvements for startup time reduction in solar steam turbines. *J Eng Gas Turbines Power*. 2015;137(4).
20. Spelling J, Jöcker M, Martin A. Annual performance improvement for solar steam turbines through the use of temperature-maintaining modifications. *Sol Energy*. 2012;86(1):496-504.
21. Domínguez R, Baringo L, Conejo AJ. Optimal offering strategy for a concentrating solar power plant. *Appl Energy*. 2012;98:316-325.
22. Pousinho HMI, Contreras J, Pinson P, Mendes VMF. Robust optimisation for self-scheduling and bidding strategies of hybrid CSP-fossil power plants. *Int J Electr Power Energy Syst*. 2015;67:639-650.
23. Xu T, Zhang N. Coordinated operation of concentrated solar power and wind resources for the provision of energy and reserve services. *IEEE Trans Power Syst*. 2017;32(2):1260-1271.
24. Yang Y, Guo S, Liu D, Li R, Chu Y. Operation optimization strategy for wind-concentrated solar power hybrid power generation system. *Energy Convers Manag*. 2018;160:243-250.
25. Cojocaru EG, Vasallo MJ, Bravo JM, Marín D. A lifetime-extending model-based predictive control for scheduling in concentrating solar power plants. *IEEE Int Conf Ind Technol*. 2018:1732-1737.

26. Tibshirani R, Saunders M, Rosset S, Zhu J, Knight K. Sparsity and smoothness via the fused lasso. *J R Stat Soc Ser B Stat Methodol*. 2005;67:91-108.
27. Gallieri M. Principles of LASSO MPC. In: *Lasso-MPC - Predictive Control With ℓ 1-Regularised Least Squares*. Cham, Switzerland: Springer International Publishing; 2016: 47-63.
28. Bertsimas D, Copenhaver MS, Mazumder R. The trimmed lasso: sparsity and robustness. 2017. arXiv:1708.04527.
29. Vasallo MJ, Bravo JM, Gelu Cojocaru E, Gegúndez ME. Calculating the profits of an economic MPC applied to CSP plants with thermal storage system. *Sol Energy*. 2017;155(Suppl C):1165-1177.
30. Boyd S, Vandenberghe L. *Convex Optimization*. Cambridge, UK: Cambridge University Press; 2004.
31. Llorente I, Álvarez JL, Blanco D. Performance model for parabolic trough solar thermal power plants with thermal storage Comparison to operating plant data. *Sol Energy*. 2011;85(10):2443-2460.
32. Red Eléctrica de España. 2018. Accessed May 16, 2018. http://www.esios.ree.es/
33. OMIE. 2018. Accessed May 25, 2018. http://www.omie.es/
34. Yang Z, Ce L, Lian L. Electricity price forecasting by a hybrid model, combining wavelet transform, ARMA and kernel-based extreme learning machine methods. *Appl Energy*. 2017;190(Suppl C):291-305.
35. User's manual for TMY2s. 2018. Accessed May 25, 2018. http://rredc.nrel.gov/solar/pubs/tmy2/
36. Law EW, Prasad AA, Kay M, Taylor RA. Direct normal irradiance forecasting and its application to concentrated solar thermal output forecasting — a review. *Sol Energy*. 2014;108:287-307.
37. Kraas B, Schroedter-Homscheidt M, Madlener R. Economic merits of a state-of-the-art concentrating solar power forecasting system for participation in the Spanish electricity market. *Sol Energy*. 2013;93:244-255.
38. Law EW, Kay M, Taylor RA. Calculating the financial value of a concentrated solar thermal plant operated using direct normal irradiance forecasts. *Sol Energy*. 2016;125:267-281.
39. MATLAB version (R2007a). Natick, MA: The MathWorks Inc; 2007.
40. Löfberg J. YALMIP: a toolbox for modeling and optimization in MATLAB. Paper presented at: 2004 IEEE International Conference on Robotics and Automation; 2004; Taipei, Taiwan.
41. Achterberg T. SCIP: solving constraint integer programs. *Math Program Comput*. 2009;1(1):1-41.

How to cite this article: Cojocaru EG, Bravo JM, Vasallo MJ, Marín D. A binary-regularization-based model predictive control applied to generation scheduling in concentrating solar power plants. *Optim Control Appl Meth*. 2019;1–24. https://doi.org/10.1002/oca.2498

APPENDIX

A.1 | Synthetic energy price forecasts

In the six months simulation included in this paper, $p(s)$, with $s = 1, \dots, 181{\cdot}24$, are the actual energy prices. Synthetic one-day-ahead and two-day-ahead predictions can be obtained by means of the expressions $\tilde{p}^{1D}(s) = \eta_1 p(s-24) + (1-\eta_1)p(s)$ and $\tilde{p}^{2D}(s) = \eta_2 p(s-48) + (1-\eta_2)p(s)$ with $s = 48, \dots, 181 \cdot 24$. Note that, if $\eta_1 = \eta_2 = 1$, then the synthetic prediction is a persistent prediction. On the other hand, if $\eta_1 = \eta_2 = 0$, predictions without error are considered. In this paper, parameters η_1 and η_2 were supposed equal, and have been tuned to obtain the RMSE values commented in Section 4.1.1.

It is important to remark that, at day D for hours $t > t_{subm}$, the energy prices of day $D+1$ are known. At day D, we have the indexes $i = 0, 1, \dots, 23$ and $j = 1, \dots, N$ used in the sliding window of the MPC strategy. Therefore, at day D, the equivalence $p(j/i) = p(24(D-1)+j+i)$ is clear. In the MPC sliding window, forecasted energy prices $\tilde{p}(j/i)$ equivalent to $\tilde{p}(24(D-1)+j+i)$ are used. If $i \leq t_{subm}$, the prediction is defined by the following expression:

$$\tilde{p}(j/i) = \begin{cases} p(j/i) & j+i \leq 24 \\ \tilde{p}^{1D}(j/i) & 25 \leq j+i \leq 48 \\ \tilde{p}^{2D}(j/i) & 49 \leq j+i. \end{cases}$$

If $i > t_{subm}$, the prediction is defined by

$$\tilde{p}(j/i) = \begin{cases} p(j/i) & j+i \leq 48 \\ \tilde{p}^{1D}(j/i) & 49 \leq j+i. \end{cases}$$

A.2 | Nomenclature

Notation	Description	Simulation values
Indices, superscripts, and time parameters		
$\Delta w, \Delta t_w, \Delta t_o$	Time length of the sliding window, time step for MPC control update and time step for MPC model, respectively	$\Delta w = 48$ h, $\Delta t_w = 1$ h, $\Delta t_o = 1$ h
t_{subm}	Deadline hour in the day D for the submission of the generation schedule for the next day $D+1$	$t_{subm} = 10:00$ h
$t_{schedule\_end}$	End time of the committed generation schedule	$t_{schedule\_end} = 24:00$ h
N	Number of time intervals in the sliding window	$N = \frac{\Delta w}{\Delta t_o}$
i, j	Each step when the MPC generates its output and each step within the sliding window, respectively	$i = 0, \ldots, \frac{24}{\Delta t_w} - 1$, $j = 1, \ldots, N$
t	Instantaneous variable for time	$t(i) = i\Delta t_w$
N_{TI}	Number of time instants in the TI interval	$N_{TI} = \frac{t_{schedule\_end} - t(i)}{\Delta t_o}$
$.^t, .^D$	Superscripts expressing instantaneous variable and daily-scheduling-related variable, respectively	
Parameters		
$P_{c\,\min}, P_{d\,\min}$	Minimum values for charging and discharging thermal power on the HTF side due to minimum value in salt pump flow rate (MW)	20.2 MW, 15 MW
P_{start_up}	Approximated value for the fraction of mean thermal power in the PB inlet used to increase thermal state in the PB during an hour with startup (MW)	14 MW
$P_{c\max\_exch}, P_{d\max\_exch}$	Maximum values for charging and discharging thermal power on the HTF side due to heat-exchanger limitations (MW)	100 MW, 124 MW
$P_{d\max\_onlyTES}$	Maximum value for discharging thermal power on the HTF side in the TES-only mode due to the input limitations of the turbine in this mode (MW)	119 MW
$\Delta P_{HTF\_stu\_\max}$	Maximum value of the fraction of mean thermal power in PB inlet used to generate electricity during an hourly period when a startup is performed (MW)	103 MW
$P_{HTF\,\min}, P_{HTF\,\max}$	Minimum and maximum values for thermal power entering the PB (MW)	20 MW, 140 MW
$E_{\min}, E_{\max}$	Minimum and maximum values for energy in TES (MW h)	0 MW h, 1010 MW h
$T_{\min\_u}, T_{\min\_d}$	Minimum up time and minimum down time for the turbine (h)	2 h
a, b	Parameters of linear approximation of function relating turbine-generated gross electric power with thermal power entering the PB (dimensionless and MW)	0.4, −3.1 MW
$\eta_{gross2net}$	Ratio for considering parasitic electric consumption	0.95
η_{exch_TES}	Efficiency of the HTF-TES heat exchangers	0.95
pc	Percentage to establish a minimum operating point when the turbine starts	0.5
K	Unit value of the final TES energy level (€ /MW h)	1e-07 € /MW h
$\bar{\phi}$	Reference mean value for deviation penalty cost (€/MW h)	6 €/MW h
$C_{\Delta_\beta}, C_{\Delta_\lambda}, C_\Delta$	Unit cost of the hourly power variation when the turbine is in startup, in shutdown, or in normal operation, respectively (€ /MW h)	
$\phi(j/i)$	Estimation of the deviation penalty cost at hour j (€ /MW h)	
γ	Deviation penalty parameter (dimensionless)	
ω	Accuracy parameter for short-term DNI forecast (dimensionless)	

Notation	Description
The nomenclature explained below refers to MPC model variables, meaning that power variables are hourly mean values. Superscripts t and D can be used in the variables below.	
Energy variables	
$P_{SF}(j/i)$	Thermal power actually transferred from the SF on the HTF side in hour j (MW)
$P_{SF\_def}(j/i)$	Defocused thermal power in the SF on the HTF side in hour j (MW)
$P_{startup}(j/i)$	Fraction of the thermal power in PB inlet used to increase the thermal state in the PB when a startup occurs in hour j (MW)
$P_{HTF}(j/i)$	Fraction of the thermal power in PB inlet used to generate electricity in hour j (MW)
$P_c(j/i)$, $P_d(j/i)$	Charging and discharging thermal power on the HTF side in hour j (MW)
$P_{d\max\_mixed}(j/i)$	Maximum value for discharging thermal power in mixed mode on the HTF side in hour j (MW)
$P_e(j/i)$, $P_{enet}(j/i)$	Turbine-generated gross and net electric power in hour j (MW)
$E(j/i)$	TES energy level at the beginning of hour j (MW h)
$\lvert\Delta P_e(j/i)\rvert$	Absolute value of the hourly increment of gross electric power generated by the turbine in hour j (MW/h)
$\overline{\lvert\Delta P_e^B\rvert}$, $\overline{\lvert\Delta P_e\rvert}$	Mean of the absolute values of the hourly increments of the generated electric power, calculated removing ($\overline{\lvert\Delta P_e^B\rvert}$) and without removing ($\overline{\lvert\Delta P_e\rvert}$) increments in startups and shutdowns, respectively (MW/h)
Binary variables	
$\alpha(j/i)$, $\beta(j/i)$, $\lambda(j/i)$	Equal to 1 if during hour j the turbine is in normal operation, in startup, or in shutdown, respectively
$\mu(j/i)$, $\delta(j/i)$	Equal to 1 if during hour j the TES is charging or discharging, respectively
Input Data	
$P_{SF\max}(j/i)$	Maximum thermal power available from the SF on the HTF side in hour j (MW)
$\tilde{P}^{\omega}_{SF\max}(j/i)$	Forecasted maximum thermal power available from the SF on the HTF side in hour j (MW)
$P_{eref}(j/i)$	Committed generation schedule still to be met, expressed in net electric power (MW)
$P_{e\_SP}(1,i)$	Power generation setpoint (MW)
$\tilde{p}(j/i)$	Forecasted electricity sale price during hour j (€/MW h)
$\alpha_{\mathbb{S}(i)}$	Values before the start hour of the sliding window for binary variable $\alpha(j/i)$, with $\alpha_{\mathbb{S}(i)} = \{\alpha_{0/i}, \alpha_{-1/i}, \ldots, \alpha_{-\max(T_{\min\_u}, T_{\min\_d})/i}\}$
$E_{0/i}$	Initial value of the TES energy level (MW h)
$P_{e0/i}$	Initial value of the turbine output (MW)
Acronyms	
CSP	Concentrated solar power
nRMSE	normalised Root mean square error
DAS	Day-ahead scheduling
PB	Power block
DNI	Direct normal irradiance
PTC	Parabolic trough collector
HTF	Heat transfer fluid
RMSE	Root mean square error
MILP	Mixed-integer linear programming
SF	Solar field
MIP	Mixed-integer programming
TES	Thermal energy storage
MPC	Model-based predictive control

Bibliografía

[1] Manuel Jesús Vasallo and José Manuel Bravo. A novel two-model based approach for optimal scheduling in CSP plants. *Solar Energy*, 126:73 – 92, 2016.

[2] Manuel Jesús Vasallo and José Manuel Bravo. A MPC approach for optimal generation scheduling in CSP plants. *Applied Energy*, 165:357 – 370, 2016.

[3] J. Löfberg. YALMIP : A toolbox for modeling and optimization in MATLAB. In *Proceedings of the CACSD Conference*, Taipei, Taiwan, 2004.

[4] Edward W. Law, Abhnil A. Prasad, Merlinde Kay, and Robert A. Taylor. Direct normal irradiance forecasting and its application to concentrated solar thermal output forecasting — A review. *Solar Energy*, 108(0):287 – 307, 2014.

[5] Zhang Yang, Li Ce, and Li Lian. Electricity price forecasting by a hybrid model, combining wavelet transform, ARMA and kernel-based extreme learning machine methods. *Applied Energy*, 190:291 – 305, 2017.

[6] WEB de OMIE. http://www.omie.es/. Último acceso: 01.12.2019.

[7] WEB de Red Eléctrica de España. http://www.esios.ree.es/. Último acceso: 01.12.2019.

[8] Gregor Erbach, European Parliamentary Research Service. Understanding electricity markets in the EU, 2016. http://www.europarl.europa.eu/RegData /etudes/BRIE/2016/593519/EPRS_BRI(2016)593519_EN.pdf. Último acceso: 01.12.2019.

[9] Fereidoon P. Sioshansi. Electricity market reform: What has the experience taught us thus far? *Utilities Policy*, 14(2):63 – 75, 2006.

[10] Antonio J. Conejo, Javier Contreras, Rosa Espínola, and Miguel A. Plazas. Forecasting electricity prices for a day-ahead pool-based electric energy market. *International Journal of Forecasting*, 21(3):435 – 462, 2005.

[11] Ricardo Fernández-Blanco Carramolino. *Price-Based Market Clearing in Pool-Based Electricity Markets*. PhD thesis, Universidad de Castilla-La Mancha, Ciudad Real, 2014.

[12] Klaus Mayer and Stefan Trück. Electricity markets around the world. *Journal of Commodity Markets*, 9:77 – 100, 2018.

[13] Steven Stoft. Power system economics. *Journal of Energy Literature*, 8:94–99, 2002.

[14] Web de Energía y Sociedad. http://www.energiaysociedad.es. Último acceso: 01.12.2019.

[15] Kavalov, B and Peteves, S.D. The Future of Coal, 2007. http://publications.jrc.ec .europa.eu/repository/handle/JRC36671. Último acceso: 01.12.2019.

[16] BP. BP Statistical Review of World Energy, 2018. https://www.bp.com/content /dam/bp/business-sites/en/global/corporate/pdfs/energy-economics /statistical-review/bp-stats-review-2018-full-report.pdf. Último acceso: 01.12.2019.

[17] Guri Bang. Energy security and climate change concerns: Triggers for energy policy change in the United States? *Energy Policy*, 38(4):1645 – 1653, 2010. Energy Security - Concepts and Indicators with regular papers.

[18] Atul Sharma. A comprehensive study of solar power in India and World. *Renewable and Sustainable Energy Reviews*, 15(4):1767 – 1776, 2011.

[19] IRENA (2016). The Power to Change: Solar and Wind Cost Reduction Potential to 2025. https://www.irena.org/publications/2016/Jun/The-Power-to-Change-Solar-and-Wind-Cost-Reduction-Potential-to-2025. Último acceso: 01.12.2019.

[20] S. Teske, J. Leung, L. Crespo, M. Bial, E. Dufour, Ch. Richter, and E. Rochon. Solar thermal electricity: Global outlook 2016. *European Solar Thermal Electricity Association*, 2016.

[21] D.O. Akinyele and R.K. Rayudu. Review of energy storage technologies for sustainable power networks. *Sustainable Energy Technologies and Assessments*, 8:74 – 91, 2014.

[22] IRENA (2018). Renewable Energy Statistics 2018. https://www.irena.org/ publications/2018/Jul/Renewable-Energy-Statistics-2018. Último acceso: 01.12.2019.

[23] X. Jin Yang, Hanjun Hu, Tianwei Tan, and Jinying Li. China's renewable energy goals by 2050. *Environmental Development*, 20:83 – 90, 2016.

[24] Mark Z. Jacobson and Mark A. Delucchi. Providing all global energy with wind, water, and solar power, Part I: Technologies, energy resources, quantities and areas of infrastructure, and materials. *Energy Policy*, 39(3):1154 – 1169, 2011.

[25] Mark A. Delucchi and Mark Z. Jacobson. Providing all global energy with wind, water, and solar power, Part II: Reliability, system and transmission costs, and policies. *Energy Policy*, 39(3):1170 – 1190, 2011.

[26] IRENA (2018). Renewable Power Generation costs in 2017. https://www.irena.org /publications/2018/Jan/Renewable-power-generation -costs-in-2017. Último acceso: 01.12.2019.

[27] WEB de SolarPACES. How CSP Works. https://www.solarpaces.org/csp-technologies/csp-how-it-works/. Último acceso: 01.12.2019.

[28] R. Guédez, J. Spelling, B. Laumert, and T. Fransson. Optimization of Thermal Energy Storage Integration Strategies for Peak Power Production by Concentrating Solar Power Plants. *Energy Procedia*, 49:1642 – 1651, 2014. Proceedings of the SolarPACES 2013 International Conference.

[29] Pitz-Paal, R and Dersch, J and Milow, B. German Aerospace Center. European Concentrated Solar Thermal Road-Mapping, 2004. https://www.promes.cnrs.fr /uploads/pdfs/ecostar/ECOSTAR.Roadmap.pdf. Último acceso: 01.12.2019.

[30] IRENA (2017). Electricity Storage and Renewables: Costs and Markets to 2030, 2017. https://www.irena.org/-/media/Files/IRENA/Agency/Publication /2017/Oct/IRENA_Electricity_Storage_Costs_2017.pdf. Último acceso: 01.12.2019.

[31] Johan Lilliestam and Robert Pitz-Paal. Concentrating solar power for less than USD 0.07 per kwh: finally the breakthrough? *Renewable Energy Focus*, 26:17 – 21, 2018.

[32] International Energy Agency. Technology Roadmap - Concentrating Solar Power, 2010. https://www.iea.org/publications/freepublications/publication /csp_roadmap.pdf. Último acceso: 01.12.2019.

[33] F.J. Santos-Alamillos, D. Pozo-Vázquez, J.A. Ruiz-Arias, L. Von Bremen, and J. Tovar-Pescador. Combining wind farms with concentrating solar plants to provide stable renewable power. *Renewable Energy*, 76:539 – 550, 2015.

[34] IRENA (2012). Renewable Energy Technologies: Cost Analysis Series. Volume 1: Power Sector. Issue 2/5. Concentrating Solar Power, June. https://www.irena.org /documentdownloads/publications /re_technologies_cost_analysis-csp.pdf. Último acceso: 01.12.2019.

[35] Tomislav M. Pavlovic, Ivana S. Radonjic, Dragana D. Milosavljevic, and Lana S. Pantic. A review of concentrating solar power plants in the world and their potential use in Serbia. *Renewable and Sustainable Energy Reviews*, 16(6):3891 – 3902, 2012.

[36] Jean-Claude Sabonnadière. *Renewable Energy Technologies*. Wiley, 2009.

[37] Kody M. Powell, Khalid Rashid, Kevin Ellingwood, Jake Tuttle, and Brian D. Iverson. Hybrid concentrated solar thermal power systems: A review. *Renewable and Sustainable Energy Reviews*, 80:215 – 237, 2017.

[38] Salvador Izquierdo, Carlos Montañés, César Dopazo, and Norberto Fueyo. Analysis of CSP plants for the definition of energy policies: The influence on electricity cost of solar multiples, capacity factors and energy storage. *Energy Policy*, 38(10):6215 – 6221, 2010.

[39] Andrey Yasinskiy, Javier Navas, Teresa Aguilar, Rodrigo Alcántara, Juan Jesús Gallardo, Antonio Sánchez-Coronilla, Elisa I. Martín, Desireé De Los Santos, and Concha Fernández-Lorenzo. Dramatically enhanced thermal properties for TiO_2-based nanofluids for being used as heat transfer fluids in concentrating solar power plants. *Renewable Energy*, 119:809 – 819, 2018.

[40] Franz Trieb, Christoph Schillings, Marlene O'Sullivan, Thomas Pregger, and Hoyer-Klick C. Global potential of concentrating solar power. In *Proceedings of the SolarPACES*, Berlin, Germany, 2009.

[41] Müller-Steinhagen, H and Trieb, Franz. Concentrating solar power, - A review of the technology, 2004. https://www.dlr.de/tt/Portaldata/41/Resources /dokumente/institut/system/publications/Concentrating_Solar_Power_Part_1.pdf. Último acceso: 01.12.2019.

[42] Wang Fuqiang, Cheng Ziming, Tan Jianyu, Yuan Yuan, Shuai Yong, and Liu Linhua. Progress in concentrated solar power technology with parabolic trough collector system: A comprehensive review. *Renewable and Sustainable Energy Reviews*, 79:1314 – 1328, 2017.

[43] Evangelos Bellos and Christos Tzivanidis. Alternative designs of parabolic trough solar collectors. *Progress in Energy and Combustion Science*, 71:81 – 117, 2019.

[44] Rodrigo Milani, Alexandre Szklo, and Bettina Susanne Hoffmann. Hybridization of concentrated solar power with biomass gasification in Brazil's semiarid region. *Energy Conversion and Management*, 143:522 – 537, 2017.

[45] Pietropaolo Morrone, Angelo Algieri, and Teresa Castiglione. Hybridisation of biomass and concentrated solar power systems in transcritical organic Rankine cycles: A micro combined heat and power application. *Energy Conversion and Management*, 180:757 – 768, 2019.

[46] A.T. Kearney and ESTELLA. Solar Thermal Electricity 2025, June 2010. http://www.estelasolar.org/wp-content/uploads/2015/11/2010-Solar-Thermal-Electricity-2025-ENG.pdf. Último acceso: 01.12.2019.

[47] A. Fernández-García, E. Zarza, L. Valenzuela, and M. Pérez. Parabolic-trough solar collectors and their applications. *Renewable and Sustainable Energy Reviews*, 14(7):1695 – 1721, 2010.

[48] Cheryl E Kennedy. Progress to develop an advanced solar-selective coating. Technical report, National Renewable Energy Lab.(NREL), Golden, CO (United States), 2008.

[49] Md Tasbirul Islam, Nazmul Huda, A.B. Abdullah, and R. Saidur. A comprehensive review of state-of-the-art concentrating solar power (CSP) technologies: Current status and research trends. *Renewable and Sustainable Energy Reviews*, 91:987 – 1018, 2018.

[50] H.M. Sandeep and U.C. Arunachala. Solar parabolic trough collectors: A review on heat transfer augmentation techniques. *Renewable and Sustainable Energy Reviews*, 69:1218 – 1231, 2017.

[51] Malika Ouagued, Abdallah Khellaf, and Larbi Loukarfi. Estimation of the temperature, heat gain and heat loss by solar parabolic trough collector under Algerian climate using different thermal oils. *Energy Conversion and management*, 75:191–201, 2013.

[52] Evangelos Bellos, Christos Tzivanidis, and Kimon A Antonopoulos. A detailed working fluid investigation for solar parabolic trough collectors. *Applied thermal engineering*, 114:374–386, 2017.

[53] A. Maccari, D. Bissi, G. Casubolo, F. Guerrini, L. Lucatello, G. Luna, A. Rivaben, E. Savoldi, S. Tamano, and M. Zuanella. Archimede Solar Energy Molten Salt Parabolic Trough Demo Plant: A Step Ahead towards the New Frontiers of CSP. *Energy Procedia*, 69:1643 – 1651, 2015. International Conference on Concentrating Solar Power and Chemical Energy Systems, SolarPACES 2014.

[54] Omar Behar, Abdallah Khellaf, and Kamal Mohammedi. A review of studies on central receiver solar thermal power plants. *Renewable and Sustainable Energy Reviews*, 23:12 – 39, 2013.

[55] M. Abbas, H. Aburideh, Z. Belgroun, Z. Tigrine, and N. Kasbadji Merzouk. Comparative Study of Two Configurations of Solar Tower Power for Electricity Generation in Algeria. *Energy Procedia*, 62:337 – 345, 2014. 6th International Conference on Sustainability in Energy and Buildings, SEB-14.

[56] Giovanni Manente, Sergio Rech, and Andrea Lazzaretto. Optimum choice and placement of concentrating solar power technologies in integrated solar combined cycle systems. *Renewable Energy*, 96:172 – 189, 2016.

[57] Soteris A. Kalogirou. Solar thermal collectors and applications. *Progress in Energy and Combustion Science*, 30(3):231 – 295, 2004.

[58] WEB de SolarPACES. CSP Projects Around the World, 2019. https://www.solarpaces.org/csp-technologies/csp-projects-around-the-world/. Último acceso: 01.12.2019.

[59] Evangelos Bellos. Progress in the design and the applications of linear Fresnel reflectors - A critical review. *Thermal Science and Engineering Progress*, 10:112 – 137, 2019.

[60] Nishith B. Desai and Santanu Bandyopadhyay. Line-focusing concentrating solar collector-based power plants: a review. *Clean Technologies and Environmental Policy*, 19(1):9–35, Jan 2017.

[61] H.L. Zhang, J. Baeyens, J. Degrève, and G. Cacères. Concentrated solar power plants: Review and design methodology. *Renewable and Sustainable Energy Reviews*, 22:466 – 481, 2013.

[62] Fausto Cavallaro. Multi-criteria decision aid to assess concentrated solar thermal technologies. *Renewable Energy*, 34(7):1678 – 1685, 2009.

[63] Andreas Poullikkas, George Kourtis, and Ioannis Hadjipaschalis. Parametric analysis for the installation of solar dish technologies in Mediterranean regions. *Renewable and Sustainable Energy Reviews*, 14(9):2772 – 2783, 2010.

[64] Frauke G. Braun, Elizabeth Hooper, Robert Wand, and Petra Zloczysti. Holding a candle to innovation in concentrating solar power technologies: A study drawing on patent data. *Energy Policy*, 39(5):2441 – 2456, 2011.

[65] V.V. Tyagi, S.C. Kaushik, and S.K. Tyagi. Advancement in solar photovoltaic/thermal (PV/T) hybrid collector technology. *Renewable and Sustainable Energy Reviews*, 16(3):1383 – 1398, 2012.

[66] Mohd Zainal Abidin Ab Kadir, Yaaseen Rafeeu, and Nor Mariah Adam. Prospective scenarios for the full solar energy development in Malaysia. *Renewable and Sustainable Energy Reviews*, 14(9):3023 – 3031, 2010.

[67] Sandia National Laboratories. Stirling Energy Systems Set New World Record for Solar-to-Grid Conversion Efficiency, 2008. https://www.newswise.com/articles /sandia-stirling-energy-systems-set-new-world-record-for-solar-to-grid-conversion-efficiency. Último acceso: 01.12.2019.

[68] N. Caldés, M. Varela, M. Santamaría, and R. Sáez. Economic impact of solar thermal electricity deployment in Spain. *Energy Policy*, 37(5):1628 – 1636, 2009.

[69] Martin Forster. Theoretical investigation of the system S_nO_x /S_n for the thermochemical storage of solar energy. *Energy*, 29(5):789 – 799, 2004. SolarPACES 2002.

[70] Antoni Gil, Marc Medrano, Ingrid Martorell, Ana Lázaro, Pablo Dolado, Belén Zalba, and Luisa F. Cabeza. State of the art on high temperature thermal energy storage for power generation. Part 1 - Concepts, materials and modellization. *Renewable and Sustainable Energy Reviews*, 14(1):31 – 55, 2010.

[71] C.Y. Zhao and Z.G. Wu. Thermal property characterization of a low melting-temperature ternary nitrate salt mixture for thermal energy storage systems. *Solar Energy Materials and Solar Cells*, 95(12):3341 – 3346, 2011.

[72] Y. Tian and C.Y. Zhao. A review of solar collectors and thermal energy storage in solar thermal applications. *Applied Energy*, 104:538 – 553, 2013.

[73] Pilkington Solar International GmbH. Survey of Thermal Storage for Parabolic Trough Power Plants, 2000. http://marcellacroix.espaceweb.usherbrooke.ca /ENERGIE/Thermal-storage.pdf. Útimo acceso: 01.12.2019.

[74] Y. Jemmal, N. Zari, and M. Maaroufi. Thermophysical and chemical analysis of gneiss rock as low cost candidate material for thermal energy storage in concentrated solar power plants. *Solar Energy Materials and Solar Cells*, 157:377 – 382, 2016.

[75] Ugo Pelay, Lingai Luo, Yilin Fan, Driss Stitou, and Mark Rood. Thermal energy storage systems for concentrated solar power plants. *Renewable and Sustainable Energy Reviews*, 79:82 – 100, 2017.

[76] Ulf Herrmann, Bruce Kelly, and Henry Price. Two-tank molten salt storage for parabolic trough solar power plants. *Energy*, 29(5):883 – 893, 2004. SolarPACES 2002.

[77] Stephen Boyd and Lieven Vandenberghe. *Convex optimization*. Cambridge university press, 2004.

[78] Christodoulos A Floudas. *Nonlinear and mixed-integer optimization: fundamentals and applications*. Oxford University Press, 1995.

[79] J. Usaola. Operation of concentrating solar power plants with storage in spot electricity markets. *Renewable Power Generation, IET*, 6(1):59–66, January 2012.

[80] Christoph Kost, Christoph M. Flath, and Dominik Most. Concentrating solar power plant investment and operation decisions under different price and support mechanisms. *Energy Policy*, 61(0):238 – 248, 2013.

[81] Regina Lamedica, Ezio Santini, Alessandro Ruvio, Laura Palagi, and Irene Rossetta. A MILP methodology to optimize sizing of PV - Wind renewable energy systems. *Energy*, 165:385 – 398, 2018.

[82] Pelin Damci Kurt. *Mixed-integer programming methods for transportation and power generation problems*. PhD thesis, The Ohio State University, 2014.

[83] E.F. Camacho, M. Berenguel, and C. Bordons. Adaptive generalized predictive control of a distributed collector field. *Control Systems Technology, IEEE Transactions on*, 2(4):462–467, 1994.

[84] Sunil K. Agrawal Radhakrishnan Mahadevan and Francis J. Doyle III. Differential flatness based nonlinear predictive control of fed-batch bioreactors. *Control Engineering Practice*, 9(8):889–899, 2001.

[85] M. Mahfouf, A. J. Asbury, and D. A. Linkens. Unconstrained and constrained generalised predictive control of depth of anaesthesia during surgery. *Control Engineering Practice*, 1(12):1501–1515, 2003.

[86] C. Bordons and J.R. Cueli. Predictive controller with estimation of measurable disturbances. Aplication to an olive oil mill. *Journal of Process Control*, 14(3):305–315, 2004.

[87] D.R. Ramírez, E.F. Camacho, and M.R. Arahal. Implementation of min-max MPC using hinging hyperplanes. Application to a heat exchanger. *Control Engineering Practice*, 12(6):700–709, 2004.

[88] J. Qin and T. A. Badwell. An overview of industrial model predictive control technology. In *Proceedings of the conference on Chemical Process Control*, 1997.

[89] Rudolf Emil Kalman et al. Contributions to the theory of optimal control. *Bol. soc. mat. mexicana*, 5(2):102–119, 1960.

[90] Rudolph Emil Kalman. A new approach to linear filtering and prediction problems. *Journal of basic Engineering*, 82(1):35–45, 1960.

[91] S. Joe Qin and Thomas A. Badgwell. A survey of industrial model predictive control technology. *Control Engineering Practice*, 11(7):733 – 764, 2003.

[92] J. Richalet, A. Rault, J. L. Testud, and J. Papon. Model predictive heuristic control: Applications to industrial processes. *Automatica*, 14:413–428, 1978.

[93] C. R. Cutler and B. C. Ramaker. Dynamic Matrix Control - a Computer Control Algorithm. In *Proc. Automatic Control Conference*, San Francisco, 1980.

[94] José Manuel Bravo Caro. *Control predictivo no lineal robusto basado en técnicas intervalares*. PhD thesis, Universidad de Sevilla, 2004.

[95] D. W. Clarke and P. J. Gawthrop. Self-tuning Control. In *Proceedings IEEE*, volume 123, pages 633–640, 1979.

[96] D. W. Clarke, C. Mohtadi, and P.S. Tuffs. Generalized Predictive Control - Part I. The Basic Algorithm. *Automatica*, 23(2):137–148, 1987.

[97] E. F. Camacho and C. Bordons. *Model Predictive Control*. Springer Verlag, 2nd edition, 1999.

[98] A. Bemporad, M. Morari, V. Dua, and E. N. Pistikopoulos. The explicit linear quadratic regulator for constrained systems. *Automatica*, 38(1):3–20, 2002.

[99] D. R. Ramírez. *Control predictivo min-max: análisis, caracterización y técnicas de implementación*. PhD thesis, Universidad de Sevilla, 2002.

[100] C. J. Baldwin, K. M. Dale, and R. F. Dittrich. A Study of the Economic Shutdown of Generating Units in Daily Dispatch. *Transactions of the American Institute of Electrical Engineers. Part III: Power Apparatus and Systems*, 78(4):1272–1282, Dec 1959.

[101] L. L. Garver. Power Generation Scheduling by Integer Programming-Development of Theory. *Transactions of the American Institute of Electrical Engineers. Part III: Power Apparatus and Systems*, 81(3):730–734, April 1962.

[102] Max Jacob Steinberg, Theodore Hunter Smith, et al. *Economy loading of power plants and electric systems*. J. Wiley & Sons, Inc., 1943.

[103] K. Hara, M. Kimura, and N. Honda. A Method for Planning Economic Unit Commitment and Maintenance of Thermal Power Systems, year=1966, volume=PAS-85, number=5, pages=427-436, doi=10.1109/TPAS.1966.291680, issn=0018-9510,. *IEEE Transactions on Power Apparatus and Systems*.

[104] Janna Martinek, Jennie Jorgenson, Mark Mehos, and Paul Denholm. A comparison of price-taker and production cost models for determining system value, revenue, and scheduling of concentrating solar power plants. *Applied Energy*, 231:854 – 865, 2018.

[105] Paul Denholm and Marissa Hummon. Simulating the value of concentrating solar power with thermal energy storage in a production cost model. 2012.

[106] R. Sioshansi and P. Denholm. The Value of Concentrating Solar Power and Thermal Energy Storage. *IEEE Transactions on Sustainable Energy*, 1(3):173–183, Oct 2010.

[107] Jennie Jorgenson, Paul Denholm, and Mark Mehos. Estimating the value of utility-scale solar technologies in California under a 40 % renewable portfolio standard. Technical report, National Renewable Energy Lab.(NREL), Golden, CO (United States), 2014.

[108] Paul Denholm, Jennie Jorgenson, Mackay Miller, Ella Zhou, and Caixia Wang. Methods for Analyzing the Economic Value of Concentrating Solar Power with Thermal Energy Storage. Technical report, National Renewable Energy Lab.(NREL), Golden, CO (United States), 2015.

[109] H.M.I. Pousinho, H. Silva, V.M.F. Mendes, M. Collares-Pereira, and C. Pereira Cabrita. Self-scheduling for energy and spinning reserve of wind/CSP plants by a MILP approach. *Energy*, 78:524 – 534, 2014.

[110] Michael J. Wagner, Alexandra M. Newman, William T. Hamilton, and Robert J. Braun. Optimized dispatch in a first-principles concentrating solar power production model. *Applied Energy*, 203:959 – 971, 2017.

[111] HMI Pousinho, J Contreras, P Pinson, and VMF Mendes. Robust optimisation for self-scheduling and bidding strategies of hybrid CSP-fossil power plants. *International Journal of Electrical Power and Energy Systems*, 67(0):639 – 650, 2015.

[112] G He, Q Chen, C Kang, and Q Xia. Optimal Offering Strategy for Concentrating Solar Power Plants in Joint Energy, Reserve and Regulation Markets. *IEEE Transactions on Sustainable Energy*, 7(3):1245–1254, July 2016.

[113] Mario Petrollese, Daniele Cocco, Giorgio Cau, and Euro Cogliani. Comparison of three different approaches for the optimization of the CSP plant scheduling. *Solar Energy*, 150:463–476, 2017.